

Effect of substituting baking water with brewer's spent grain supernatant on the micro-structure and crumb texture of white wheat flour bread

by

Nicola Jean van Zyl

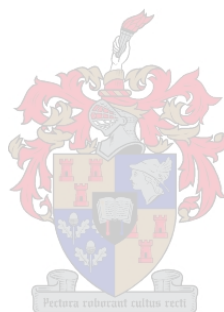
Thesis presented in partial fulfilment of the requirements for the degree of

Master of Science, in the Department of Food Science,

Faculty of AgriSciences

at

Stellenbosch University



Supervisor: Prof Marena Manley

Co-supervisors: Prof Johann Görgens & Dr Eugene van Rensburg

April 2019

Declaration

By submitting this thesis electronically, I declare that the entirety of the work contained therein is my own, original work, that I am the sole author thereof (save to the extent explicitly otherwise stated), that reproduction and publication thereof by Stellenbosch University will not infringe any third-party rights and that I have not previously in its entirety or in part submitted it for obtaining any qualification.

Nicola Jean van Zyl

April 2019

Date

Abstract

The ubiquitous opinion regarding brewer's spent grain (BSG), is that it is currently underutilised, based on its residual nutritional contents and potential for re-use. This is a process by-product that is available throughout the year, in most countries, at a very low cost from micro- to industrial-sized breweries.

For this research assignment, freshly produced BSG was processed using a screw-press which enabled the extraction of BSG-supernatant, a liquid consisting of 98% water. Using the supernatant would require less energy-intensive processing, compared to preparing a composite-flour from the spent grain through drying and milling of BSG.

Very little research has been undertaken with the objective of determining the effect on bread quality parameters when using an alternative baking water. The functional role of baking water in producing a quality bread product was reviewed. The knowledge gained therefrom enabled the evaluation of the potential of BSG-supernatant as an alternative baking water in white bread formulations.

The experimental design and research objectives of this investigation were employed in order to review the proposed removal of the excess moisture within fresh BSG. The liquid fraction is separated from its solid, fibrous origin and clarified through the gravimetric sedimentation of suspended fibrous-particulates. The BSG-supernatant's effect on the dough's rheological behaviour and quality scores were evaluated according to bread industry standards and regulations.

Macro- and micro-structural properties of the bread samples were evaluated using Texture Analysis (TA), C-Cell Visual Analysis (2D) and X-ray micro-Computed Tomography (3D) across a shelf-life period (Days 2, 3 and 4).

The micro-structural properties of bread loaves were evaluated in terms of their cell properties within the crumb-structure, as well as its porosity and water holding capacity (WHC). BSG-supernatant was determined to have no significant effect on the micro-structural properties of the bread loaf, although the crumb-structure of the BSG-supernatant breads had a greater WHC than did that of the control formulations.

The control- and treatment formulations were compared on a 5% significance level and it was concluded that BSG-supernatant can be used as an alternative baking water, for white bread formulations, without being detrimental to loaf quality.

Opsomming

Die alomteenwoordige opinie aangaande BSG, is dat dit tans onderbenut word, gebasseer op die oorblywende voedingsinhoud, en BSG se potensiaal vir hergebruik. Dit is tans 'n afvalprodukt wat dwarsdeur die jaar beskikbaar is in meeste nasies, vanaf mikro- en industriële brouerye teen 'n baie lae tarief.

Vir hierdie ondersoek is vars geproduseerde BSG verwerk met behulp van 'n skroefpers wat die ekstraksie van *BSG-supernatant*, 'n vloeistof wat uit 98% water bestaan, moontlik gemaak het. Die gebruik van die *supernatant* benodig minder energie-intensiewe prosessering, in vergelyking met die voorbereiding van BSG-meel deur die dehidrasie en maal van vars BSG.

Baie min navorsing is beskikbaar, met betrekking tot die effek op broodkwaliteits eienskappe wanneer 'n alternatiewe bakwater gebruik word om brood te produseer. 'n Omvattende literatuuroorsig is saamgestel om vas te stel wat die funksionele eienskappe is wat water bied in 'n brood formulering en produksie prosedures. Die funksionele rol van bakwater in die vervaardiging van 'n goeie gehalte broodprodukt is as gevolg hersien. Die kennis wat in die proses versamel is, het die evaluering van die potensiaal van *BSG-supernatant* as 'n alternatiewe bakwater gerealiseer.

Die eksperimentele ontwerp en navorsingsdoelwitte van hierdie ondersoek is in diens geneem om die ekstraksie van die oortollige vog (water) binne vars BSG te oorweeg as 'n alternatiewe bakwater. Die *BSG-supernatant* is geskei van die gesuspendeerde veselagtige materiaal, deur die vloeistof te laat staan. Die *BSG-supernatant* se effek op die broodmeel se reologiese eienskappe en brood kwaliteit is geëvalueer volgens broodbedryf-standaarde en regulasies.

Makro- en mikrostruktuur eienskappe van broodmonsters, van beide 'n oorspronklike en *BSG-supernatant* brood formulasies, is geëvalueer met behulp van Tekstuur-analise (TA), C-Cell Visuele Analise (2D) en *X-ray micro-Computed Tomography* (*X-ray* μ CT) tydens 'n brood se rakkertydperk (Dae 2, 3 en 4 na- produksie).

Die mikrostrukturele eienskappe en veranderinge tydens 'n vasgestelde rakkertyd, was evalueer deur die sel-struktuur binne-in die brood se krummel-struktuur te vergelyk met die van die kontrole s'n. Die mikrostruktuur van die brode was ook evalueer deur te kyk na die porositeit van die brood se spons-struktuur.

Dit was bepaal dat die *BSG-supernatant* geen negatiewe invloed op die mikrostruktuur van 'n wit-brood het nie. Daar is tog 'n merkwaardige gevolgtrekking gemaak, dat die WHC van die *BSG-supernatant* brode 'n verbeterde krummel-struktuur WHC gehad het.

Die *BSG-supernatant* en oorspronklike wit-brood formulering was vergelyk op 'n 5% betekenisvlak, waartydens die gevolgtrekking gemaak is dat die *BSG-supernatant* as 'n effektiewe, alternatiewe bakwater benut kan word in wit-brood formulasies, sonder om die kwaliteit van die finale brood produk te benadeel.

Acknowledgements

Firstly, I would like to thank my supervisor, Professor Marena Manley. I am honoured to be able to say that I have worked alongside you. Your experience and wisdom were quintessential to the progress and completion of this research assignment. I hope we have the opportunity to work together again.

Additionally, I would like to extend my sincere gratitude to the following individuals, organisations and institutions for enabling the progress and conclusion of this research assignment:

My Family and close friends, you have always believed in me, regardless of my triumphs or failures. I appreciate and love you with all my heart;

My co-supervisors: Professor Johann Görgens and Doctor Eugene van Rensburg. Thank you for helping me define and conceptualise the vision for this project, through enabling me to pursue beyond the confines of my familiar academic field, and into the practical innovation that is process engineering;

The Winter Cereal Trust Bursary Scheme, for awarding a two-year bursary, from January 2017 to December 2018, enabling me to pursue my dream of studying towards a Masters degree in Food Science. I would also like to thank the Trust for providing the financial resources to attend the annual Winter Cereal Trust meeting in Pretoria (2018);

The National Research Foundation (NRF) for awarding a Masters Freestanding scholarship (2018);

Kim O'Kennedy and Carien Roets at Sasko Research and Development Laboratory, Paarl, South Africa, I would like to thank you for your input and support during the sourcing of wheat, milling of bread flour and rheological analyses. Your guidance was crucial to the progress and completion of this investigation;

Prof Martin Kidd, from the Centre of Statistical Consultation, Stellenbosch University, for his advice in planning the experiments and for his statistical analysis;

Lia Bothma, at Anchor Yeast Bakery Specialties in Johannesburg, South Africa, for your technical support during this research assignment's initial stages, the hands-on training in the Baking Laboratory on the premises as well as your hospitality;

The Department of Food Science, Stellenbosch University: I could not have wished for a more supportive community of academics and support personal. As a department, I will miss each and every one of you, who have made my time there truly inspiring and unforgettable;

A big thank you to the Central Analytical Facility (CAF) X-ray Unit, Stellenbosch University, for your guidance during the process of X-ray micro-Computed Tomography image acquisition, assistance with sample volume processing, data extraction and last but not least, the coffee. It was amazing;

Lukas Swart, thank you for indulging my vision, and your invaluable assistance with the logistics concerning the setup, operation and maintenance of the screw-press and accompanying materials;

To the Department of Process Engineering at Stellenbosch University: Thank you for accommodating me in your workshop and laboratory whilst I was doing sample preparation. I would also like to thank the support staff for being so kind, helpful and patient towards me;

A big thank you to the Newlands Brewery (Cape Town, South Africa) for supplying the brewer's spent grain required for this investigation;

Last but not least my colleague, Zandr  Germishuys, thank you for your reliable assistance, patience and guidance;

Oh, and Willem, if you are reading this, I love you.

“Waste is a resource out of place” - Bill Coors (1916-2018)

List of Abbreviations

α	Alpha
β	Beta
\pm	Plus-minus
*	Interaction indicator
%	Percentage
% w/w	Percentage weight, per weight of flour
$^{\circ}\text{C}$	Degrees Celsius
μA	Micro-ampere
μCT	Micro-Computed Tomography
μm	Micrometre
\bar{x}	Mean
2D	Two-dimensional
3D	Three-dimensional
AB InBev	Anheuser-Busch International Beverages
AACC	American Association of Cereal Chemists
ANOVA	Analysis of variance
a_w	Water activity
AX	Arabinoxylan(s)
$^{\circ}\text{Bx}$	Degrees Brix
BA	Baking absorption
BSG	Brewer's spent grain
BU	Brabender Units
<i>ca.</i>	Circa (around; approximately)
CAF	Central Analytical Facility
Cl	Chlorine
$\text{CO}_2(\text{g})$	Carbon dioxide gas
cP	Centipoise
CSIR	Council for Scientific and Industrial Research
DAFF	Department of Agriculture, Forestry, and Fisheries (of South Africa)
DDT	Dough development time
db	Dry base
dH ₂ O	Deionised water
dough _{temp}	Dough temperature
DSC	Differential scanning calorimetry
Eq.	Equation
<i>etc.</i>	Et cetera (and so forth)

<i>et al.</i>	Et alia (and others)
EtOH	Ethanol
FAO	Food and Agriculture Organisation of the United Nations
FN	Falling Number
FOV	Field-of-view
GG	Guar gum
g	Gram
g/cm ³	Gram per cubic centimetre
GLM	General linear models
H ₀	Null hypothesis
H ₁	Alternative Hypothesis
HMF	Hydroxymethylfurfural
HPLC	High Performance Liquid Chromatography
HU	Houndsfield Units
J	Joules
kg	kilogram
kg/hL	Kilogram per hectolitre
kV	kilovolt
L	Distensibility
L	Litre
LSD	Least significant difference(s)
min	Minute(s)
mb	Moisture base
mL	Millilitre
mm	Millimetre
mm ³	Cubic millimetre
n	Number of samples
MT	Mixing time
Na	Sodium
NaCl	Sodium chloride
NIR	Near infrared
NMR	Nuclear magnetic resonance
NSP, NSPs	Non-starch polysaccharide, Non-starch polysaccharides
P	Tenacity
P/L	Curve configuration ratio
PTFE	Polytetrafluoroethylene
ROI, ROIs	Region-of-interest, Regions-of-interest
VOI, VOIs	Volume-of-interest, Volumes-of-interest

RVA	Rapid Visco Analyser
s	seconds
SAGL	South African Grain Laboratory
TA	Texture Analysis
TDS	Total dissolved solids
TSS	Total suspended solids
T ₀	Initiation temperature
T _c	Conclusion temperature
T _p	Peak temperature
TSS	Total suspended solids
VA	Visual Analysis
VG	Volume Graphics
W	Deformation energy
WAC	Water absorption capacity
WBC	Water binding capacity
WHC	Water holding capacity
water _{temp}	Temperature of water source
XG	Xanthum gum

List of Tables

Table 1 HPLC analysis specifications and conditions	23
Table 2 Details of the bread formulation(s) used during the baking of bread samples	25
Table 3 Parameters that were recorded for each batch of bread formulation	25
Table 4 Summary of X-ray μ -Computed Tomography scan parameters used for image acquisition of all bread samples	28
Table 5 Parameters calculated and recorded, for each VOI including: whole bread sample and all VOI's part of the <i>Bread sample VOI reconstruction</i>	29
Table 6 Parameters calculated and recorded, for each VOI, during Foam Structure Analysis	30
Table 7 Proximate analysis of BSG-supernatant (n=6)	34
Table 8 Compositional analysis of BSG-supernatant through the use of high-performance liquid chromatography	34
Table 9 Wheat kernel quality, as measured by a NIR Grain Analyser (n = 3)	35
Table 10 Proximate and compositional analysis of the bread flour. Results are reported as mean \pm standard deviation	35
Table 11 Alveograph analysis on bread flour. Results are reported as mean \pm standard deviation (n = 6)	36
Table 12 Test Hypotheses for this investigation	36
Table 13 Mixograph, Farinograph and FN parameters as affected by the replacement of water with BSG-supernatant.	37
Table 14 Pasting properties, as determined by the Rapid Visco Analyser (RVA), of the bread flour used, as influenced by replacing water with BSG-supernatant	38
Table 15 GLMs of the effects on the pasting properties of the dough. The effects include the <i>treatment</i> , control or BSG-supernatant, <i>age</i> of the supernatant and their interaction, as <i>Treatment*Age</i>	38
Table 16 General Linear Models (GLM) of the parameters measured during Texture Analysis on the second, third and fourth day after bread sample production. The effect is significant when $P \leq 0.05$.	

*represents an interaction.	41
Table 17 Firmness and Resilience as measured during texture analysis, across days two, three and four of the bread sample's shelf-life.	41
Table 18 General Linear Models for C-Cell Visual Analysis parameters, describing the effect of the variables being considered on the bread sample's slice shape and colour parameters.	43
Table 19 General Linear Models for Cell size and Holes morphology.	46
Table 20 Bread quality parameters as measured by C-Cell visual analysis (Treatment*Age interaction). (n = 120 slices per Day)	49
Table 21 General linear models for the Bread VOI morphology.	50
Table 22 Bread morphology as measured by X-ray μ CT, on three consecutive shelf-life days.	51
Table 23 General Linear Models for bread size parameters and porosity, regarding the Bread sample VOI reconstruction.	52
Table 24 Determining the percentage increase/decrease, between Bread sample VOI reconstruction volumes of interest (VOI) due to the difference in bread formulation (treatment).	53
Table 25 Determining the percentage increase/decrease, between bread the control- and treatment bread formulations, across three shelf-life days (2, 3 and 4).	54
Table 26 General Linear Models for the crumb density of bread samples as affected by the VOIs within the Bread sample VOI reconstruction VOIs, as affected by Treatment, Sample Age and Volume of Interest (VOI).	57
Table 27 Determining the difference, between the control- and treatment formulations as affected by the interaction between treatment*VOI factors.	58
Table 28 General Linear Models for crumb properties as analysed using the Foam Structure analysis function of the VGStudio Max software package ($P \leq 0.05$)	60
Table 29 Treatment vs. Volume of interest. Determining the difference, if any, between Bread sample VOI reconstruction volumes of interest (VOI) and treatment applied.	61
Table 30 Treatment vs. Sample Age. Determining the difference in foam structure (micro-structural) properties, between the two bread formulations, as affected by the interaction between the VOI and Treatment applied.	63

List of Figures

- Figure 1** A schematic representing the process of extracting the liquid-fraction within BSG, using a screw-press.21
- Figure 2** BSG-supernatant sample preparation: Defrosting the BSG-liquid and separating it into its liquid and solid fractions. The two bottles are each designated to a BSG-supernatant bread-formulation batch. In total, this process was repeated three times, once for each replicate of the experimental design, ca. 24 h before bread sample production.22
- Figure 3** Replicate design for bread sample production for each respective analysis. This design was repeated three times, over a period of three weeks (21 days).26
- Figure 4** A systematic representation of the process used to extract information from the image acquisition of bread samples using X-ray micro-Computed Tomography. ¹Region Of Interest, ²Volume Of Interest, ³reconstruction of bread VOIs.31
- Figure 5** A visual representation of the Top Crust-VOI that forms part of the Bread House VOI. a) front perspective b) sagittal perspective c) top perspective d) three-dimensional (3D) perspective of VOI32
- Figure 6** Trough viscosity as determined by RVA and affected by the interaction between the treatment and the age of treatment water. Vertical lines denote 95% confidence intervals. Indicated scripts that differ indicate a significant difference ($P \leq 0.05$). *represents an interaction.39
- Figure 7** Time required to reach peak viscosity, as determined by RVA and affected by the interaction between the treatment and the age of the BSG-supernatant. Vertical lines denote 95% confidence intervals. Indicated scripts that differ indicate a significant difference ($P \leq 0.05$). *represents an interaction.39
- Figure 8** Final viscosity of the flour-water slurry as determined by RVA, as affected by the treatment and the age of the treatment water. Vertical lines denote 95% confidence intervals. Scripts that differ indicate a significant difference ($P \leq 0.05$). *represents an interaction.40
- Figure 9** Firmness of bread, as determined by the texture analyser and affected by the interaction between the treatment and the age of the sample. Vertical lines denote 95% confidence intervals. Indicated scripts that differ indicate a significant difference ($P \leq 0.05$). *represents an interaction. ...42
- Figure 10** Resilience of the bread sample slices, as determined by the texture analyser and affected by the interaction between the treatment and the age of the bread sample. Vertical lines denote 95% confidence intervals. Indicated scripts that differ indicate a significant difference ($P \leq 0.05$).

*represents an interaction.....	42
Figure 11 Total concavity (%) of the bread samples as measured by C-Cell VA and affected by the age of the sample. Vertical lines denote 95% confidence intervals. Indicated scripts that differ indicate a significant difference ($P \leq 0.05$).	43
Figure 12 Slice area measured by C-Cell VA, and affected by the interaction between the experimental treatment and replicate. Vertical lines denote 95% confidence intervals. Indicated scripts that differ indicate a significant difference ($P \leq 0.05$). *represents an interaction.....	44
Figure 13 Slice brightness, as measured by C-Cell VA, and affected by the age of the bread sample. Vertical lines denote 95% confidence intervals. Indicated scripts that differ indicate a significant difference ($P \leq 0.05$).	44
Figure 14 L^* colour component, as measured by C-Cell VA, and affected by the age of the bread sample. Vertical lines denote 95% confidence intervals. Indicated scripts that differ indicate a significant difference ($P \leq 0.05$).	45
Figure 15 a^* colour component, as measured by C-Cell VA, as affected by the replicate factor. Vertical lines denote 95% confidence intervals. Indicated scripts that differ indicate a significant difference ($P \leq 0.05$).	45
Figure 16 b^* colour components measured by C-Cell VA and affected by the age of the bread sample. Vertical lines denote 95% confidence intervals. Indicated scripts that differ indicate a significant difference ($P \leq 0.05$).	46
Figure 17 Number of cells within a bread slice as measured by C-Cell VA and affected by the interaction between the experimental treatment and replicate. Vertical lines denote 95% confidence intervals. Indicated scripts that differ indicate a significant difference ($P \leq 0.05$). *represents an interaction...	47
Figure 18 Volume of the cells within the bread slice, as measured by C-Cell VA and affected by the interaction between the treatment and the age of the bread sample. Vertical lines denote 95% confidence intervals. Indicated scripts that differ indicate a significant difference ($P \leq 0.05$).	47
Figure 19 The area of the bread loaf, as measured by X-ray μ CT and affected by the treatment. Vertical lines denote 95% confidence intervals. Indicated scripts that differ indicate a significant difference ($P \leq 0.05$).	50
Figure 20 The area of the bread slice/crust, as affected by the VOI effect measured by X-ray μ CT. Vertical lines denote 95% confidence intervals. Indicated scripts that differ indicate a significant difference ($P \leq 0.05$).	52

- Figure 21** Total VOI volume as affected by the VOI effect, measured by X-ray μ CT. Vertical lines denote 95% confidence intervals. Indicated scripts that differ indicate a significant difference ($P \leq 0.05$). ...55
- Figure 22** VOI porosity, as a function of its internal volume of air, as measured by X-ray μ CT, and affected by the interaction between the VOI, and the Treatment effects. Vertical lines denote 95% confidence intervals. Indicated scripts that differ indicate a significant difference ($P \leq 0.05$).55
- Figure 23** VOI porosity, as a function of its internal volume of material (crumb), as measured by X-ray μ CT and affected by the VOI-effect. Vertical lines denote 95% confidence intervals. Indicated scripts that differ indicate a significant difference ($P \leq 0.05$).56
- Figure 24** VOI porosity, as a function of its internal volume of air, as measured by X-ray μ CT, and affected by the interaction between the progress in loaf shelf-life (Sample Age) and its interaction with the VOI-effect. measured in days. Vertical lines denote 95% confidence intervals. Indicated scripts that differ indicate a significant difference ($P \leq 0.05$).56
- Figure 25** Grey-value distribution of the bread as affected by the VOI-effect. Vertical lines denote 95% confidence intervals. Indicated scripts that differ indicate a significant difference ($P \leq 0.05$).58
- Figure 26** Grey-value distribution of the bread as affected by the age of the sample. Vertical lines denote 95% confidence intervals. Indicated scripts that differ indicate a significant difference ($P \leq 0.05$).59
- Figure 27** Relative density of the bread sample as affected by the VOI-effect. Vertical lines denote 95% confidence intervals. Indicated scripts that differ indicate a significant difference ($P \leq 0.05$).59
- Figure 28** Foam structure analysis of the mean cell size within the bread micro-structure as affected by the VOI-effect. Vertical lines denote 95% confidence intervals. Indicated scripts that differ indicate a significant difference ($P \leq 0.05$).62
- Figure 29** Foam structure analysis of the maximum cell size within the bread micro-structure as affected by the VOI-effect. Vertical lines denote 95% confidence intervals. Indicated scripts that differ indicate a significant difference ($P \leq 0.05$).62

Table of Contents

Effect of substituting baking water with brewer’s spent grain supernatant on the micro-structure and crumb texture of white wheat flour bread.....	i
Declaration.....	I
Abstract.....	II
Uittreksel.....	Error! Bookmark not defined.
Acknowledgements.....	IV
List of Abbreviations	VII
List of Tables	X
List of Figures	XII
Table of Contents	XV
Chapter 1:	1
Introduction	1
Chapter 2:	4
Literature Review.....	4
Functional role of baking water in the physicochemical changes that occur during bread production – a review	4
Introduction	4
The interaction of water with other formulation components	5
Wheat-flour starch	5
Wheat-flour proteins	6
Wheat-flour lipids.....	7
Non-starch polysaccharides	7
Minor formulation constituents.....	9
Water addition and mixing	10
Baking absorption.....	12
Increasing the baking absorption of a bread formulation.....	12
Dough conditioning.....	14
Baking.....	15
Setback.....	16

Bread product quality and shelf-life	16
Starch retrogradation	18
Moisture migration and redistribution	18
Conclusion	19
Chapter 3	21
Materials and Methods	21
BSG-supernatant extraction	21
Proximate and compositional analysis	22
Wheat-flour production	23
Proximate analysis	23
Rheology	24
Breadmaking process	24
Bread micro-structural analysis	25
C-Cell Visual Analysis	26
Texture Analysis	27
X-ray micro-Computed Tomography	27
Statistical Analysis	32
Chapter 4	34
Results	34
Proximate and compositional analysis	34
BSG-supernatant	34
Bread flour	35
Dough Rheology	35
Texture analyses	40
C-Cell Visual Analysis	43
X-ray micro-Computed Tomography Analyses	50
Bread size and porosity	50
Bread Crumb Density	57
Foam structure analysis: cell size and distribution within the bread sample foam structure ...	60
Chapter 5	64

Discussion	64
BSG-supernatant composition.....	64
Bread flour quality.....	65
Effect of BSG-supernatant on Rheology	66
Bread Analyses	67
Texture Analysis	67
C-Cell Visual Analysis.....	67
X-ray micro-Computed Tomography.....	68
Microstructural changes: A consequence of bread staling	68
Chapter 6	71
Conclusion	71
Recommendations.....	72
Chapter 7:	73
References	73
Addendum: A.....	84

This thesis is presented in the format prescribed by the Department of Food Science at Stellenbosch University. The language, style and referencing format used are in accordance with the requirements of the *International Journal of Food Science and Technology*.

Chapter 1:

Introduction

Malted barley is used to extract its fermentable sugars during the mashing step of beer production (Lynch *et al.*, 2016). The malted barley is hydrated with water and kept at a temperature between 60°C and 75°C to produce wort (Lynch *et al.*, 2016) a sugary liquor, which is rich in fermentable sugars. The wort is drained from the brewer's spent grain (BSG) to proceed in the beer production process, whilst the BSG is removed from the process entirely. Brewer's spent grain accounts for up to *ca.* 85% of the total brewing residue of the beer industry (Aliyu and Bala, 2013; Gil-Martinez, 2016). The beer-production by-product is an environmental concern due to the large volumes produced annually on a global scale (Stojceska *et al.*, 2008; Lynch *et al.*, 2016). The Council for Scientific and Industrial Research (CSIR) determined that an excess of 300 000 tons of BSG is produced annually in South Africa (CSIR, 2008). This number is estimated to have grown closer to 600 000 tons in 2018.

When there are no established alternative routes for the utilisation of BSG, it is primarily designated to landfills (Thiago *et al.*, 2014). A fraction of the total BSG produced is utilised on-site in anaerobic digesters for organic gas-production and/or transported to the nearest farm for a low-cost livestock feed (Aggelopoulos and Bekatorou, 2013) with the majority of the BSG still designated to landfills as it becomes spoiled and unsuitable for its use as livestock feed, within a seven day period (El-Shafey *et al.*, 2004).

Peer-reviewed publications on the utilisation of BSG, include the incorporation of BSG into food products, intended for humans. The focus of recent literature has been centred around determining its composition (Mussatto, 2014; Severini *et al.*, 2015; Kemppainen *et al.*, 2016; Lynch *et al.*, 2016; Madubuike and Okolo, 2016), variability in composition (Moreira *et al.*, 2012, 2013) and the incorporation of BSG composite-flour into baked food products to increase potential health benefits for the consumer (Santos *et al.*, 2003; Aliyu and Bala, 2011; Lynch *et al.*, 2016). The nutritional and health benefits associated with incorporating BSG composite-flour into food products, include lowering plasma cholesterol, aiding in lipid metabolism, and reducing the glycaemic index of its surrounding food matrix (Izydorczyk and Dexter, 2008).

The use of BSG composite-flour in food products has been reviewed as an innovative method of increasing the antioxidant, fibre and protein content of the original product. These products include bread (Stojceska, 2011; Waters *et al.*, 2012; Ktenioudaki *et al.*, 2013b, 2015), cookies (Öztürk *et al.*, 2002), extruded snacks (Stojceska *et al.*, 2008; Ktenioudaki *et al.*, 2013a), and pasta (Sobukola *et al.*, 2013). It has been illustrated that when the BSG composite-flour is incorporated into a bread formulation, the molecular weight, degree of -polymerisation and -branching of the arabinoxylan (AX) fraction within the BSG-composite flour, has a direct influence on the bread dough- and loaf quality (McCarthy, 2013; Reis *et al.*, 2015).

Although it is an attractive solution to reducing waste, the production of BSG composite-flour is a very energy intensive process (Weger *et al.*, 2017). Native BSG consists of *ca.* 65 to 80% moisture (Kotlar *et al.*, 2011; Gil-Martinez, 2016), and would require an extended residence time in a dehydrator to reduce its high initial moisture content. The practical and cost-related limitations that accompany the use of a BSG composite-flour include the large volumes of wet spent grain that would need to be dried and milled, both of which are time-consuming processes even with modern equipment. Producing a composite flour from BSG is thus not a very practical nor sustainable solution towards BSG waste reduction as a whole.

Another popular research objective is to produce value-added extractives from BSG. The application of pre-treatment(s) to promote the solubility of BSG, have been investigated in order to extract any residual compounds of interest, such as arabinoxylans (AX) (Mussatto and Roberto, 2006; Reis *et al.*, 2014), polyphenols (Moreira *et al.*, 2012), phytochemicals (Bartolomé *et al.*, 1997; del Río *et al.*, 2013; McCarthy *et al.*, 2013; Meneses *et al.*, 2013), oligosaccharides (Carvalho *et al.*, 2004; Kotlar *et al.*, 2011; Ikram *et al.*, 2017) and lipids (Niemi *et al.*, 2012). The fermentation of BSG, which has undergone acid hydrolyses, has also been reviewed as a means of xylitol production (Aliyu and Bala, 2011). Other methods of BSG utilisation include using the fresh biomass as a growth medium for microbial organisms, which in turn produce valuable metabolites such as ethanol, hydrogen-gas and probiotics (Mbagwu and Ekwealor, 1990; Duarte *et al.*, 2008; Giroto *et al.*, 2015; Weger *et al.*, 2017; Poladyan *et al.*, 2018).

Bread, in particular, white bread, is a staple food in households around the world. In the Republic of South Africa in 2017 alone, over a billion white bread (*ca.* 700 g loaves), accompanied by another billion brown bread (*ca.* 700 g loaves) and a relatively small amount, *ca.* 32 million whole wheat loaves were produced (SAGL, 2018). Baring this in mind, *ca.* 60% (per weight of flour) of each bread formulation consists of water, making it the second most abundant ingredient in bread formulations (Roels *et al.*, 1993; Mondal and Datta, 2008). This equates to a rough estimate of 5.4×10^8 litres of drinkable water, used annually, to produce bread, disregarding the processes surrounding the production of bread which also requires clean and safe drinking water, for example, wheat tempering. Wheat tempering is the process of increasing the moisture content of wheat kernels in order to retain the optimum moisture content post-milling.

South Africa, like many other countries around the world, is subject to episodes of drought that last between two- to three years, during which access to safe, clean drinking water necessary for all consumer life, becomes a scarce commodity. This was recently illustrated in the incredible drought that lasted from the beginning of 2016 to the start of 2018 (Anonymous, 2017) which nearly lead to the cut-off of clean water supply to the city of Cape Town, surrounding towns and settlements.

This research undertaking was designed in order to obtain knowledge on the rheology and microstructural properties, including the foam structure of dough and bread, prepared using BSG-supernatant. This would deliver insight on the functional properties of BSG-supernatant as an alternative baking water and its effect(s) on bread quality.

Instead of diluting the gluten-network protein within a bread formulation, through the substitution of wheat-flour with hydrocolloids (Davidou *et al.*, 1996; Linlaud *et al.*, 2009; Fadda *et al.*, 2014), grain-, vegetable-(Wang *et al.*, 2017; Lu *et al.*, 2018) or seed- isolates (Sęczyk *et al.*, 2017; Švec and Hrušková, 2018), or through the use of composite-flours (Hemdane *et al.*, 2017, 2018), replacing the water in the bread formulation with an alternative baking water, such as BSG-supernatant, is proposed as a viable means of increasing waters absorption and/or water holding capacity of the bread product's crumb.

Very little research has been completed with the objective of determining the effect on quality parameters of a baked product as a result of using an alternative baking water. Hassan *et al.* (2013), concluded that using fermented skim milk, acidic cheese whey and buttermilk as an alternative baking water, increased the loaf slice firmness, and decreased the overall acceptability across a three-day shelf-life period, when compared to their control bread formulation made with water (Hassan and El-Shazly, 2013).

Since producing a composite-flour from BSG has clear limitations regarding its sustainability, the extraction of the excess moisture from within fresh, wet BSG is considered a possible means of increasing the potential shelf-life and reducing the transport costs to the final destination, whether it be to a local farm or the nearest landfill. This research assignment proposes the reuse of the extracted water as an alternative baking water in white bread formulations. The rationale behind this is that large volumes of clean, drinking water are used to produce bread, independent of its formulation. The BSG-supernatant will be used as an alternative baking water, through complete substitution of the clean, drinkable water in the original white-bread formulation.

The first objective of this research assignment encompasses the characterisation of the BSG-supernatant through composition and proximate analyses. The second objective includes measuring and evaluating the effect of BSG-supernatant as a baking water on dough rheology parameters, with reference to the specifications used by the bread industry for quality control purposes (DAFF, 2017; SAGL, 2018). The third objective includes the analysis of the bread samples made using the BSG-supernatant as an alternative baking water, in a lean bread formulation. Texture Analysis and C-Cell Visual Analysis are currently used as standardised quality control analyses employed by the bread industry and so they were included in this project's experimental design. X-ray micro-Computed Tomography (X-ray μ CT) was employed as a third, yet non-destructive, analysis method in order to investigate the microstructural changes within white bread (*ca.* 700 g) as a consequence of using BSG-supernatant as an alternative baking water. Microstructural changes are also measured and evaluated across a shelf-life period (days 2, 3 and 4) to include the evaluation of the bread staling phenomena. X-ray μ CT has already been determined to be an effective, non-destructive method for measuring, evaluating and comparing the effect of different bread formulations on the microstructural characteristics of bread's foam structure (Falcone *et al.*, 2004).

Chapter 2:

Literature Review

Functional role of baking water in the physicochemical changes that occur during bread production – a review

Introduction

The structural, chemical and sensory properties of a baked food product are dependent on the physical properties of the water it contains (Leung *et al.*, 1983). Water is present in all food(s). Water can be present in one- or more of the following physical states: as a solvent, a plasticizer, water of hydration, and adsorbed on internal- and external surfaces (Curren & King, 2002). In biological systems, such as those of food products, the interaction of the formulation components with water determines the observed macro- and micro-structural changes and properties of the food product (Leung *et al.*, 1983).

The two main ingredients that constitute a bread formulation, and determine bread quality are the bread-flour and the amount of water used during dough formation (Roels *et al.*, 1993; Mondal and Datta, 2008). During bread production, a critical process parameter is to consider the quality of the wheat flour used, in terms of its moisture- and protein content, accompanied by the amount (% w/w) of water used to form a functional dough and desirable baked bread product (Cauvain and Young, 2000; Goesaert *et al.*, 2005).

Due to water being the second most abundant ingredient in a bread-dough formulation, the ratio of flour-to-water (% w/w of flour) and the interaction between water and the wheat-flour's components, starch and protein, directly influences the appearance and the quality of the bread product. Although the purpose of water in a bread formulation is clear, the functionality evaluated through the water's interactions as an ingredient and its effect on bread quality, has as of yet not been thoroughly reviewed.

As part of a bread-dough formulation, water is a solvent medium and a plasticizer in the presence of other ingredients (Cauvain and Young, 2000). It has been determined that decreasing the amount of water added to a dough-formulation has a greater effect on the resulting dough's quality than does an increase in the level of water addition (Mani *et al.*, 1992; Linlaud *et al.*, 2009). Wheat flour's interaction with water is of such importance that rheology, a science dedicated to determining the behaviour of flour-water mixtures, has gained international recognition for being able to predict the quality of a baked product, based on the combination of the quality and quantity of the wheat flour and water in a bread formulation.

The water absorption capacity (WAC) of flour has been determined to depend solely on the direct interaction of flour components with water molecules during all baking stages (Roman-Gutierrez *et al.*, 2002). Essentially, the interaction between wheat-flour components, water and other bread-

dough ingredients determine the bread product's quality (Roels *et al.*, 1993). Water is absorbed by formulation components, during their manufacture as well as when they are incorporated into a dough-formulation.

Although the water activity (a_w) concept accounts for the availability of unbound water, it does not sufficiently describe the structural changes in food, as a function of temperature changes and the mobility of moisture. Breadmaking includes several physicochemical changes that are driven by the combination of moisture and heat, including the proofing and baking stages. The water activity (a_w) and moisture content of the dough- and bread product are known to have a thermodynamic relationship, which is dependent on the temperature of the food system at the time it is measured (Andrade *et al.*, 2011).

The interaction of water with other formulation components

The quality of bread-flour is measured through proximate analysis and rheological tests that have been accepted globally by the baking industry. A quality white bread-flour is required by, regulation (DAFF, 2016) to have a greater ratio of wet- to dry gluten, a low degree of damaged starch and a low falling number. A lean dough formulation comprises wheat flour, water, yeast, salt, sugar, and shortening (FAO, 1947; Cauvain and Young, 2000).

Wheat-flour starch

Wheat starch is classified as A-class starch granules (Hoseney, 1986), which are located within the amyloplasts of wheat kernels (Delcour and Hoseney, 2010a). Amylose is a large, relatively insoluble compound in water and accounts for 18-33% of the starch composition within the wheat's endosperm (Delcour and Hoseney, 2010b). An amylose molecule consists of a backbone with branches of α -D-glucose bound monomers. These glucose molecules are bound linearly through glycosidic α -(1 \rightarrow 4)-bonds and branch through α -(1 \rightarrow 6)-glucose bonds, to increase the surface area and size of the molecule. The degree of branching within an amylose molecule is proportional to its solubility, attributed to the slightly polarised (α -1 \rightarrow 6)-D-glucose bonds at the origin of each branched segment (Delcour and Hoseney, 2010c).

Amylopectin is similar to amylose, in that it is composed of the same monosaccharides and the same bonds involved in branching of its linear backbone (Angold, 1975; Delcour and Hoseney, 2010a). The major difference between amylose and amylopectin is the degree of branching, with amylopectin being able to form branches that are the size of smaller amylose molecules. Amylopectin has three different branch types, referred to as A, B and C sidechains consisting of α -(1 \rightarrow 4)-D-glucose (Delcour and Hoseney, 2010a). Amylopectin's branch types can be described in terms of their composition; A-chains consist of only α -(1 \rightarrow 4)-D-glucose, whilst B-chains have α -(1 \rightarrow 4)-D-glucose and α -(1 \rightarrow 6)-D-glucose and C-chains have both α -(1 \rightarrow 4)-D-glucose and α -(1 \rightarrow 6)-D-glucose and a reducing end (Delcour and Hoseney, 2010a).

Amylose is seen as the more mobile of the two (soluble) whilst amylopectin's molecular size, due to its extensive branching and behaviour in solutions, are indicative of a relatively immobile,

branched polysaccharide. The reducing end is able to interact with water during the formation of a flour-water mixture, such as during dough formation (Delcour and Hoseneey, 2010d).

The reduction in amylose's molecular weight is due to the action of α -amylase. The activity of α -amylase is linked to the formation of a softer dough (Barrera *et al.*, 2007). Through liberating (α -1 \rightarrow 4)-D-glucose monomers and polymers from amylose's structure, glucose molecules are more readily available to yeast as a substrate, eventually contributing to the characteristic slight sweetness associated with white bread products. During mixing, the hydrating starch network evolves as the amylose accumulates in the centre of starch granules, due to phase separation (Hug-Iten *et al.*, 1999).

Damaged starch is a portion of the wheat-flour's total starch, dependent mostly on the density of the wheat kernel's endosperm and the milling process used to produce bread-flour (Irvine, 1975; Kent and Evers, 1994a; AACC International, 1999a; Cauvain, 2001). Excessive absorption of baking water occurs during mixing when the bread-flour has a level (%) of damaged starch greater than that recommended by international baking standards (Cauvain & Young, 2000; Barrera, Pérez, Ribotta & León, 2007). As the α -amylase digests damaged starch, it produces dextrans with a lower molecular weight, as compared to that of sound starch. The Water Holding Capacity (WHC) of dextrans are directly proportional to their molecular weight and degree of branching. When the damaged starch content of the bread-flour is too great, a sticky dough is produced, which comprises the bread quality as the product's crumb-structure, and porosity are strongly influenced by the WHC of dough produced.

Wheat-flour proteins

The composition and quality of wheat proteins often referred to as the flour's strength, directly influences the baked loaf's volume and crumb characteristics, including crumb-distribution, -density, -size, -firmness and resilience (Zghal *et al.*, 2001). In order to utilise the inherent characteristics of wheat proteins, Goesaert *et al.* (2005), reviewed the different wheat proteins in terms of their Osborne fraction, solubility, their composition, and their respective biological- and functional roles in bread dough formulations. The formation of a gluten-network is dependent on the amount of water absorbed by the flour and the quality- and quantity of its wheat flour proteins (Barak *et al.*, 2014; Ahmed and Thomas, 2015). The functional properties of gluten are dependent on non-covalent and hydrogen bonds as well as hydrophobic interactions (Schofield, 1986). Wheat proteins, glutenin and gliadin, determine the rheological properties of bread-dough (Hug-Iten *et al.*, 1999) and their respective quality and quantities determine the quality of the bread product formed (Vodovotz, 2007).

It has been determined that an increase in the ratio of hydrophilic to hydrophobic gliadins has a significant impact on the bread-making quality of a wheat-flour (Roels *et al.*, 1993; Shehzad *et al.*, 2013). The functional role of gliadin can be summarised as being quintessential to the elasticity and cohesive strength of the dough formed (Schofield, 1986). Increasing the ratio of gliadin to glutenin has undesirable consequences when it comes to the formation of a continuous gluten network. It

has been determined that this is due to the smaller molecular size of gliadin which is able to interfere with the formation of an extensive network of hydrated glutenin. The resulting protein network has a noticeable increase in extensibility, and a decrease in gas-retention during baking, translating into a bread product with a collapsed, dense pore- and crumb-structure.

When the gluten-network is developed, it proceeds to form a gluten-gel that behaves like hydrocolloid in water (Larsson, 1986). The gluten-gel is the result of hydrophobic interactions with lipids and absorbs water and swells until it reaches its absorption limit (Larsson, 1986). Polar lipids associate with the gluten-gel to form a lamellar phase, which acts as a membrane (Larsson, 1986). The gel and its membrane are disrupted during mixing to form a smaller bilayer, named liposomes, which aid in the development of gas cells with a strong gas retention capacity (Larsson, 1986).

Wheat-flour lipids

There are three sources of lipids that are commonly used in bread production, including endogenous wheat-flour lipids, shortening and surfactants (hydrocolloids) (Pareyt *et al.*, 2011). Even though the protein content of wheat flour is used to determine its baking potential, it is often overlooked that the interaction between wheat-proteins and lipids are also important for producing a quality loaf of bread (Rosell, 2011). Macmurray *et al.* (1970), described the relative abundance of the lipids that are naturally present in white bread-flour (Macmurray and Morrison, 1970).

Shortening is added to dough formulations in order to compensate for the germ-oils lost during the isolation of milling fractions that makeup bread-flour. The functional role of lipids in a bread-dough formulation revolves around their respective polarities and interaction with wheat-flour proteins. Glutenin binds more readily to glycolipids and gliadin bind more readily to phospholipids (Rosell, 2011). As a result, phospholipids aid in the viscosity of the dough whilst glycolipids aid in strengthening its gluten network. Polar-lipids are known to have a significantly positive effect on the dough quality parameters and volume of the bread product (Rosell, 2011). These polar lipids are able to align at gas-cell interface, increasing the extensibility of cell-walls, and consequently prevents coalescence of smaller gas cells to form voids in the proofing dough (Pareyt *et al.*, 2011). When outweighing the polar lipid concentration, within a dough formulation as a whole, non-polar lipids are detrimental to dough volume (Rosell, 2011).

Non-starch polysaccharides

Non-starch polysaccharides (NSP) account for all of the wheat-components, excluding for lipids and proteins, that are not bound *via* α -glycosidic linkages (Meuser and Suckow, 1986). These polysaccharides play an important role in the water binding capacity (WBC) of the wheat flour used to produce baked products (Meuser and Suckow, 1986). Non-starch polysaccharides are also known to associate with the wheat-proteins, specifically glutenin- β -sheets, during mixing (Fadda *et al.*, 2014).

Compounds in wheat flour which are classified as NSP include β -glucan(s), hemicelluloses, pentosans and gluco- and galactomannans (Meuser and Suckow, 1986). Glycoproteins are

generally classified as an NSPs as it consists of a very large polysaccharide portion, and a very small protein terminal (Meuser and Suckow, 1986). Pentosans is a collective term used for water-soluble NSP, and account for *ca.* 0.4 to 0.9% of the total yield of white wheat flour (Meuser and Suckow, 1986; Cauvain and Young, 2000). These water-soluble pentosans are made up of arabinoxylans (AX) and arabinogalactans (glycoprotein).

Arabinoxylans consist of an elongated backbone of D-xylopyranose monosaccharides, bound through β -(1→4) glycosidic bonds, that are able to branch from their C₂ and C₃ positions of the xylopyranose units, to bind with chains of L-arabinofuranose (Meuser and Suckow, 1986). The degree of branching influences the solubility of arabinoxylan, dependent on the interaction of the large molecule's side-chains within its current environment (Meuser and Suckow, 1986). Arabinogalactans are made up of glycopyranosyl and arabinose monosaccharides, bound together to form a linear backbone with several branched, linearly bound chains of arabinose monosaccharides which bind *via.* β -(1→3) and β -(1→6) to galactose (Meuser and Suckow, 1986).

Both arabinogalactan and arabinoxylan, when hydrated and agitated during mixing, are able to form a gel-like substance through a process termed oxidative gelation (Meuser and Suckow, 1986). As the name suggests, the gel formation is dependent on the presence of an oxidising agent in the bread formulation (Meuser and Suckow, 1986), most commonly incorporated as ascorbic acid.

During gelation the diferulic acid, a product of the oxidation of the ferulic acid within arabinoxylan, acts as a coupling-unit between its resident molecule and glycoproteins (Meuser and Suckow, 1986). The gel network produced is insoluble and consists of *ca.* 25% protein and *ca.* 75% arabinoxylan. It is inferred that *ca.* 0.15% of the flour's total mass consists of gel-able glycoproteins which constitute *ca.* 10% protein and *ca.* 90% arabinoxylan (Meuser and Suckow, 1986), although the amount of protein bound to arabinoxylan is still inconclusive.

The formed gel forms a membrane, surrounding the forming gas-inclusions during dough conditioning. This membrane sustains and improves the gas retention capacity of the dough (Meuser and Suckow, 1986) during resting, proofing and baking, improving the proof height and oven-spring of the dough- and baked loaf (Gray and Bemiller, 2003; Izydorczyk, 2009; Kwaśniewska *et al.*, 2014). The gel-membrane is not susceptible to heat degradation. This property is enabled by the membrane's ability to retain a small amount of bound water during baking, supplying the unstable gelatinised amylopectin with consistent hydration until its own deposit is depleted over time (Meuser and Suckow, 1986).

The insoluble NSP account for *ca.* 1.6 to 2.1% of the total yield of white wheat flour (Meuser and Suckow, 1986; Cauvain and Young, 2000). The insoluble NSP consists of polysaccharides made up of glucose and mannose units, as well as arabinoxylan with a greater frequency of branching than its soluble counterpart (Meuser and Suckow, 1986). The insoluble NSP swell when hydrated, simultaneously forming a deposit of bound water that is able to migrate towards the gelatinised starch during bread storage. This has been proposed to decrease the rate of starch retrogradation (Meuser and Suckow, 1986). Although this is beneficial to the baked product's shelf-life, if the insoluble NSP

fraction within the bread formulation is too great, it is detrimental to the quality of the resulting bread loaf's appearance and structure (Izydorczyk, 2009). It has been determined that this is possibly due to steric hindrance of the NSPs between the proteins involved in gluten formation and their affinity for available water (Izydorczyk, 2009). Kwaśniewska et al. (2014), concluded that the presence of both soluble- and insoluble arabinoxylan positively influences the baked product when the prevalence of soluble pentosans outweighed the prevalence of insoluble NSP (Kwaśniewska et al., 2014).

Minor formulation constituents

Saccharomyces cerevisiae, commonly known as baker's yeast, is a live microorganism that forms part of a lean bread-dough formulation (Kent and Evers, 1994b). Yeast is incorporated as either fresh yeast-cake or as dried instant yeast granules (FAO, 1947). Water solubilises the yeast during mixing, enabling it to metabolise the fermentable sugars it comes into contact with. Yeast metabolises fermentable sugars to produce CO₂(g) and ethanol (EtOH), essential to the increase in dough volume during proofing, and pore structure formation during baking.

All bread formulations contain sodium chloride (NaCl) or a suitable salt-mimicking compound (FAO, 1947; Kent and Evers, 1994b; Cauvain, 2001). Through ionising in water, sodium (Na⁺) and chloride (Cl⁻) -ions occupy binding sites along glutenin and gliadin, making it possible for hydrophobic interaction(s) between the two gluten proteins as they aggregate and start to form the gluten-network required for a functional bread-dough (Cauvain, 2009a). The addition of salt to dough formulations produces a more complex protein structure with hydrating wheat proteins (Beck *et al.*, 2012). In the absence of sodium-chloride or a sodium-chloride alternative, the flour-water mixture hydrates very quickly, at the cost of the gluten network's development (Avramenko *et al.*, 2018). Beck *et al.* used a Farinograph to conclude that decreasing the sodium chloride (NaCl) concentration in a dough formulation increases the WAC of the flour and baking absorption (BA) of the formulation as a whole (Beck *et al.*, 2012). The dough produced has an increased level of stability, flexibility and less stickiness compared to a dough made without salt (NaCl) (Linlaud *et al.*, 2009; Beck *et al.*, 2012).

Sucrose is a disaccharide compound that is composed of a glucose and a fructose monosaccharide, which is incorporated into bread formulations in the form of granulated sugarcane/beet sugar. Sugar is soluble in water and aids in the activation and proliferation of yeast cells, as it is an immediately available substrate for viable yeast cells to metabolise (FAO, 1947; Rosell, 2011). Due to sucrose being a reducing sugar, it is able to partake in the Maillard browning reaction, contributing to the formation of the characteristic toasted bread-crust (FAO, 1947). It has also been determined that increasing the concentration of sucrose within a dough formulation as a whole, interferes with the dehydration, and consequent retrogradation of gelatinised amylopectin (Hoseney, 1986).

After α -amylase cleaves the glucose-monosaccharides from the amylose-backbone, it leaves a reducing-end that is more hydrophilic in nature and available to take part in redox reactions within

the dough system's continuous phase. By including additional α -amylase into a bread formulation it is possible to delay the rate at which the dough's crumb starts to set during baking which is correlated with an increase in bread loaf volume.

Surfactants (polyglycols), referred to as dough-improvers, are hydrocolloids that have both a hydrophilic and hydrophobic region, which enable them to simultaneously interact with water, wheat proteins and starch components. When added to a bread-dough formulation, dough improvers promote dough quality and functional characteristics beneficial to the bread product's shelf-life (Goesaert *et al.*, 2005; Kwaśniewska *et al.*, 2014). Through interacting with wheat-proteins during mixing and binding to starch-polymers during baking, dough improvers are able to increase bread product quality by promoting distribution of moisture throughout the baking dough (Goesaert *et al.*, 2005). Lipase is a well-known dough improver, which increases the polarity of the wheat-flour lipids it comes into contact with, during mixing (Purhagen *et al.*, 2011).

Ascorbic acid is a dough improver and known fungicide. Ascorbic acid's anti-microbial activity has been determined to be the most effective additive at lower dosages, when compared to other preservatives such as propionic acid and calcium propionate (Kwaśniewska *et al.*, 2014). Ascorbic acid is added to bread formulations primarily as an oxidising agent, to promote oxidative gelation during mixing.

Soy-flour is a defatted flour made from soybeans (Vodovotz, 2007; Kwaśniewska *et al.*, 2014). The soybean-flour is still enzymatically active when added to bread formulations and it favours consumer acceptance by increasing the product's observed whiteness index (WI) (Vodovotz, 2007; Kwaśniewska *et al.*, 2014).

Water addition and mixing

The amount of water added in a dough formulation is determined using standardised rheological methods. A Farino- and Consistograph measure the WAC of the wheat flour as the change in the resistance of the dough against a mixing blade. These methods are repeated at multiple levels (water (g)/flour (g)) of water addition, in order to determine the optimum amount of water to incorporate as part of the dough formulation. The purpose of mixing is to hydrate and homogenise the bread formulation's ingredients (Cauvain, 2001). If this is not done sufficiently, due to the insufficient/excessive hydration and/or mixing of the ingredients, the resulting dough will not have the functional characteristics required to produce the desired bread quality (Cauvain and Young, 2000; Vodovotz, 2007; Rosell, 2011). The mixing action also incorporates air into the developing dough, which produces nucleation-sites for the carbon dioxide produced by yeast metabolism (Cauvain, 2001).

At the start of mixing, the low-moisture (*ca.* 10-15%) ingredients are homogenised, thereafter the water hydrates the monomolecular layer of the forming dough. Once *ca.* 60-65% of the water is added to the dry ingredients the first aqueous phase is formed, within which soluble formulation components are solubilised and dispersed as a consequence of mixing (MacRitchie, 1986). As the

rest of the water is incorporated, a second aqueous phase is formed (MacRitchie, 1986). This phase acts as a continuous medium for the transport of substrates required by chemical reactions, such as the metabolism of fermentable sugars to produce carbon dioxide (CO₂) and ethanol (EtOH) (MacRitchie, 1986). However, it is important to note there is no correlation between water mobility and the extent of mixing (Ablett *et al.*, 1986).

The temperature of the water and the temperature of the floury, low-moisture ingredients have a thermodynamic influence on the rate of the physical changes that occur during mixing. When water is at and above 20°C, its intramolecular hydrogen bonds are able to dissociate and form new intermolecular bonds with molecules in its immediate vicinity. The increased temperature of the water, acting as a solute, not only favours the rate of starch-granule swelling during BA but the rate at which amylase can process starch polysaccharides into smaller, less soluble starch moieties. The temperature of the water is also used as a means of yeast activation, by increasing the overall energy of the dough-system, through the incorporation of heat and kinetic (mixing action) energy, the activation energy required for chemical reactions to occur, is supplied during the processing of dough systems. The temperature of the water, when incorporated, should not be greater than 36°C, in order to not inhibit and/or cease yeast longevity (FAO, 1947).

Initially, the flour-water matrix has a pH of *ca.* 6, which is below that of glutenin- and gliadin's isoelectric point at pH 7.5 (Avramenko *et al.*, 2018). Consequently, the hydrophobic and largest portion of gliadins (*ca.* 55-95%) are encouraged to interact with the hydrophobic glutenin-proteins as they both repel water and proceed to aggregate (Roels *et al.*, 1993). The developed gluten-network predominantly consists of glutamine, proline and leucine amino acids which, through the incorporation of energy through mixing, become appropriately orientated to promote dough stability, extensibility and gas-retention capacity (Vodovotz, 2007; Shehzad *et al.*, 2013). The development of gluten and water acting as a solvent for ingredients is a quintessential step in producing a dough-matrix that will through consequential resting, proofing and baking produce a bread loaf with desirable quality and sensory characteristics (Cauvain and Young, 2000).

The ultimate viscoelasticity and extension modulus of the dough is determined by the degree of hydration of wheat-flour (Ablett *et al.*, 1986) and other formulation components. Increasing the content of water (%) in a bread-dough formulation increases the extent of the ingredients' plasticity (Ahmed and Thomas, 2015).

During an investigation of the baking absorption (BA) vs. mixing time (MT), Roels *et al.* (1993) concluded that the resulting bread volume is dependent on the amount of water added during mixing, the gliadin quality of the bread flour and the mixing time required to form a dough with desirable consistency (Roels *et al.*, 1993). A study by Gao *et al.* (2015), concluded that through only altering processing conditions, such as mixing time and speed combinations, the same formulation can be used to produce loaves of bread with different crumb-structures and textures (Gao *et al.*, 2015).

Baking absorption

Baking absorption (BA) is defined as the collective water absorption of the components within a white bread formulation, during mixing (Roels *et al.*, 1993; Goesaert *et al.*, 2005; Wang *et al.*, 2017). The WAC of the wheat-flour being used is thus a major contributor to the BA of the formulation. The BA is determined by a magnitude of factors, dictated by the wheat flour's composition and followed by mixing practices employed (Mani *et al.*, 1992; Roels *et al.*, 1993). Roels *et al.* (1993), investigated the relationship between BA and mixing time (MT) (Roels *et al.*, 1993). Through evaluating different levels of BA and different MT of six wheat flours from different cultivars, with standardised protein content, the varied water-addition levels were compared based on their effect on the bread dough's consistency. The authors concluded that the BA is directly proportional to the MT (Roels *et al.*, 1993). During mixing, the rate of baking absorption (BA), is significantly increased with the increase in the level of damaged starch within the wheat-flour sample (Roels *et al.*, 1993).

Increasing the level of water addition (%) to a dough formulation increases the bread product's crumb density if not accompanied by an increased mixing time (Haraszi *et al.*, 2004; Osella *et al.*, 2007). The BA of a bread-dough formulation can be altered through wheat-flour substitution. It has been determined to have a positive effect on the bread loaf's volume although it does not have a significant effect on the bread product's crumb-size or -density (Zghal *et al.*, 2001). During their investigation, Pühr *et al.* (1992), kept the amount of flour constant in each formulation, with varying levels of BA, which resulted in bread loaves with a decreased crumb-density (Pühr and D'Appolonia, 1992). It has been proposed that increasing the gluten-strength within a dough-formulation would be a suitable counter measure to curb the effect of an increased BA on the crumb-strength and resilience of the bread product (Zghal *et al.*, 2001; Shehzad *et al.*, 2013)

The quality of wheat-flour proteins influences the optimum mixing time of the formulation, and proofing- and baking time of the bread-dough formed (Li *et al.*, 2012). The successful development of a gluten-network is dependent on the combination of the availability of water and sufficient mixing (Li *et al.*, 2012). The gluten-network formed has a marginal influence on the dough development time (DDT), as measured by Farinograph (Haraszi *et al.*, 2004; Shehzad *et al.*, 2013). This suggests that there is a short time window when the gluten-network produced, can increase the BA of a bread-dough as its protein-network further strengthens upon exposure to energy, transferred from the mixer's blade(s).

Increasing the baking absorption of a bread formulation

The viscosity and extensibility of a bread dough are known to be influenced significantly by the level of water addition (%), referred to as baking absorption, and the water-soluble gliadin content of the flour used, referred to here as the flour's WAC (Mani *et al.*, 1992). The gliadin wheat-protein has a greater WAC than does its glutenin counterpart (Hug-Iten *et al.*, 1999; Barak *et al.*, 2014), consequently by increasing the total gliadin concentration within a dough formulation the BA of the formulation would increase. However, the addition of gliadin isolate would decrease the glutenin-to-

gliadin ratio within the dough formulation as an entirety, and so would require optimisation of the increase in gliadin concentration for the desired BA and intended micro-structural properties of the bread product.

The interaction of hydrocolloids with other formulation ingredients is driven by its polarity and molecular size, as well as the availability of unbound water. Hydrocolloidal compounds are usually amphiphilic and are able to interact and bind to other components in its direct environment, such as water, starch and proteins (Davidou *et al.*, 1996; Linlaud *et al.*, 2009; Fadda *et al.*, 2014). Hydrocolloids compete with gluten-proteins for available water and contributes to the increase in the BA of the dough-formulation. Xanthum gum (XG), and guar gum (GG) are two commonly used hydrophilic hydrocolloids. XG has a β -D-glucose backbone with tri-saccharide side chains and GG has a β -D-mannose backbone with a galactose side chain; galactose to mannose ratio of 2:1 (Linlaud *et al.*, 2009). Linlaud *et al.*, (2009), illustrated that substituting 1.5% of the bread-flour weight with these hydrocolloids, along with increasing the salt (NaCl) concentration with 2% (w/w) shows a synergistic relationship, significantly improving the BA, the mixing time required to reach the optimum dough consistency, dough stability and overall bread-dough functionality (Linlaud *et al.*, 2009).

The rate of endohydrolysis of the α -(1 \rightarrow 4)-D-glycosidic linkages, increases with the addition of α -amylase to the formulation, and so increases the rate at which amylose is cleaved into smaller amylose molecules, with an overall increase in amylose di- and tri-saccharides with reducing-terminals on their glucose backbone (Gray and Bemiller, 2003; Delcour and Hoseney, 2010d; Zhou *et al.*, 2011).

Wang *et al.*, (2017), investigated the effect on BA when bread-flour, in a white bread dough formulation, is substituted with Oat β -glucan concentrate at a 5% level (Wang *et al.*, 2017). The composite dough had a greater BA compared to the original formulation (Wang *et al.*, 2017). The authors used Farinographic results to illustrate a significant increase in BA from 59% to 67% (Wang *et al.*, 2017). It was concluded that the increase in BA significantly decreased the dough's gluten-network strength, stability and proof height of the dough (Wang *et al.*, 2017).

Hemdane *et al.*, (2017; 2018), investigated the bread-making qualities of a composite-flour, composed of 80% (w/w) bread-flour and 20% regular-bran (RB) (Hemdane *et al.*, 2017, 2018). Using H^1 -NMR, the effect of bran incorporation on water mobility, in both bread dough and product, was investigated (Hemdane *et al.*, 2017, 2018). The composite-flour had an increased WAC, which translated to a *ca.* 16% increase in BA of the dough (Hemdane *et al.*, 2017). The presence of RB modified the gluten-starch network, due to immobilising water away from the hydrating flour components (Hemdane *et al.*, 2018). Bran particles were determined to have aligned on the exterior of forming gas-cells, and so decreasing the gas-retention capacity of the dough (Hemdane *et al.*, 2017). The authors concluded that the composite-flour, significantly decreased the resulting bread's size and volume, consequently increasing the crumb-firmness and -density of the bread significantly (Hemdane *et al.*, 2018). The authors postulated that this was due to the dilution of bread-flour proteins due to the use of a composite flour. The particle size of the regular-bran was found to not

have a significant effect on the bread product's quality (Hemdane *et al.*, 2018).

Lu *et al.*, (2018), determined the effect of substituting 5%, 10% and 15% of bread flour in a bread formulation with white button, shiitake and porcini mushroom powder. The mushroom powder had a greater WAC than the flour, per gram (Lu *et al.*, 2018). They determined the effect on dough- and bread quality in terms of macro- and micro-structural properties of the bread product, concluding that the white button mushroom powder, at a substitution level of 5% of the bread-flour, resulted in an increase in BA of the formulation, with the least significant effect on bread loaf quality (Lu *et al.*, 2018). The mushroom powder significantly increased the BA by *ca.* 5.7% (gH₂O/100g flour) for the composite formulation, accompanied by an increase in dietary fibre- and protein content within the bread product (Lu *et al.*, 2018). The effects were determined to be as follows: The white button mushroom composite-flour's dough peak consistency (500 BU), dough development time (DDT), stickiness, adhesiveness and dough moisture content (%), as well as the height, gumminess (texture) and moisture content of the bread product all showed no significant difference from the 100% wheat-flour formulation (Lu *et al.*, 2018). The only significant difference between the two formulations in question, was determined to be the decrease in dough extensibility, possibly related to the dilution of the gluten-protein content through decreasing the percentage of wheat-flour (Lu *et al.*, 2018; Luo *et al.*, 2018).

Recently, Švec *et al.*, (2018), reviewed the effect on bread dough and product quality when substituting wheat-flour, with linseed fibre, at levels of 2.5% and 5% (Švec and Hrušková, 2018). Linseed fibre is a process by-product from linseed-oil extraction that has a particle size of *ca.* 500 to 700 µm (Sęczyk *et al.*, 2017; Švec and Hrušková, 2018). The authors concluded that linseed fibre, at a 5% level of substitution of the wheat-flour (w/w), significantly increases the BA of the bread formulation (Švec and Hrušková, 2018). As linseed fibre is composed of *ca.* 50% dietary fibre independent of its varietal origin, the increase in BA was attributed to the increase in total dietary fibre content of the formulation (Sęczyk *et al.*, 2017; Švec and Hrušková, 2018) The linseed fibre did however significantly decrease the extensibility and pasting properties of the dough as compared to the 100% wheat-flour formulation (Švec and Hrušková, 2018).

Hassan *et al.* (2013) concluded that the replacement of baking water with fermented skim milk, acidic cheese whey or buttermilk, all had an effect on the rheological properties of the resulting dough and quality of the bread product (Hassan and El-Shazly, 2013). All three alternative baking waters increased the BA of the bread formulation (Hassan and El-Shazly, 2013). The observed increase in WAC of the flour was attributed to the increased solute concentration of each of the alternative baking waters (Hassan and El-Shazly, 2013). However, all of the doughs produced from their respective alternative baking water, resulted in doughs with a decreased extensibility, resistance and resilience (Hassan and El-Shazly, 2013).

Dough conditioning

During mixing, the developing glutenin-network is hydrophobic in nature, and so the hydrophilic

constituents become redistributed as a function of the mobility of moisture within a dough's developing matrix. The occurrence, and rate of moisture migration within a resting dough, is dependent on the relative abundance of water in each of its phases including mobile-, bound and/or available water (Mani *et al.*, 1992). The solubility of arabinoxylans (AX) has been shown to increase when the dough is allowed to rest before being proofed. The increase in arabinoxylans' solubility is linked to the endoxylanase activity within the dough matrix (Rosell, 2011). Letting the dough rest, also favours the nucleation of yeast cells and their first stages of fermentation. The growth and regrowth of the gas-bubbles in bread-dough directly influences the resulting bread loaf's volume, crumb-structure and porosity (Rosell, 2011; Beck *et al.*, 2012).

The ability of a dough's matrix to retain carbon dioxide, CO₂(g), influences its ability to proof effectively (Barak *et al.*, 2014). The proofing of bread-dough, usually occurs in an artificial environment, with a relative humidity of *ca.* 80% and a temperature of 40°C±1°C (Cauvain and Young, 2000). These conditions favour the de-solubilisation of CO₂(g), which then leads to the expansion of yeast-nucleation sites, to form bubble-like structures filled with CO₂(g) (Cauvain and Young, 2000). If the bread-dough were to proof insufficiently, due to a lack of gas-retention or compromised proofing conditions, the bread product will deviate from its intended quality in terms of volume, crumb-density and overall appearance (Barak *et al.*, 2014).

Each growing bubble is encapsulated by the continuous gluten-gel. The bubble-structure of the dough gradually evolves during proofing along with the de-solubilisation of carbon dioxide (CO₂) which gradually increases the dough's volume (Rosell, 2011). After a rest period, the dough is typically reshaped to disrupt larger gas-bubbles, redistributing the retained CO₂(g) into smaller gas-cells (Hug-Iten *et al.*, 1999). The stability of the dough's gas-cell structure, prior-, during- and after proofing determines the stability of the bubble structure of the baking dough and consequently the volume and crumb-structure of the bread loaf (Rosell, 2011).

Baking

Glass transitions are second-order, time and temperature dependent transitions that are characterised by a change in state, but not in phase. Glass transitions of food matrix's occur within temperature ranges, and not specific temperatures (Goesaert *et al.*, 2005; Rahman, 2009). The glass transition temperature of bread-dough decreases as the amount of water added, during mixing of the formulation, increases (Ahmed and Thomas, 2015). The most notable glass transition during bread making is possibly the melting of amylopectin crystallites during hydration and baking, prior to gelatinisation (Bloksma, 1986; Hosoney, 1986; Delcour and Hosoney, 2010b).

Starch gelatinisation is a phase transition which is dependent on the sufficient availability of water. The gelatinisation of wheat starch is affected by the following parameters: pH, water- and dough temperature along with the abundance of salts and minerals within the baking water (Cauvain and Young, 2000). As the proofed dough is placed into the oven, the water within the confines of the dough-matrix starts to mobilise. The three significant temperatures of starch gelatinisation, that

represent the physicochemical changes of wheat-flour starch granules, are known as the initiation temperature, T_0 ca. 45°C, the peak temperature, T_P ca. 60°C and the conclusion temperature, at T_c ca. 75°C (Goesaert *et al.*, 2005; Delcour and Hoseneey, 2010a).

The baking dough has a soft continuous phase, which swells with the increase in the volume of unbound water (Ablett *et al.*, 1986). Starch gelatinisation is a granule-by-granule process and is dependent on the loss of birefringence of the starch granule, which is dependent on sufficient hydration (Delcour and Hoseneey, 2010e). During gelatinisation, a small change in water activity (a_w) is observed, indicating that the water that was absorbed/reabsorbed, was the result of redistribution of water (bound-, free-, and mobile) within the dough's baking matrix (Ablett *et al.*, 1986). The unbound water originates from the denaturation of protein that occurs, within the same temperature range as that of starch gelatinisation (Larsson, 1986), and water is momentarily available for absorption by starch granules (Thorvaldsson and Skjöldebrand, 1998). Whilst the unbound water is continuously mobilised from within the baking crumb-structure, it also condenses at the dough's coldest point, located just below its geometric centre, due to the temperature difference (Thorvaldsson and Skjöldebrand, 1998). This process repeats itself until all starch granules have completed gelatinisation, or the source of unbound water becomes depleted.

Once the dough has been transformed into a gelatinous mass, the crumb- and pore structure starts to take shape, similar to that of the final product's. When the internal temperature of the baking product is within ca. 80-100°C, its gas-phase gradually becomes continuous as the pore structure is established (Mills *et al.*, 2005). Unbound water vaporises, along with residual ethanol (EtOH) produced during yeast metabolism. The developing vapour pressure expands the dough's pore structure as the ethanol(g) and water(g) migrate towards the baking crust. Within the last stages of baking, the characteristic bread crust is formed. As the crust is more porous than the central crumb-structure, the residual mobilised vapours are able to escape into the oven's headspace.

Setback

Setback is a glass transition that occurs just as the freshly baked bread proceeds to cool. Setback starts to occur as the bread loaf is removed from the oven and its coldest centre cools from ca. 95°C to ca. 30°C, whilst firming the loaf crumb-structure as the baked product cools down further. This occurs due to the rapid retrogradation of amylose, until it reaches room temperature, ca. 25°C (Delcour and Hoseneey, 2010d; Rosell, 2011). Lind *et al.*, (1991), determined the desorption isotherms of white bread crust as the white bread product proceeded to cool from ca. 90°C to ca. 30°C (Lind and Rask, 1991). The authors concluded that as setback occurs, moisture migrates from the internal crumb-structure towards the crust (Lind and Rask, 1991). As a consequence the moisture content of the baked bread does vary until setback has completed at ca. 30°C.

Bread product quality and shelf-life

The baking time- and temperature combination, as well as the shape of the dough and/or baking pan, determines the amount of moisture left in the final baked product (Ablett *et al.*, 1986). The

moisture content of the bread product directly influences its structural quality, texture and shelf-life stability (Ablett *et al.*, 1986). And so the optimisation of mixing, dough conditioning and baking conditions have been studied and correlated with an increase in bread product quality and its shelf-life resilience (Jahromi *et al.*, 2014). The principle of flour-quality and optimum water addition along with the duration of mixing, resting, proofing and baking time are all considered to be effective methods to increase the shelf-life of the bread product produced (Gray and Bemiller, 2003; Purhagen *et al.*, 2011; Lu *et al.*, 2018).

Processing aids and additives are incorporated into bread formulations in order to increase dough functional characteristics, improve processing efficiency, conserve sensory-, and nutritional quality whilst promoting product quality as the bread product proceeds to age. Purhagen *et al.* (2011), emphasised the benefit of adding α -amylase to a bread dough formulation; these benefits include increasing the moisture retention of the bread's micro-structure, through decreasing the rate at which complex retrograded amylopectin networks are formed (Purhagen *et al.*, 2011).

Pareyt *et al.* (2011) emphasised that increasing the overall polar-lipid concentration, in a dough formulation, benefits the dough matrix's gas retention capacity, consequently promoting the stability of the bread product's micro-structure and its WHC (Pareyt *et al.*, 2011).

Buera *et al.*, (1998), determined the adsorption isotherm of a white bread at 26°C, as well as the effect of moisture content (%) on the initiation (T_0) and conclusion (T_c) glass transition temperatures of the white bread loaf (Buera *et al.*, 1998). The sorption isotherm of bread at this temperature follows a Flory-Huggins (Type 3) shape (Andrade *et al.*, 2011). As starch gelatinisation is reversible to the point where starch retrogradation occurs, the adsorption isotherm calculated for a bread product, can be used to illustrate that during starch retrogradation, moisture is redistributed within the bread product itself.

The outskirts of a loaf, referred to as its bread-crust, can be seen as a secondary moisture transfer zone. The moisture migration within the bread's micro-structure, that contributes to micro-structural changes of the bread-crumbs, can be divided into two transfer zones, namely: between the crumb and crust, and between the crust and direct atmosphere (Purhagen *et al.*, 2011; Monteau *et al.*, 2017). Monteau *et al.* determined that the total loss of moisture, that occurs during bread staling is accounted for by 75% of the water vapour being transferred to the atmosphere surrounding the bread loaf, and 25% of the vapour eventually gained by the crust. The vapour migrates through the bread's internal pore-structure, building up enough vapour pressure for the majority of the water vapour to move through the micro-structure of the upper crust's structure and into the atmosphere outside the bread product (Monteau *et al.*, 2017). The 25% can be accounted for by the condensation that occurs when the water vapour is continuously transferred into the crust and is unable to migrate into the environment surrounding the bread product (Monteau *et al.*, 2017). This also explains how dehydration of the crumb and the softening of the crust can occur simultaneously during bread storage (Choi *et al.*, 2010; Monteau *et al.*, 2017; Morren *et al.*, 2017).

Fadda *et al.*, (2014), concluded that the main causes of bread-staling are as follows: amylopectin

retrogradation, water redistribution, the effect of starch-gluten interactions and in some instances due to the wheat-proteins competing with NSPs for water during dough mixing (Fadda *et al.*, 2014).

The staling of a bread is a consequence of the rate of decrease in the WHC of the bread's crumb-structure (Leung *et al.*, 1983; Zeleznak and Hosenev, 1996; Hug-Iten *et al.*, 2003), which determines the rate of moisture redistribution, and crumb-firming as the product's shelf-life progresses. The homogeneity of the bread loaf's crumb- and pore-structure is correlated to its WHC (Cauvain and Young, 2000; Mondal and Datta, 2008). The combination of the effects of moisture-loss and redistribution, along with amylopectin regaining its birefringence during starch retrogradation, is collectively referred to as bread staling (Zeleznak and Hosenev, 1996; Vodovotz, 2007; Purhagen *et al.*, 2011; Fadda *et al.*, 2014; Monteau *et al.*, 2017).

Optimising the bread-dough formulation, and each stage involved in the breadmaking process (Roels *et al.*, 1993) has been determined to be more effective than the addition of starch-acting, anti-staling agents (Purhagen *et al.*, 2011) to the bread's formulation. And so, it is hypothesised that the migration of water vapour is favoured by an open pore-structure, attributed to the lack of condensation that occurs at the crumb-crust interface of the bread product.

The cell-walls of pores in the bread loaf's foam-like structure are formed as a result of esterified arabinoxylan (Li *et al.*, 2012). Michniewicz *et al.*, (1992), hypothesised that NSPs, such as arabinoxylans, interfere with the aggregation of amylose chains during product storage, through promoting the water holding capacity (WHC) of the crumb (Fadda *et al.*, 2014) and so promotes the product's quality across its shelf-life (Michniewicz *et al.*, 1992). By increasing the WHC of a bread product, the rate of moisture loss and starch retrogradation during bread loaf ageing is decreased (Fadda *et al.*, 2014).

Starch retrogradation

Amylopectin regains its birefringence during the ageing of bread. The rate of retrogradation is determined by the rate of moisture migration primarily due to hysteresis (Hosenev, 1986; Gray and Bemiller, 2003; Vodovotz, 2007). It is hypothesised that the hysteresis taking place during bread ageing, can be attributed to a phenomenon known as capillary condensation (Andrade *et al.*, 2011). The rate of starch retrogradation is strongly correlated to an overall decrease in the bread-crumbs' WHC and moisture content (Hosenev, 1986).

Moisture migration and redistribution

Through the use of Texture Analysis (TA) and Differential Scanning Calorimetry (DSC), Purhagen *et al.*, (2008), determined that the loss and migration of water (moisture) has a greater influence on the staling of bread than does the occurrence of amylopectin-retrogradation (Purhagen *et al.*, 2008). As the shelf-life period of a bread product progresses, the moisture within its crumb-structure becomes redistributed in a process referred to as moisture migration (Czuchajowska and Pomeranz, 1989; Buera *et al.*, 1998).

The interface between the crust and the surrounding atmosphere has been determined to be

where the greatest rate of moisture loss occurs (Monteau *et al.*, 2017). The moisture migration occurs due to a favourable water vapour gradient within the bread product, which aids in the redistribution of water from the crumb, with a greater initial moisture content, to the crust, with a lower initial moisture content (Czuchajowska and Pomeranz, 1989; Thorvaldsson and Skjöldebrand, 1998).

The water entrapped within the structural confines of the bread product is able to soften the food foam as it ages, due to water's ability to plasticize glassy polymers found within the microstructure of bread (Ablett *et al.*, 1986). The water within the bread product has a high thermodynamic activity (>95%), enabling the water to migrate freely through the crumb-structure of a bread-foam as long as the favourable chemical potential gradient exists within the bread's structural confines (Fessas and Schiraldi, 2001). As the different polymer phases within the bread product become increasingly incompatible as the bread product ages (hours, days) the polymers can utilise their water's thermodynamic activity to aid in conformational and phase changes such as amylopectin steadily regaining its birefringence (Vodovotz, 2007).

Conclusion

The physical state(s) and quantity of water within, and in the direct environment of bread formulation components have an immediate effect on the appearance, texture and shelf-life of the bread product. The composition and amount (% w/w) of the water used, influences the behaviour of water as a solvent and plasticizer, thereby affecting the glass-transitions taking place within the dough during baking, cooling and the product's shelf-life.

The moisture that is able to migrate from within the dough structure, to its external environment, is accounted for by unbound/available water. After baking, there are no more physicochemical changes that require an external source of moisture. All physical changes within the bread product's structure are due to the redistribution of moisture, dependent on time and temperature conditions within its direct environment.

Without water, a bread formulation consists of a strange, out-of-place list of ingredients, with their individual composition and physical properties. Water is the golden thread that gives functionality to bread formulation components. The interaction between wheat bread-flour components, water and other formulation ingredients are influenced by the mixing time and its influence on the BA of the formulation, along with the time and temperature combination of both the proofing and baking stages.

Increasing the BA of a bread dough-formulation, through slight formulation adjustments and/or total mixing time, would have a lesser effect on the bread product's quality than would decreasing the amount of water added during mixing. When a composite-flour consists of less than 95% bread-flour the total gluten-protein fraction is significantly diluted, producing a bread product with inferior structural characteristics and quality across its shelf-life. Instead of using a composite-flour, which dilutes the original concentration of the gluten-network proteins in the dough-formulation, using an alternative liquid is a viable means of increasing the formulation's BA. Very little research has been

completed with the objective of determining the effect, of using an alternative baking water on the quality of a white bread product.

Whilst water is essential to producing a bread product, its behaviour during the progress of the product's shelf-life, determines the product's keeping quality. The phenomenon known as bread staling is the consequence of the combination of starch retrogradation and moisture migration, which are both driven by the loss of the WHC of the bread's crumb-structure. During the first few hours of the bread loaf's shelf-life, a water-vapour gradient is established between the higher-moisture zones within the loaf, towards the lower-moisture zone of its enveloping crust. The moisture gradient is also utilised by the starch-granules within the bread's structure, to regain its birefringence. starch retrogradation

The rate of bread staling can potentially be optimised by improving the WHC of the bread's crumb-structure, which has been correlated to the homogeneity of its crumb- and pore- distribution. The WHC of the bread product's crumb-structure is dependent on the BA of the dough-formulation which can be optimised through the use of a quality bread-flour, dough-improvers, composite-flours and/or the use of an alternative baking water. An alternative baking water would need to contain compounds such as NSPs, α -amylase and/or fermentable sugars, which are all known to improve the BA of a bread dough-formulation, and as a consequence improve the WHC of a bread's crumb-structure.

Chapter 3

Materials and Methods

BSG-supernatant extraction

The BSG from two separate ale beer batches, of the same beer formulation, consisting of 1000 kg BSG each, were obtained from the Newlands Spring Brewing Company, in Newlands, South Africa. A 200 kg sample from each batch was used for the extraction of the liquid fraction from the BSG (**Figure 1**).

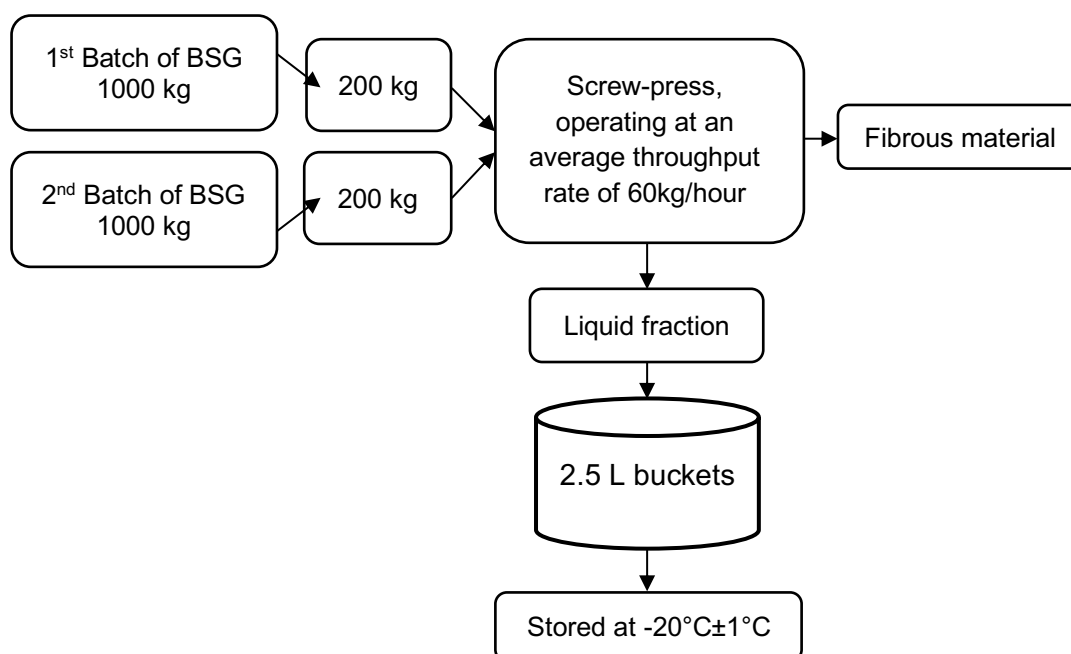


Figure 1 A schematic representing the process of extracting the liquid-fraction within BSG, using a screw-press.

In order to minimise potential contamination during transportation, the BSG, from each batch of beer, was sealed in a sanitised square plastic container. The BSG was transported, within 10 h of being produced, to the Department of Process Engineering, at Stellenbosch University. Both batches of BSG arrived within twenty-four hours of each other. The liquid fraction of the BSG was then subsequently extracted using a continuous screw press (NEW eco-tec Verfahrenstechnik GmbH, Mühldorf, Germany) with a 0.3m long x 0.15m diameter screen cage (2.2 kW three-phase motor).

A total of 400 kg BSG was processed, made up of equal 200 kg samples from each batch of BSG. The fractions separated during screw-press extraction consisted of the fibrous material and the liquid fraction, which included *ca.* 25% of fine particulate sediment. A 50 L liquid sample was then carefully sealed into sterilised 2.5 L plastic buckets, and stored in a walk-in freezer, kept at $-20^{\circ}\text{C}\pm 1^{\circ}\text{C}$, at the Department of Food Science, Stellenbosch University, South Africa. The final sample preparation step, preceding a replicate of bread sample production, was to defrost four 2.5 L buckets, over 3 h

in a water bath, set at $21^{\circ}\text{C}\pm 1^{\circ}\text{C}$. The water-bath was used to enable homogenous defrosting of the BSG-liquid sample. Thereafter, the following was repeated twice: The contents of two buckets were decanted into a 5 L sterilised plastic jug, and the undissolved solids were allowed to settle, to the bottom of the jug, for 10 min.

Thereafter the top fraction, ca. $3.5\text{ L} \pm 0.2\text{ L}$, was decanted into two sanitised 2 L plastic bottles and stored at 4°C , for no longer than 24 h prior to its incorporation into its designated bread batch (**Figure 2**).

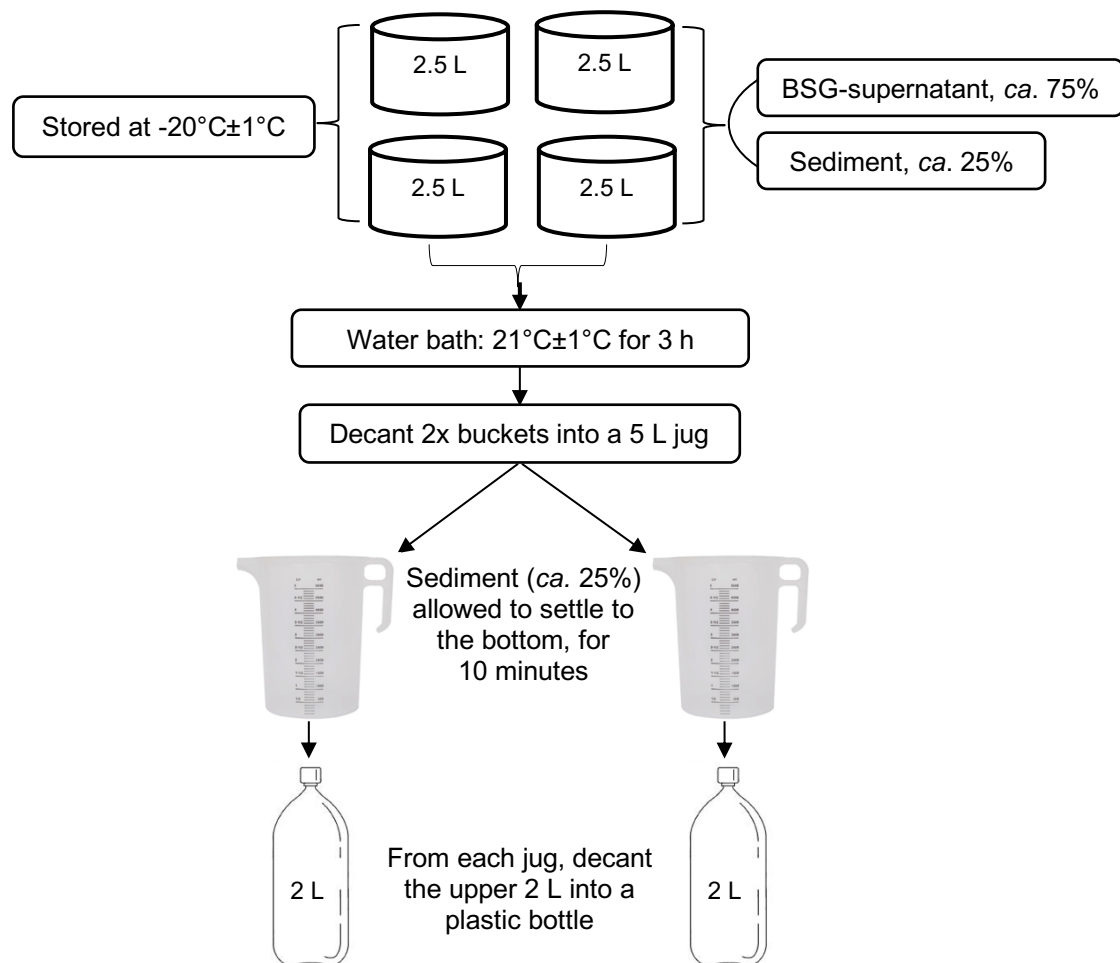


Figure 2 BSG-supernatant sample preparation: Defrosting the BSG-liquid and separating it into its liquid and solid fractions. The two bottles are each designated to a BSG-supernatant bread-formulation batch. In total, this process was repeated three times, once for each replicate of the experimental design, ca. 24 h before bread sample production.

Proximate and compositional analysis

The proximate analysis of BSG-supernatant was performed using the following methods of analysis: Moisture content (%) (AACC: 44-15.02), Protein (%) (AACC: 46-30.01), Total Dissolved Solids (%) (AACC: 44-15.02), Ash (%) (AACC: 08-02.01), °Brix using a refractometer (AACC: 80-51.01) and acidity/alkalinity using Hydrogen-Ion Activity (pH) - Electrometric Method (AACC International,

1999b,c,d,e).

In order to determine the composition of the BSG-supernatant, High-Performance Liquid Chromatography (HPLC) was employed (**Table 1**). The sample preparation included defrosting each supernatant sample, the homogenisation thereof, after which an aliquot of 25 mL, for each replicate, was filtered through a 0.2 µm nylon membrane. The filtered liquid was then hydrolysed using sulphuric acid (H₂SO₄), including a fifteen-minute incubation at 121°C.

Table 1 HPLC analysis specifications and conditions

HPLC specification	Unit
Column	Aminex HPX-87H Ion Exclusion Column with a Cation-Hydrogen cartridge
Mobile phase	5 mm** sulphuric acid
Flow rate	0.6 mL/min
Temperature	65°C
1 st Detector: sugar-compounds	Refractive Index (RI)
2 nd Detector: hydrolysis by-products	Ultra Violet (UV) detector set at 220 nm → 280 nm

*High Performance Liquid Chromatography

**millimolar

Wheat-flour production

The bread-flour production and rheological analyses were completed at the Research and Development Laboratory of Sasko Mills in Paarl, South Africa.

Whole wheat kernels were sourced locally from Bethlehem and Malmesbury. A total of 70 kg of wheat (18 kg Malmesbury with 52 kg Bethlehem) was homogenised using a Boerner Divider and cleaned using a Carter Day Dockage Tester. The grade of the wheat used, was determined using Near Infrared (NIR) spectroscopy (Perten IM9500) (AACC International, 2017; SAGL, 2018) on whole-wheat kernels.

The wheat was divided into batches of 5 kg to 10 kg, thereafter enough distilled water (dH₂O) was added to the wheat, to reach a moisture content of *ca.* 15.5% after 24 h of tempering. The tempered wheat was then milled to produce bread-flour, using a Bühler Mill (MLU-202, six stream), according to the standardised AACC method, 26-22.01 (AACC International, 1999a).

The wheat-flour was specifically produced for this investigation, in order to rule out the effect of treatments and/or fortification applied to commercial bread-flour. The bread-flour was used within a month of milling, and stored at 15°C in airtight, plastic containers during the period leading up to bread sample production.

Proximate analysis

Proximate analysis of the wheat-flour was completed at the same location as the wheat-flour production. The moisture content of the flour was determined using the convection oven method (AACC-method: 44-15.02) with a Chopin Laboratory Oven (AACC International, 1999b). Protein content (12_{mb}%) was determined using the combustion analysis method (AACC: 46-30.01), through

the use of a Dumatherm (Dumas Analytical System, C. Gerhardt-Analytical Systems, Dijkstra Vereenigde, Nederland) instrument (AACC International, 1999c). The ash content of the flour was determined using the muffle-furnace method (AACC International, 1999d).

Rheology

The analyses that accommodated the replacement of water with BSG-supernatant, included the Farinograph (AACC International, 2011), Mixograph (AACC International, 1999g), Falling Number (AACC International, 1999h) and Rapid Visco Analyser (AACC International, 2009). The bread flour was further characterised using an Alveograph (AACC International, 1999i), and Starch Damage analyses (AACC International, 2007).

Breadmaking process

The bread formulation ingredients, other than the wheat-flour and BSG-supernatant, were sourced and supplied by Anchor Yeast Head Quarters, at their baking laboratory/facility in Johannesburg, South Africa. For each batch of bread formulation prepared, the flour-, water- and dough's temperature, as well as the mixing-, resting-, proofing- and baking time were recorded (**Table 2 & 3**).

The BSG-supernatant required subtle heating to *ca.* 27°C, achieved through immersing it within its sealed container, into a water bath set at 40°C. The dry ingredients including wheat-flour, yeast, salt, sugar, shortening, ascorbic acid and alpha-amylase (**Table 2**), were all added to the mixer's (Morton Mixer) bowl. The temperature(s) of the dry ingredients were recorded (**Table 3**). The temperature of the water source, either water or BSG-supernatant, was adjusted in order to reach the recommended dough temperature of *ca.* 28°C. There after the water was added to the dry ingredients in the mixing bowl. The ingredients were homogenised for 2 min on the mixer's slow-speed and mixed for a further 6 min on the mixer's high-speed. Thereafter the large dough-mass was portioned into 770 g dough balls, using a laboratory scale. The dough-balls were rounded by hand and placed on a floured countertop surface.

The dough was covered with a plastic sheet and allowed to rest for 10 min at ambient temperature, *ca.* 25°C. After the resting period lapsed, the dough was kneaded evenly by a dough sheeter, to disrupt large gas-bubbles. After sheeting, the dough was rolled into a sausage-like shape and placed fold-side down into a lightly greased bread tin (280 mm length x 110 mm height x 110 mm width). The bread tins were placed into a proofer with a relative humidity of 80±2% and temperature of 41°C±1°C for 55 min. There after the bread tins were removed from the proofer-oven and placed into a preheated, industrial bread oven to bake for 27±2 min at 210°C±5°C.

The breads were removed and placed onto a drying rack until cool enough to remove from their baking tins. The bread samples were allowed to cool, at ambient temperature, *ca.* 25°C, until an internal temperature of less than 30°C was reached. Finally, the samples were placed into their labelled, transparent sachets, sealed and stored at room temperature until their analyses on shelf-life days 2, 3 and 4 post-baking.

Table 2 Details of the bread formulation(s) used during the baking of bread samples

Ingredients*	Bread formulation	Scaled weight (g)
Bread-flour (14% _{m.b.}), %	100	2000
Water**, %	61	1220
Fresh compressed yeast, %	2.6	52
Salt (NaCl), %	2	40
Sugar, %	1.0	20
Shortening (fat), %	0.25	5
Soy-flour, %	0.2	4
Ascorbic Acid, %	0.008	0.16
Fungal α -amylase, %	0.0007	0.014

*% flour weight(g)

**potable water for *control* formulation, BSG-supernatant for *treatment* formulation

m.b. Moisture basis

Table 3 Parameters that were recorded for each batch of bread formulation

Parameter	
Scaling weight for dough, g	770g
Flour temperature, °C	19°C*
Water temperature, °C	24°C \leq water _{temp.} \leq 30°C
Mixing time, min**	8
Dough Temperature, °C	27°C \leq dough _{temp.} \leq 30°C
Resting time, min**	15
Proof time, min**	ca. 55
Oven temperature, °C	220
Baking time, min**	30
Pan height, mm***	110
Baked Loaf Yield, per formulation	four, ca. 700g each
Bread Loaf Parameters	
Bake Height, mm***	Loaf height (mm)
Oven Spring, mm***	= Bake Height (mm) – Oven Spring (mm)

*averaged value from twelve batches

**minutes

***millimeter

Bread micro-structural analysis

The crumb-structure and porosity of the bread was collectively evaluated as the micro-structure of the bread's foam structure. The same bread was used for both Texture Analysis (TA) and C-Cell Visual Analysis (VA) on the second, third and fourth-day of the bread's shelf-life.

C-Cell Visual Analysis

The quality of the loaves, from both formulations, were analysed using a C-Cell digital image analyser (Calibre Control International, Warrington, UK). On each shelf-life day, a bread loaf from each batch was sliced using a Graef 182 Master slicer (Graef GmbH & Co. KG, Arnsberg, Germany) to slices with 12.5 mm thickness, according to industry standard. The bread samples were kept in transparent sachets, after cooling to ambient temperature *ca.* 25°C). On Days 2, 3 and 4 after which allocated bread samples were analysed with the C-Cell VA and then placed back into the sample's labelled sachet until texture analysis. This process lasted no longer than 20 minutes for each bread sample analysed.

Level 1	<i>Bread formulations:</i> Control and Treatment								
Level 2	<p><i>Batch replicates, per formulation:</i> Rep 1: 4 Bread samples Rep 2: 4 Bread samples <i>Bread sample designation</i></p> <p><u>Bread #1</u> The same bread sample is used for all shelf-life day analysis through X-ray scans as it is a non-destructive method</p> <p><u>Bread #2, #3 and #4:</u> Per shelf-life day of analysis, one loaf is used per batch-replicate of each formulation for both C-Cell VA (10 x 1 slice) and Texture Analysis (5 x 2 slices)</p>								
Level 3	<p><i>Shelf-life quality determination: order of analysis</i></p> <table border="0" style="width: 100%; text-align: center;"> <tbody> <tr> <td><u>Day 0:</u></td> <td><u>Day 2:</u></td> <td><u>Day 3:</u></td> <td><u>Day 4:</u></td> </tr> <tr> <td>Bread sample production</td> <td>C-Cell VA Texture Analysis X-ray Scan</td> <td>C-Cell VA Texture Analysis X-ray Scan</td> <td>C-Cell VA Texture Analysis X-ray Scan</td> </tr> </tbody> </table>	<u>Day 0:</u>	<u>Day 2:</u>	<u>Day 3:</u>	<u>Day 4:</u>	Bread sample production	C-Cell VA Texture Analysis X-ray Scan	C-Cell VA Texture Analysis X-ray Scan	C-Cell VA Texture Analysis X-ray Scan
<u>Day 0:</u>	<u>Day 2:</u>	<u>Day 3:</u>	<u>Day 4:</u>						
Bread sample production	C-Cell VA Texture Analysis X-ray Scan	C-Cell VA Texture Analysis X-ray Scan	C-Cell VA Texture Analysis X-ray Scan						

Figure 3 Replicate design for bread sample production for each respective analysis. This design was repeated three times, over a period of three weeks (21 days).

To scan the slices using the C-Cell instrument, each slice was individually placed into the drawer of the instrument. The drawer is designed in such a way that it is impermeable to external light. Thereafter the instrument's sensitive camera was enabled to capture an image for consequent analysis by the instrument's accompanying software. This was repeated until ten slices of each bread loaf had been scanned/imaged. The instrument's accompanying software (C-Cell Colour, Version 3) then analysed the images captured during each slice's scan, to extract quantitative data in the form of slice parameters.

The parameters measured during C-Cell analysis were as follows: Slice Area, Total Concavity (%), Slice Brightness, Number of Cells, Number of Holes, Area of Holes and Cell Diameter. The following parameters were also considered to further evaluate the effect of replacing the baking water within a lean dough formulation, with BSG-supernatant: Colour variables L^* , a^* and b^* , Volume of Cells, Coarse Cell Volume, Cell Wall Thickness, Volume of Holes, and Cell-Alignment.

Texture Analysis

The extent of bread-staling parameters, firmness and resilience, were analysed on days two, three and four using a TA.XT.plus Texture Analyser (Stable Micro System, Godalming, Surrey, United Kingdom) with its aluminium, cylindrical probe (35 mm diameter). The method was completed using a modified version of the approved AACC method, 74-09 (AACC, 1999). Two slices (2 x 12.5mm thickness) were placed on the instrument and the cylindrical probe descended to 60% of the original sample height, remaining there for two seconds prior to its retraction. The firmness was measured, by the cylindrical probe, as the amount of force (g) required to compress the two bread slices to 60% of its initial height. The resilience was calculated by dividing the final height (post-compression) by the initial height to determine the percentage recovery of the bread-structure after being exposed to compression.

X-ray micro-Computed Tomography

To stabilise the bread loaf during the image acquisition (scanning) period within the X-ray unit (General Electric Phoenix V|Tome|X L240 X-ray μ CT scanner) each bread loaf was placed on a florist sponge at a 60° angle, to house the bottom-end of the bread loaf. In order to minimise artefacts within the scan, the bread was kept within its plastic transparent sachet across shelf-life days two, three and four. The reference disc was embedded into the florist sponge used to support the bread sample. The disc was composed of a polytetrafluoroethylene (PTFE) polymer (10 mm thickness and 25 mm diameter) with a density of 2.5 g/cm³, obtained from Maizey Plastics (Cape Town, South Africa). Each prepared bread sample was placed into the X-ray unit and scanned using the parameters in **Table 4**. The first phase of processing a scan of bread was to reconstruct the 2D-images into a 3D-rendered scan, using the system-supplied Datos reconstruction software (Datos|x® 2.1, General Electric Sensing & Inspection Technologies GmbH, Phoenix, Wunstorf, Germany).

The process of image reconstruction enabled the rendering of a 3D-sample representation. The 3D-sample was produced using the thousands of 2D-images obtained during the X-ray scanning of each bread sample, and a Datos reconstruction software package (Datos|x® 2.1, General Electric Sensing & Inspection Technologies GmbH, Phoenix, Wunstorf, Germany) powered by a specialised desktop computer. The software (Datos|x® 2.1), reconstructed the 2D X-ray projection images, collectively referred to as image-stacks, into a 3D-volume made of individual voxels (three-dimensional pixels) that were mapped according to a 16-bit grey-value scale.

Table 4 Summary of X-ray μ -Computed Tomography scan parameters used for image acquisition of all bread samples

Units	Parameter
Voltage (kV)	180
Current (μ A)	150
Magnification	1.25
Pixel size in the X- and Y axes (mm)	0.16
Number of pixels in the X- and Y axes	2000
Resolution/Voxel Size (μ m)	160
Spot size (μ m)	~2400
Scan time, per image (ms)	666.2
Total scan time, per sample (min,s)	31 min 5 s
Original image greyscale intensity resolution	16-bit
Grey levels	$2^{16} = 65536$
Number of 2D images, per Bread sample	2800
Image acquisition time (ms)	333.1
Rotation sector ($^{\circ}$)	360

When the 2D-images were reconstructed into 3D-sample(s) it was loaded onto a desktop computer powering the VGStudio (Volume Graphics GmbH, 69115 Heidelberg, Germany V 3.1 © 2001-2017) software package. In order to isolate and extract the Volume of Interest (VOI) from the 3D reconstructed sample, a series of functions from the VGStudio software were applied. These functions are based on complex algorithms and were applied to the original sample volume in the following order: *Adaptive Gauss* filter, *Normalise Gradient* of the sample volume's surface brightness, Object Surface Determination establishing the boundaries of the VOI isolated from the original scan's volume. The bread sample's perspectives (front, top, sagittal and 3D) in the software platform were registered so that all vertical sides of the sample were perpendicular to the (x)-axes.

In order to remove all remaining artefacts from the bread's scan volume, Regions of Interest (ROI) were used to exclude all voxels outside of the bread-volume in order to capture and analyse only the bread-sample material and the air entrapped within it as part of the bread sample's foam-like structure. Through the use of eroding-and-dilating the ROI, from which the VOI is extracted, it was possible to extract the bread VOI and exclude external voxels that weren't part of the bread sample. The surface determination function enables the software to realise the boundaries of the VOI for Object Information calculation.

The process of extracting quantitative data from the three-dimensional rendered volume of each sample, was accomplished through the isolation of the bread-sample from any artefacts recorded during sample scanning. The segmentation of ROI for analysis enabled the comparison of the inner and outer-most regions of the bread loaf sample (Error! Reference source not found.).

The following equations were employed in order to transform the quantitative data acquired,

through initial sample-volume processing, into other sample parameters of interest. These included determining the (1) Relative Density (g/dm^3), and (2) Sample porosity (%).

$$\frac{\text{Mean greyvalue of VOI}}{\text{Mean greyvalue of polymer reference disc}} \times \text{density of polymer disc} \left(2.5 \frac{\text{g}}{\text{dm}^3}\right) = \text{Relative Density} \left(\frac{\text{g}}{\text{dm}^3}\right) \quad (\text{Eq. 1})$$

$$\frac{\text{Volume of air (mm}^3\text{)}}{\text{Total sample volume (mm}^3\text{)}} \times 100\% = \text{Porosity (\%)} \quad (\text{Eq. 2})$$

The X-ray μCT analysis of bread samples, consisted of two levels of bread loaf VOIs (**Figure 3**). The first being the whole loaf Volume of Interest (VOI), referred to as the *Bread VOI*, and the second consisting of a reconstruction of four individual VOIs, referred to as the *Bread sample VOI reconstruction* (**Figure 6**). The segmentation of the 3D Bread volume was completed in order to analyse sub-samples of each of the bread sample. The sub-samples consisted of four individual VOI's, including the Top Crust, Bottom Crust, and two Slices (1 & 2).

The microstructural analysis was performed on the Bread sample VOI reconstruction volumes using an additional function of the micro-Computed Tomographic analysis and image processing software termed Foam Structure Analysis (Volume Graphics, 2017). The bread volume's foam-like structure was analysed using this function, in order to quantify and investigate the changes in the sample's crumb density and microstructural properties, due to the replacement of the baking water in a lean dough formulation with BSG-supernatant.

Table 5 Parameters calculated and recorded, for each VOI including: whole bread sample and all VOI's part of the *Bread sample VOI reconstruction*

Dimensions of VOI	Units
Dimensions (voxels)	(x, y, z)
Resolution	mm
Voxel Count	-
Dimensions (x, y, z)	mm
VOI surface area	mm^2
Total Volume	mm^3
Volume of Material	mm^3
Volume of Air	mm^3
Grey value distribution	
Minimum	-
Mean	-
Maximum	-
Standard deviation	-

The isolation of the four VOIs that form part of the Bread sample VOI reconstruction enabled the processing of smaller volumes within each bread samples. This is beneficial to the computing-power required to analyse the bread-sample in detail, using algorithms present in the VGStudio software package. In order to segment the bread samples in the exact same locations, *Instrument* templates were setup using the VGStudio software in order to decrease operator related variance when constructing the *Bread sample VOI reconstruction* of four smaller VOIs, including the *Top-crust* and *Bottom-crust* and *Slice 1* and *Slice 2*. These templates were constructed for the precise segmentation of the *Bread VOI* into its four smaller volumes. The distance from the top of the top-perspective, for *Slice 1* at 75.00 mm and *Slice 2* at 180.00 mm selection. The *Top Crust* was measured at a thickness of 25.00mm from the very top of the bread sample, and the *Bottom Crust* was measured from the bottom of the bread sample to a thickness of 12.50mm. A slice-thickness of 12.50mm is the industry standard for the thickness of bread slices, and so the thickness chosen for the slice-VOIs were identical. *Foam Structure* analysis in *Advanced Cell* mode and *Strut Thickness* mode are analyses which required an increased computing power, and thus the analyses of the four sub-VOIs from the *Bread VOI* was more practical to process using these functions.

The following analyses were completed for the four VOIs within the bread sample VOI reconstruction (**Figure 6**) in both *Advanced Cell* mode and *Strut Thickness* mode. The *Advanced Cell* Foam Structure Analysis of the bread samples were completed in order to statistically analyse and visualise the size and distribution of the pores and cells within the bread's foam-like structure (Volume Graphics, 2017). By selecting the *Strut Thickness* option during the Foam Structure Analysis, the thicknesses of the material between the pores within the bread-sample were calculated. The strut thickness was measured as the maximum tangent within an inscribed sphere (Volume Graphics, 2017).

Table 6 Parameters calculated and recorded, for each VOI, during Foam Structure Analysis

Cell structure parameters	Units
Minimum cell size	mm ³
Mean cell size	mm ³
Maximum cell size	mm ³
Standard deviation	mm ³
Strut thickness parameters	
Minimum thickness	mm
Maximum thickness	mm
Mean thickness	mm
Standard deviation	mm

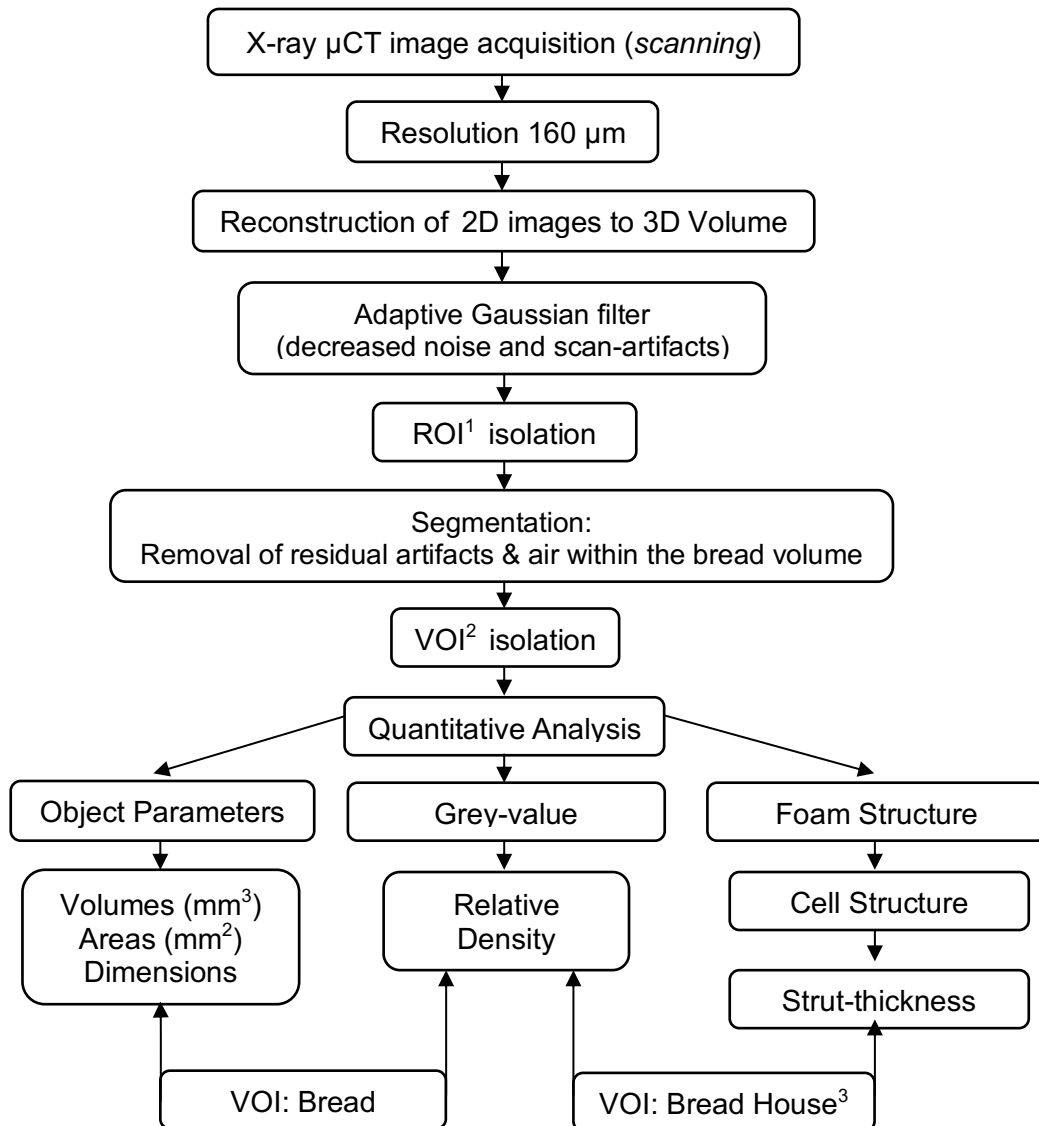


Figure 4 A systematic representation of the process used to extract information from the image acquisition of bread samples using X-ray micro-Computed Tomography. ¹Region Of Interest, ²Volume Of Interest, ³reconstruction of bread VOIs.

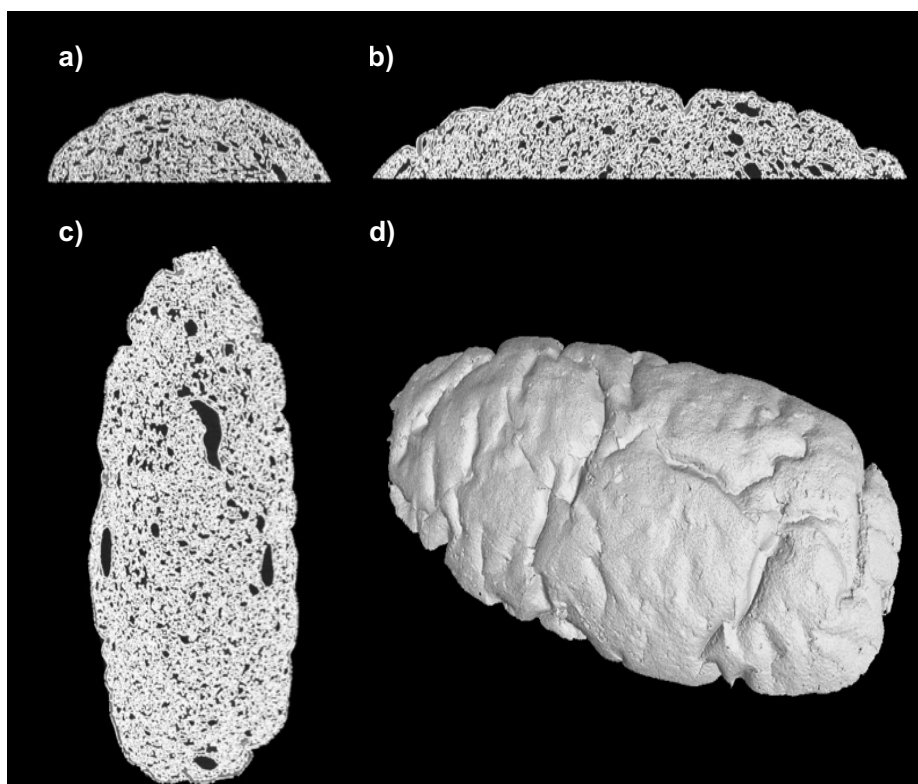


Figure 5 A visual representation of the Top Crust-VOI that forms part of the Bread House VOI. a) front perspective b) sagittal perspective c) top perspective d) three-dimensional (3D) perspective of VOI

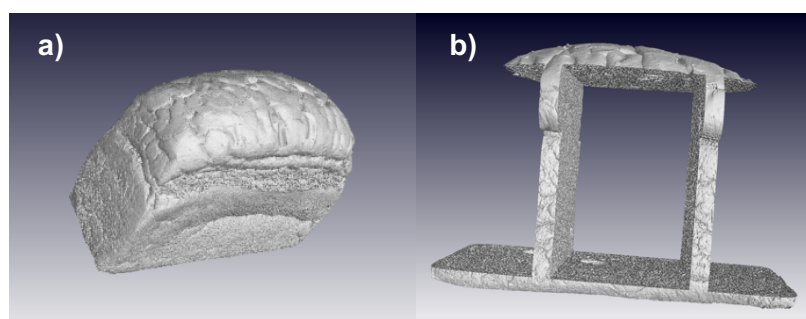


Figure 6 Screenshots captured of one of the bread samples, during *Bread sample VOI reconstruction* isolation, where a) is a three-dimensional (3D) rendering of the bread sample volume and b) is the *Bread sample VOI reconstruction*, including Top Crust (top), Bottom Crust (bottom), Slice 1 (right) and Slice 2 (left).

Statistical Analysis

Statistical analysis was carried out on the results obtained during analyses, described as repeated measures of experimental vs. control trials. This was subsequently completed, using Statistica version 13.31 (TIBCO Statistica™, Palo Alto, California, United States of America). Analysis of variance (ANOVA) was performed in order to determine which variables were dependant and independent of the treatment, replicate, and age of the product and which variables showed a

significant difference between the bread loaf quality of the Control- and BSG-supernatant formulations. The least significant difference (LSD) test was used to evaluate the mean differences at the 5% significance level ($P \leq 0.05$). General Linear Models (GLMs) were used in order to evaluate possible interactions between the factors within the experimental design (**Table 12**).

Chapter 4

Results

Proximate and compositional analysis

To enable the characterisation of the effect of BSG-supernatant on dough- and bread quality attributes, proximate (**Table 7**) and compositional (**Table 8**) analysis of the BSG-supernatant was completed. Proximate analysis determined that the supernatant is slightly acidic (pH = 4.2) and has a small concentration of total dissolved solids, protein and sugars.

The detection of monomers, that form part of the NSPs which are essential to bread loaf quality, substantiates the potential of using the BSG-supernatant to enhance bread product quality. These monomers include arabinose, xylose, furfural and hydroxymethylfurfural (HMF). The monomers are quantified, as the acid hydrolysis required for HPLC-analysis degrades the NSPs into its constituent monomers. Using this information, the arabinose to xylose ratio was determined to be ca. 3:1. The residual sugars within the supernatant, other than the abovementioned monomers, were identified as glucose and glycerol.

BSG-supernatant

Table 7 Proximate analysis of BSG-supernatant (n=6)

Moisture content, %	97.989
Protein content, %	0.743
Ash, %	0.173
Sum of TSS [*] and TDS ^{**} , %	2.011
Brix, °Bx	0.583
pH	4.2

*TSS: Total Soluble Solids

**TDS: Total Dissolved Solids

Table 8 Compositional analysis of BSG-supernatant through the use of high-performance liquid chromatography

(n = 6)	(g/L)
Glucose	6.6355
Xylose	0.6527
Arabinose	0.2273
Glycerol	0.1036
Ethanol	0.2491
Acetic Acid	0.5565
Hydroxymethylfurfural	0.0949
Furfural	0.0209

Bread flour

Bread-flour was produced specifically for this investigation in order to rule out the effect of flour-improvers, used by the industry to improve the bread flour's baking quality. The wheat kernel quality measurements (**Table 9**) were made using an IM9500 NIR (Near infrared) Grain Analyser (Perten, Australia). The bread flour was determined to be of good baking quality, based on the flour's proximate- and compositional analyses results (**Table 10**). Its composition was determined in order to rule out false positive or negative effects measured as being due to the complete substitution of water with BSG-supernatant. The ratio of wet- to dry gluten was determined to be ca. 28:1. The flour had an ideal moisture- (~14%_{omb}), protein- (12.5%_{omb}), ash- (0.5%_{adb}), and damaged starch content (<12.5%) for bread-making.

Table 9 Wheat kernel quality, as measured by a NIR Grain Analyser (n = 3)

Initial moisture content, %	11.35
Initial whole-kernel protein (12% _{omb}), %	13.35
Specific weight, kg/hL	81.64
Wet gluten (14% _{omb}), %	30.02

Table 10 Proximate and compositional analysis of the bread flour. Results are reported as mean ± standard deviation.

Proximate analysis	(n = 6)
Moisture (14% _{omb}), %	13.95±0.05
Protein (12% _{omb}), %	12.51±0.07
Ash, %	0.53±0.001
Compositional analysis	(n = 6)
Starch damage, %	10.72±0.27
Dry gluten, %	1.14±0.11
Wet gluten, %	32.44±1.61
¹ Water binding capacity (WBC), %	21.05±0.93

¹WBC is also often referred to as the WAC

Dough Rheology

The characterisation of the bread flour's baking potential is important when investigating the effect of replacing water in a bread formulation with an alternative baking water. The dough quality was quantified using rheological analyses, as the interaction between the bread flour and the water and/or BSG-supernatant would directly affect the quality of the bread product.

The Alveograph was used in order to measure the flour's ability to lend strength and extensibility to the dough, as its measured and quantified parameters are indicative of the bread loaf quality that

could be achieved by the formulation (**Table 11**). Due to the sensitivity of the more modern Alveograph, it was only possible to evaluate the flour's quality as it interacted with water. The Alveograph measures the biaxial extension of the dough sample. The parameters involved in quantifying the biaxial deformation tolerance of the dough-system includes the pressure (P) tolerance of the dough, measured during the inflation stage of the analysis (AACC International, 1999i). The length of the curve, on the alveogram, represents the extensibility of the dough (Delcour and Hosney, 2010c). The curve configuration ratio (P/L) is a parameter used by the bread industry to compare the quality of different wheat-flours and their breadmaking potential (SAGL, 2018). The flour is evaluated based on how close the curve configuration ratio is to 1.0. The deformation energy (W) is also recorded and forms part of the alveogram, and is often used to refer to the flour sample's strength (Delcour and Hosney, 2010c).

Table 11 Alveograph analysis on bread flour. Results are reported as mean \pm standard deviation (n = 6).

Stability (P), mm	84.67 \pm 2.34
Distensibility (L), mm	118.50 \pm 7.42
Deformation energy (W), ($\times 10^{-4}$ J)	293 \pm 17
Curve configuration ratio, (P/L)	0.72 \pm 0.04
Hygrometry (15% _{omb}), %	62.50 \pm 3.95

Table 12 Test Hypotheses for this investigation.

Variable	Hypothesis
Treatment	H ₀ : $\bar{x}_{\text{control}} = \bar{x}_{\text{BSG-supernatant}}$
	H ₁ : $\bar{x}_{\text{control}} \neq \bar{x}_{\text{BSG-supernatant}}$
Sample Age	H ₀ : $\bar{x}_{\text{Day 2}} = \bar{x}_{\text{Day 3}} = \bar{x}_{\text{Day 4}}$
	H ₁ : $\bar{x}_{\text{Day 2}} \neq \bar{x}_{\text{Day 3}} \neq \bar{x}_{\text{Day 4}}$
Replicates	H ₀ : $\bar{x}_{\text{Rep 1}} = \bar{x}_{\text{Rep 2}} = \bar{x}_{\text{Rep 3}}$
	H ₁ : $\bar{x}_{\text{Rep 1}} \neq \bar{x}_{\text{Rep 2}} \neq \bar{x}_{\text{Rep 3}}$
Interaction	H ₀ : $P_{\text{Treatment*Age}} \sim P_{\text{Treatment*Replicate}} \sim P_{\text{Replicate*Age}} \sim P_{\text{Treatment*Age*Replicate}} \geq 0.05$
	H ₁ : $P_{\text{Treatment*Age}} \sim P_{\text{Treatment*Replicate}} \sim P_{\text{Replicate*Age}} \sim P_{\text{Treatment*Age*Replicate}} \leq 0.05$

H₀: null hypothesis; H₁: alternative hypothesis

*represents an interaction

The Mixograph and Farinograph analyses were used in order to quantify the water absorption behaviour of the flour (**Table 13**). Both these analyses also measure the mixing properties of the dough. The percentage (%) increase/decrease in dough quality parameters were determined in order to determine the effect of the BSG-supernatant used as an alternative baking water. The BSG-

supernatant had an enzyme activity of its own, as it significantly increased the Falling Number (FN) of the flour (**Table 13**).

Table 13 Mixograph, Farinograph and FN parameters as affected by the replacement of water with BSG-supernatant.

Mixograph-35g	Control (n = 6)	BSG-supernatant (n=6)	Increase/Decrease (%)
Water absorption, %	62.81	62.81	fixed value
Midline peak height	52.48±0.71	51.92±1.03	-0.56
Right of peak slope	-6.59±0.27	-9.00±0.54	-2.41
Width at peak	29.34±2.51	26.95±3.86	-2.39
Width at 7 min	5.04±1.31	4.32±0.75	-0.72
Farinograph-250g	(n = 6)	(n = 6)	
Consistency, BU*	500	500	fixed value
Water absorption (14% _{mb}), %	65.20	66.00	0.80
Dough development time, min	6.5	5.7	-0.8
Stability, min	9.2	5.9	-3.3
Time to breakdown, min	11.3	8.5	-2.8
Amylolytic enzyme activity	(n = 6)	(n = 6)	
Falling number, s	359.83±5.24	339.83±6.15	-20

Results are reported as mean ± standard deviation

*BU: Brabender Units

The pasting properties of the flour-water and flour-supernatant mixtures were determined using a Rapid Visco Analyser (RVA) (**Table 14**). Prior to analysis, the BSG-supernatant sample was refrigerated, at 4°C. The sample age (Day) variable accounts for the period of days the supernatant was refrigerated for. The Rapid Visco Analyser (RVA) method was originally developed in order to measure the sprout damage of the wheat used to produce flour. The Falling Number (FN) method is able to measure this too. The results from these two analyses can be used in order to measure the difference between the inherent amylolytic enzyme activity within the wheat-flour sample and the difference in activity from the incorporation of the BSG-supernatant.

The RVA and Falling Number methods of analyses are based on the suspension of flour in water, which is consequentially stirred and heated according to a pre-programmed combination of stirring and temperature elevation. For the RVA analyses the results are recorded as a function of the time- and temperature in centipoise (cP), whilst the FN result is recorded as a function of time, in seconds. The RVA measures the viscosity of the flour-water suspension, using a temperature profile which emulates that of the different glass transitions which starch undergoes during the bread production process. By measuring the pasting properties of the flour-in-water and comparing it to the pasting

properties of flour-in-BSG-supernatant, it is possible to measure the influence of replacing the water in a bread formulation with an alternative baking water, in this case BSG-supernatant. The RVA inherently records the α -amylase activity within the flour-water suspension, as the difference in viscosity between a selected- and modified flour-water suspension. The measured peak viscosity indicates that the equilibrium starch-granule swelling point has been reached and is thus used as a measurement of the WHC of the flour sample. The retrogradation of starch is reflected during the cooling-cycle of the RVA analysis. After a set holding period, at constant temperature, both the peak and trough viscosity are recorded. The breakdown, also known as the flour's ability to resist the shear force experienced during mixing of bread formulation ingredients, is measured using the difference between the peak and trough viscosity values.

Table 14 Pasting properties, as determined by the Rapid Visco Analyser (RVA), of the bread flour used, as influenced by replacing water with BSG-supernatant.

Sample (n = 12)	Peak viscosity (cP)	Trough (cP)	Final viscosity (cP)	Time to peak viscosity (s)
Control	1474.92±20.76 ^c	829.00±18.81 ^c	1762.67±26.50 ^c	342.67±3.01 ^c
BSG-supernatant, Day 0	2153.55±35.84 ^b	1195.80±28.12 ^b	2294.80±30.00 ^b	358.00±6.57 ^b
BSG-supernatant, Day 7	2281.05±28.45 ^a	1377.30±6.83 ^a	2485.40±25.10 ^a	372.67±5.32 ^a
% Increase/decrease, Day 0	46.01	44.25	30.19	4.47
% Increase/decrease, Day 7	54.66	66.14	41.00	8.75
% Increase/decrease, Day 0→7	8.65	21.89	10.81	4.28

Results are reported as mean ± standard deviation, on a 14%_{mb}

Superscripts that differ, within the same column, differ significantly (P≤0.05)

The results indicate that there is a significant difference in the pasting properties between that of water and BSG-supernatant (**Table 14**). There is also a significant difference based on the sample age of the supernatant. The general linear models (**Table 15**) indicate that the treatment, age of the supernatant, as well as their interaction significantly affected the pasting properties of the bread flour (**Figures 6, 7 and 8**).

Table 15 GLMs of the effects on the pasting properties of the dough. The effects include the *treatment*, control or BSG-supernatant, *age* of the supernatant and their interaction, as *Treatment*Age*.

Effect	p-values			
	Peak viscosity (cP)	Trough (cP)	Final viscosity (cP)	Time to peak viscosity (cP)
Treatment	0.00000	0.00000	0.00000	0.00000
Age	0.00012	0.00000	0.00000	0.00145
Treatment*Age	0.00012	0.00000	0.00000	0.00145

The effect is considered significant when P≤0.05; *represents an interaction

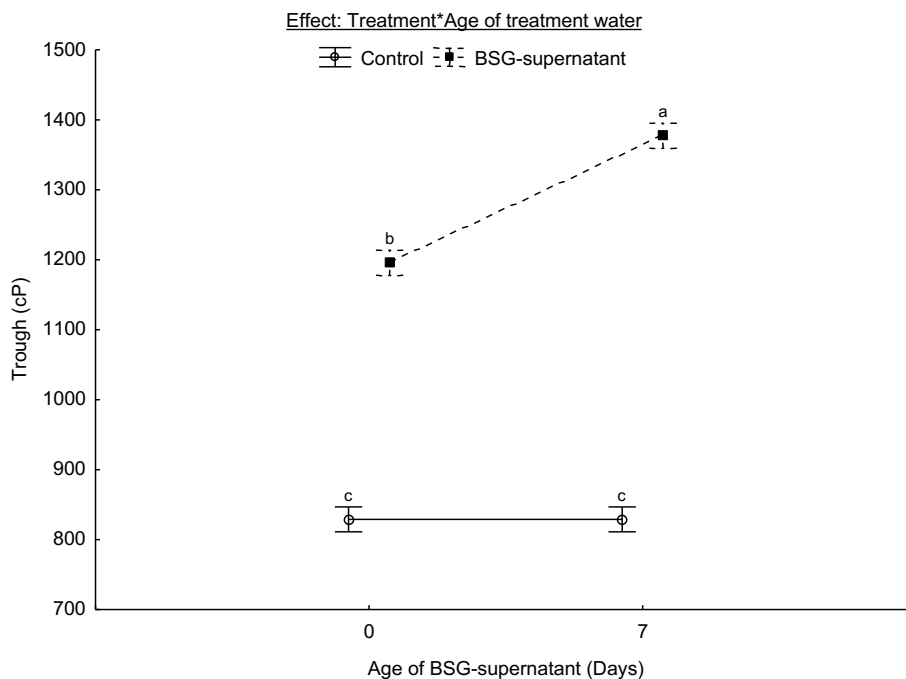


Figure 6 Trough viscosity as determined by RVA and affected by the interaction between the treatment and the age of treatment water. Vertical lines denote 95% confidence intervals. Indicated scripts that differ indicate a significant difference ($P \leq 0.05$). *represents an interaction.

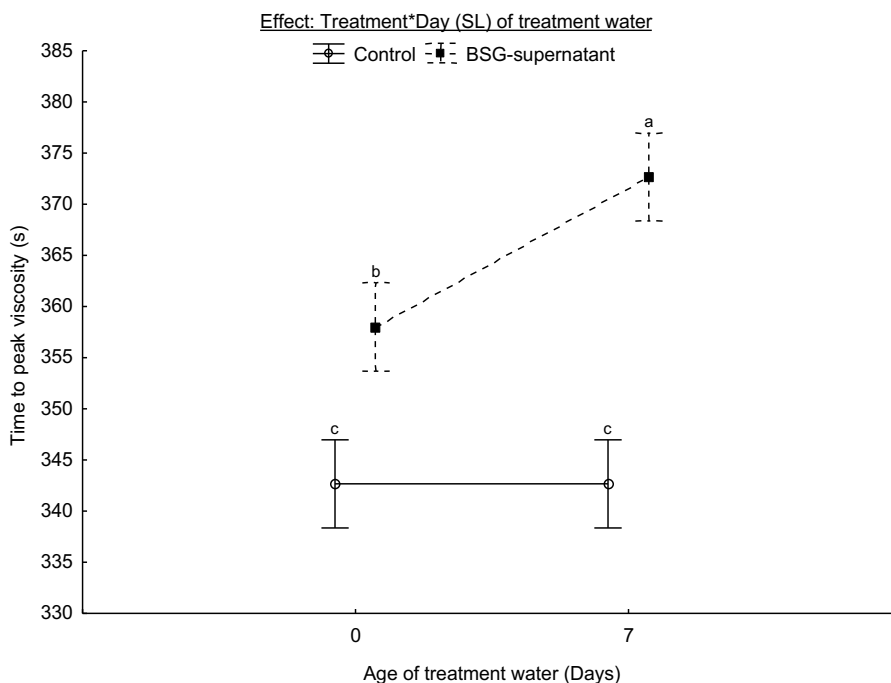


Figure 7 Time required to reach peak viscosity, as determined by RVA and affected by the interaction between the treatment and the age of the BSG-supernatant. Vertical lines denote 95% confidence intervals. Indicated scripts that differ indicate a significant difference ($P \leq 0.05$). *represents an interaction.

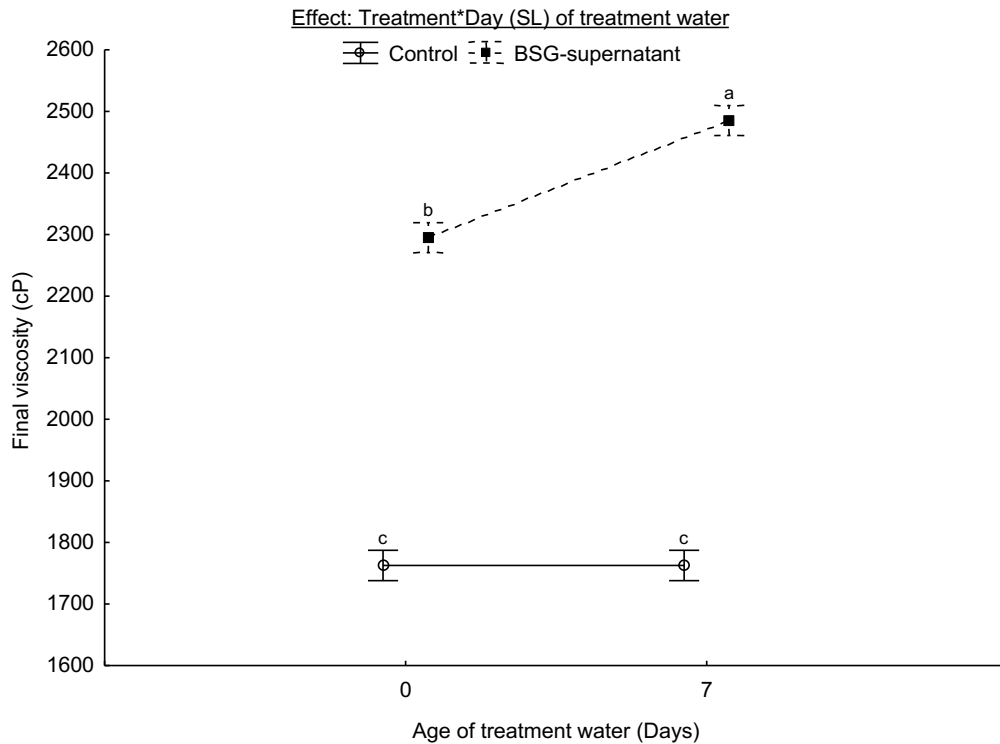


Figure 8 Final viscosity of the flour-water slurry as determined by RVA, as affected by the treatment and the age of the treatment water. Vertical lines denote 95% confidence intervals. Scripts that differ indicate a significant difference ($P \leq 0.05$). *represents an interaction.

The loaf height (mm) of the fresh (Day 0) bread samples were measured using a manual calliper. The control formulation had a 171.9mm average loaf height, whilst the BSG-supernatant formulation samples had a 168.9mm average loaf height. The BSG-supernatant formulation decreased the average loaf height by an average of 3mm, which is negligible when observed with the human eye.

Texture analyses

The general linear models indicate that only the age of the bread sample had a significant effect on both the firmness (g) and resilience (%) of the bread samples (**Table 16 & 17**). Similarly, the firmness of the samples increased significantly from shelf-life days two to four, whilst the resilience decreased significantly (**Figure 9 & 10**).

Table 16 General Linear Models (GLM) of the parameters measured during Texture Analysis on the second, third and fourth day after bread sample production. The effect is significant when $P \leq 0.05$. *represents an interaction.

Effect	p-values	
	Firmness (g)	Resilience (%)
Treatment	0.28514	0.28283
Replicate	0.18772	0.78799
Age	0.00000	0.00405
Treatment*Replicate	0.76684	0.90248
Treatment*Age	0.67502	0.96892
Replicate*Age	0.22801	0.21321
Treatment*Replicate*Age	0.65593	0.19947

The effect is considered significant when $P \leq 0.05$; *represents an interaction

Table 17 Firmness and Resilience as measured during texture analysis, across days two, three and four of the bread sample's shelf-life.

	Day 2 (n = 12)	Day 3 (n = 12)	Day 4 (n = 12)
Firmness (g)			
Control	246.09±21.44 ^c	296.40±27.97 ^b	362.63±35.76 ^a
BSG-supernatant	263.27±25.28 ^c	299.25±30.50 ^b	362.53±28.31 ^a
% Increase/decrease	6.98	0.96	0.03
Resilience (%)			
Control	60.63±4.72 ^a	58.07±4.99 ^{abc}	55.70±4.71 ^{bc}
BSG-supernatant	58.64±2.87 ^{ab}	55.35±3.85 ^{bc}	53.98±4.82 ^c
% Increase/decrease	-3.28	-4.68	-3.09

Results are reported as mean ± standard deviation

Superscripts that differ within the same column or row, per measured parameter, are significantly different from one another ($P \leq 0.05$).

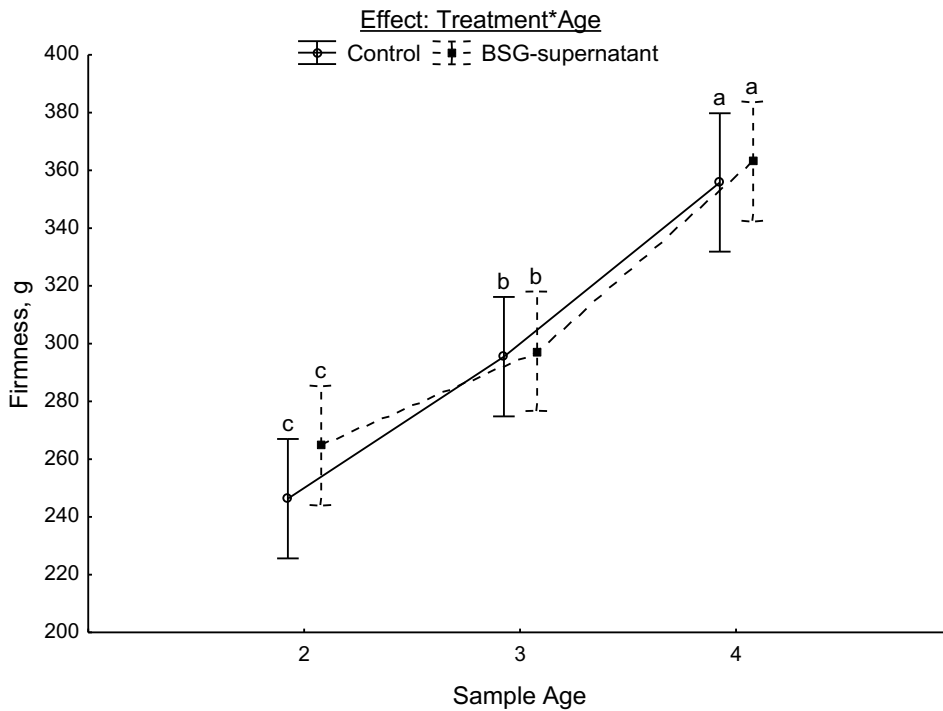


Figure 9 Firmness of bread, as determined by the texture analyser and affected by the interaction between the treatment and the age of the sample. Vertical lines denote 95% confidence intervals. Indicated scripts that differ indicate a significant difference ($P \leq 0.05$). *represents an interaction.

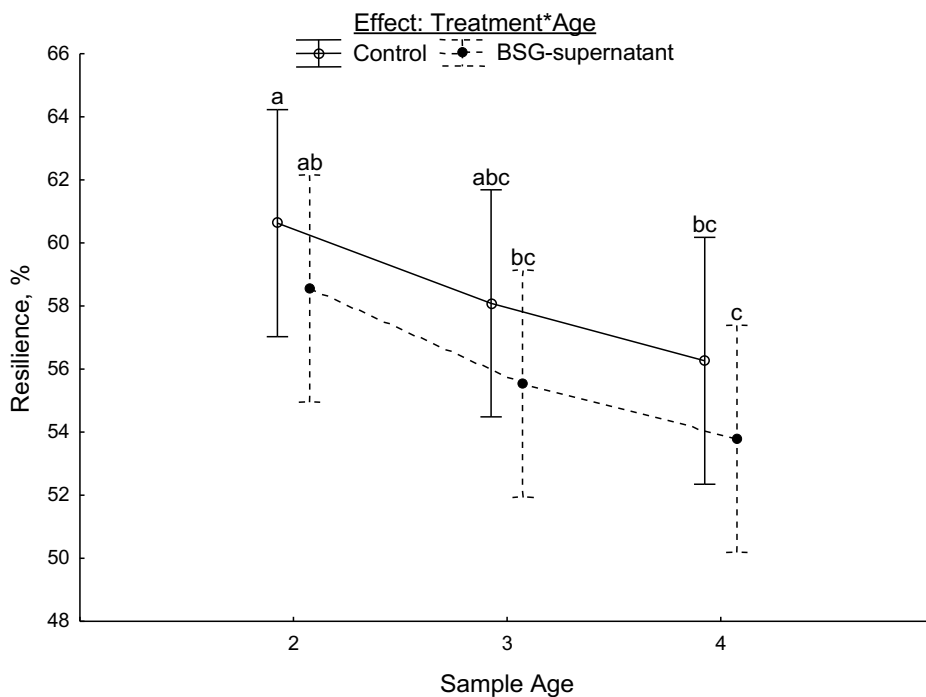


Figure 10 Resilience of the bread sample slices, as determined by the texture analyser and affected by the interaction between the treatment and the age of the bread sample. Vertical lines denote 95% confidence intervals. Indicated scripts that differ indicate a significant difference ($P \leq 0.05$). *represents an interaction.

C-Cell Visual Analysis

The GLMs from the C-Cell (**Table 18**) indicate that the age of the bread sample (Days 2, 3, and 4) significantly affected the concavity (%) (**Figure 11**) and slice area of the bread loaves (**Figure 12**).

The age of the bread sample also significantly affected the slice brightness (**Figure 13**) as well as the measured CIElab (Kenten Jones) colours (**Figure 14, 15, & 16**). The replicate effect is also evident in the a^* and b^* colour properties (**Figures 15**), with only a^* being affected by both the treatment (BSG-supernatant) and the variation between replicates.

Table 18 General Linear Models for C-Cell Visual Analysis parameters, describing the effect of the variables being considered on the bread sample's slice shape and colour parameters.

Effect	p-values					
	Total Concavity (%)	Slice Area	Slice Brightness	Colour L*	Colour a^*	Colour b^*
Treatment	0.81744	0.01150	0.96802	0.73844	0.00435	0.07597
Replicate	0.46608	0.21078	0.18391	0.16262	0.00229	0.00058
Age	0.00443	0.22695	0.00000	0.00002	0.94254	0.01279
Treatment*Replicate	0.50870	0.04465	0.45759	0.45864	0.82790	0.58962
Treatment*Age	0.75811	0.34629	0.32726	0.35517	0.06896	0.06000
Treatment*Replicate*Age	0.43278	0.11943	0.39551	0.74426	0.35205	0.40888

The effect or interaction of effects are significant when $P \leq 0.05$ ($n = 12$ per day). *represents an interaction.

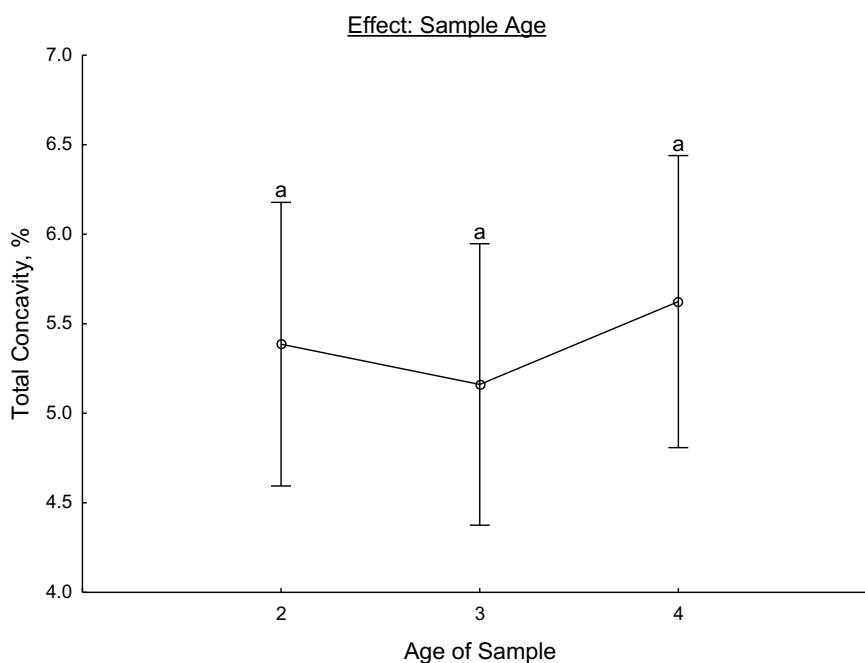


Figure 11 Total concavity (%) of the bread samples as measured by C-Cell VA and affected by the age of the sample. Vertical lines denote 95% confidence intervals. Indicated scripts that differ indicate a significant difference ($P \leq 0.05$).

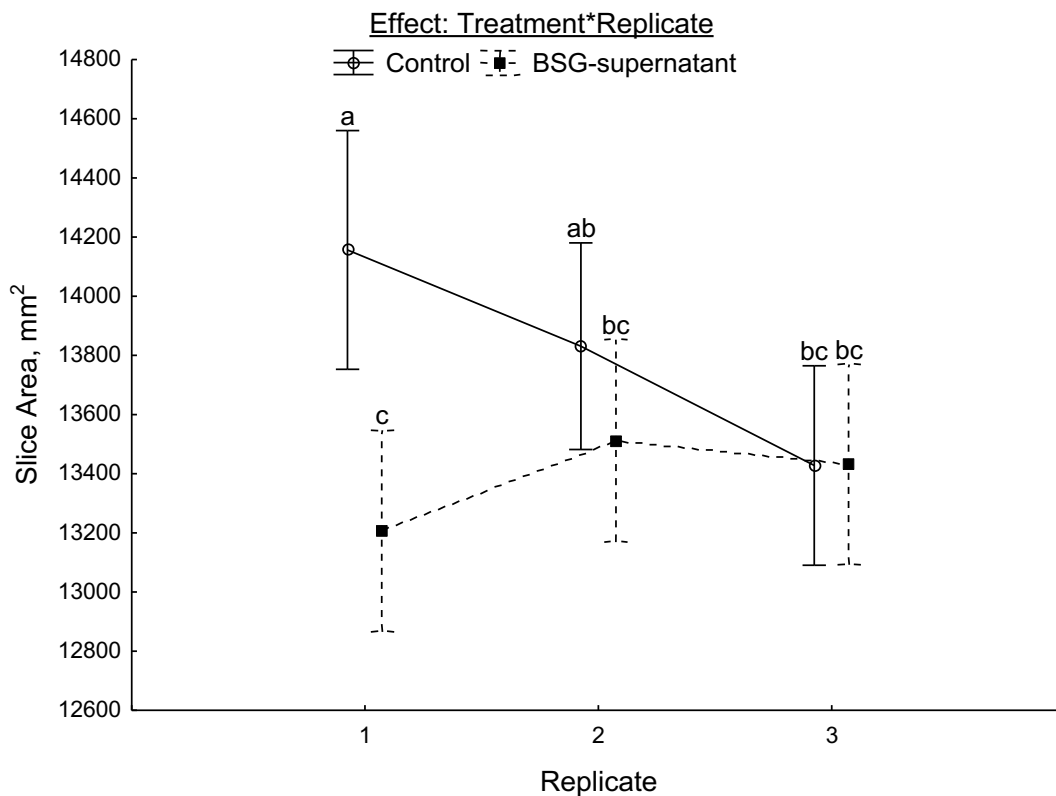


Figure 12 Slice area measured by C-Cell VA, and affected by the interaction between the experimental treatment and replicate. Vertical lines denote 95% confidence intervals. Indicated scripts that differ indicate a significant difference ($P \leq 0.05$). *represents an interaction.

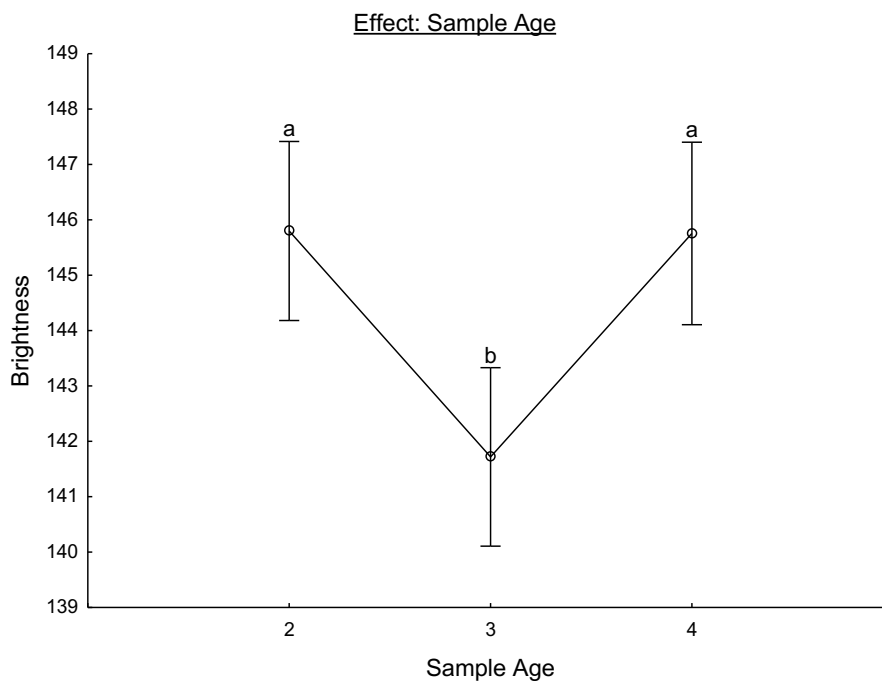


Figure 13 Slice brightness, as measured by C-Cell VA, and affected by the age of the bread sample. Vertical lines denote 95% confidence intervals. Indicated scripts that differ indicate a significant difference ($P \leq 0.05$).

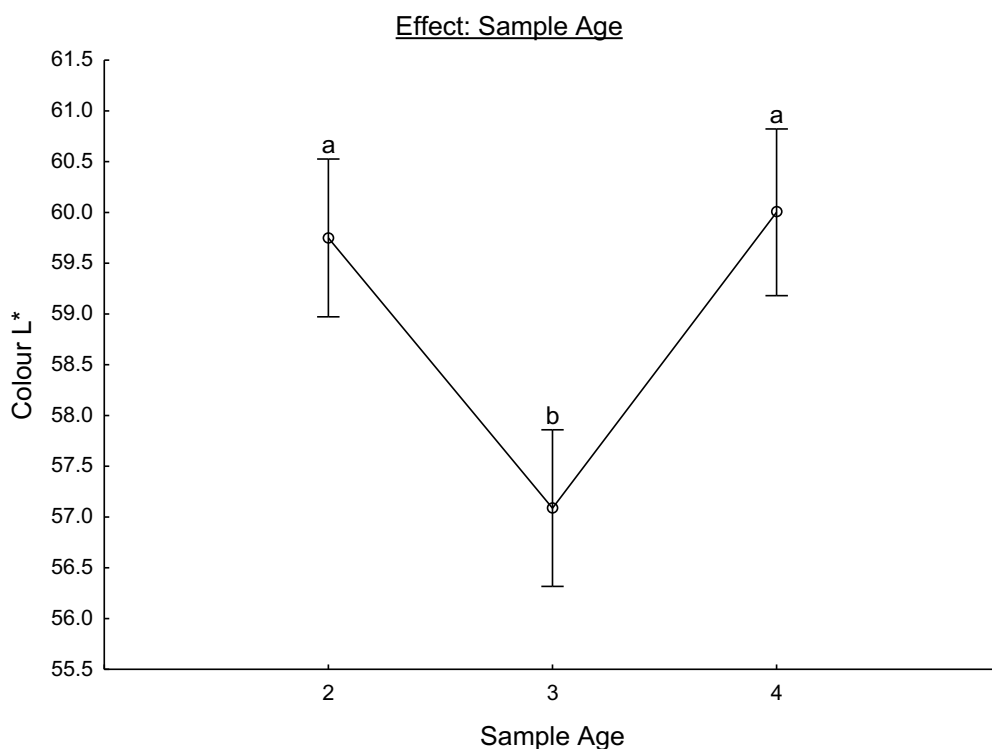


Figure 14 L* colour component, as measured by C-Cell VA, and affected by the age of the bread sample. Vertical lines denote 95% confidence intervals. Indicated scripts that differ indicate a significant difference ($P \leq 0.05$).

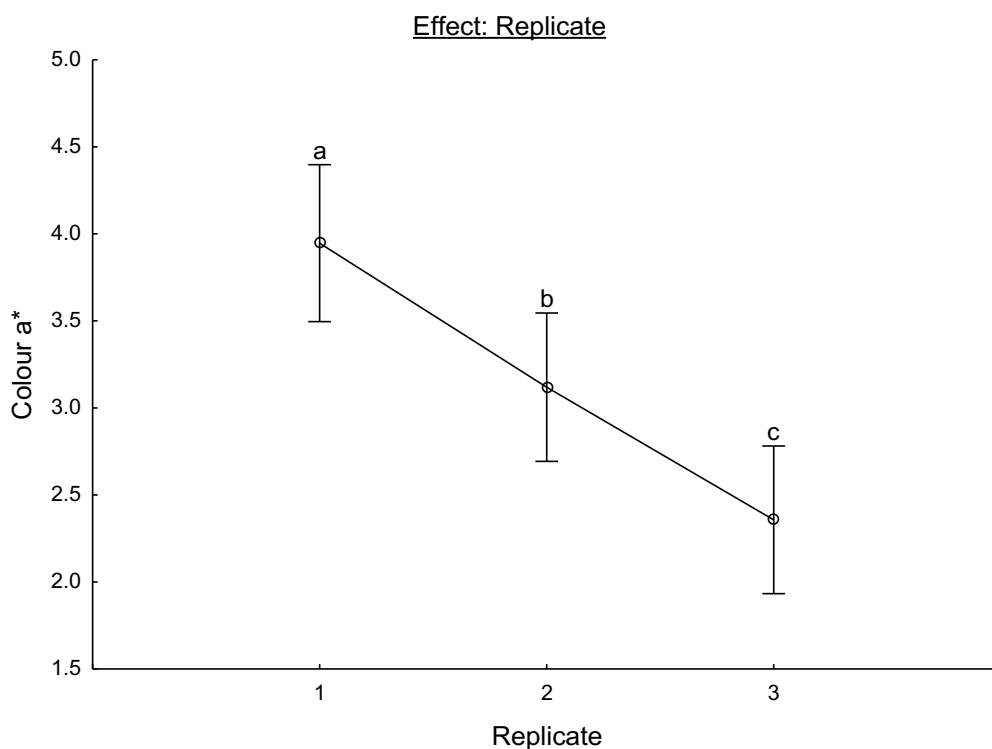


Figure 15 a* colour component, as measured by C-Cell VA, as affected by the replicate factor. Vertical lines denote 95% confidence intervals. Indicated scripts that differ indicate a significant difference ($P \leq 0.05$).

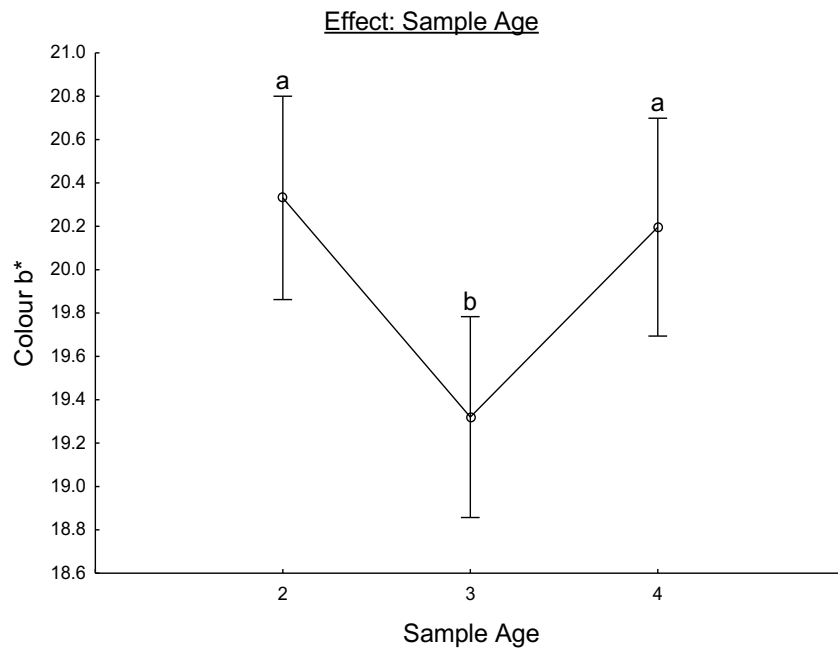


Figure 16 b* colour components measured by C-Cell VA and affected by the age of the bread sample. Vertical lines denote 95% confidence intervals. Indicated scripts that differ indicate a significant difference ($P \leq 0.05$).

The interaction between the replicate and the treatment effects, significantly affected the number of cells detected by the C-Cell VA (**Table 19**). The interaction between the treatment and the age of the bread sample significantly affected both the number of the cells (**Figure 17**) and the cell volume (**Figure 18**). The interaction between the replicate and the treatment effects, significantly affected the area of cells as well as the number of cells (**Figure 17**) detected by the C-Cell.

Table 19 General Linear Models for Cell size and Holes morphology.

Effect	p-values							Number of Holes	Area of Holes	Volume of Holes
	Number of Cells	Cell Diameter	Area of Cells	Volume of Cells	Coarse Cell Volume	Cell Wall Thickness	Cell Alignment			
Treatment	0.55424	0.32144	0.37128	0.39408	0.56133	0.42360	0.26895	0.80249	0.66378	0.93196
Replicate	0.10622	0.48555	0.01815	0.53582	0.27741	0.89216	0.08799	0.07180	0.00075	0.00092
Age	0.36920	0.17550	0.31951	0.13264	0.13823	0.15673	0.45328	0.92802	0.84037	0.89435
Treatment*Replicate	0.03436	0.31345	0.35581	0.23980	0.44136	0.25881	0.16979	0.18886	0.63486	0.60724
Treatment*Age	0.26296	0.05273	0.09331	0.04437	0.03896	0.05876	0.69967	0.05287	0.41045	0.60829
Treatment*Replicate*Age	0.69643	0.32847	0.88094	0.94770	0.87709	0.90485	0.74519	0.75725	0.88352	0.97130

The effect or interaction of effects are significant when $P \leq 0.05$. *represents an interaction.

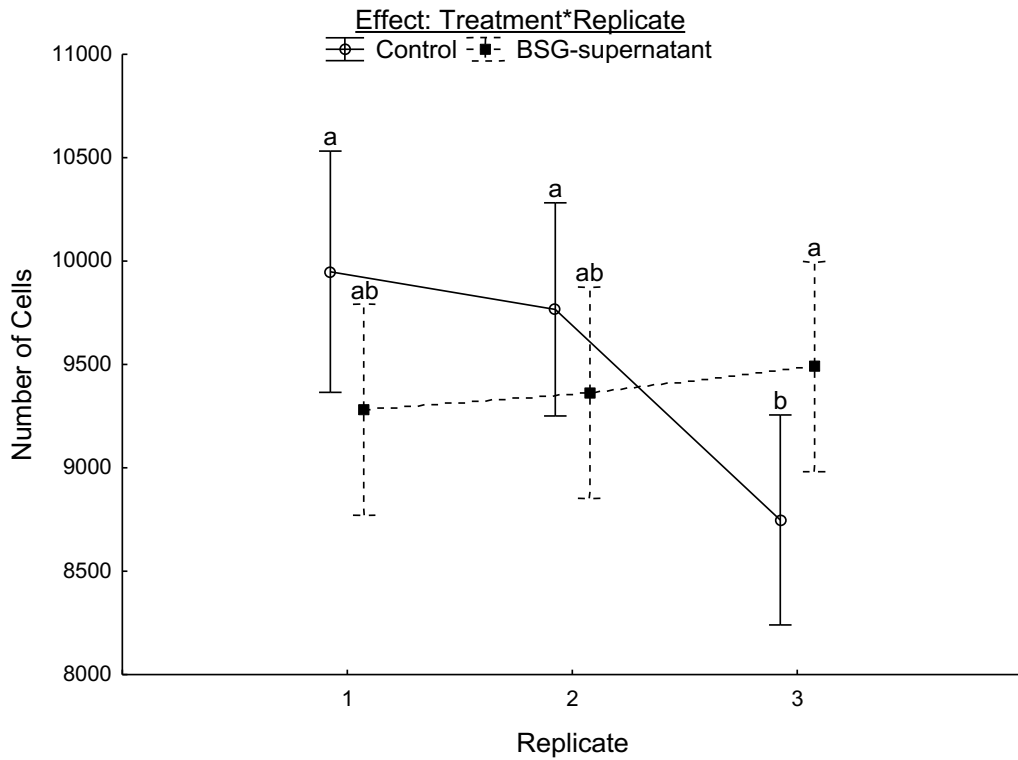


Figure 17 Number of cells within a bread slice as measured by C-Cell VA and affected by the interaction between the experimental treatment and replicate. Vertical lines denote 95% confidence intervals. Indicated scripts that differ indicate a significant difference ($P \leq 0.05$). *represents an interaction.

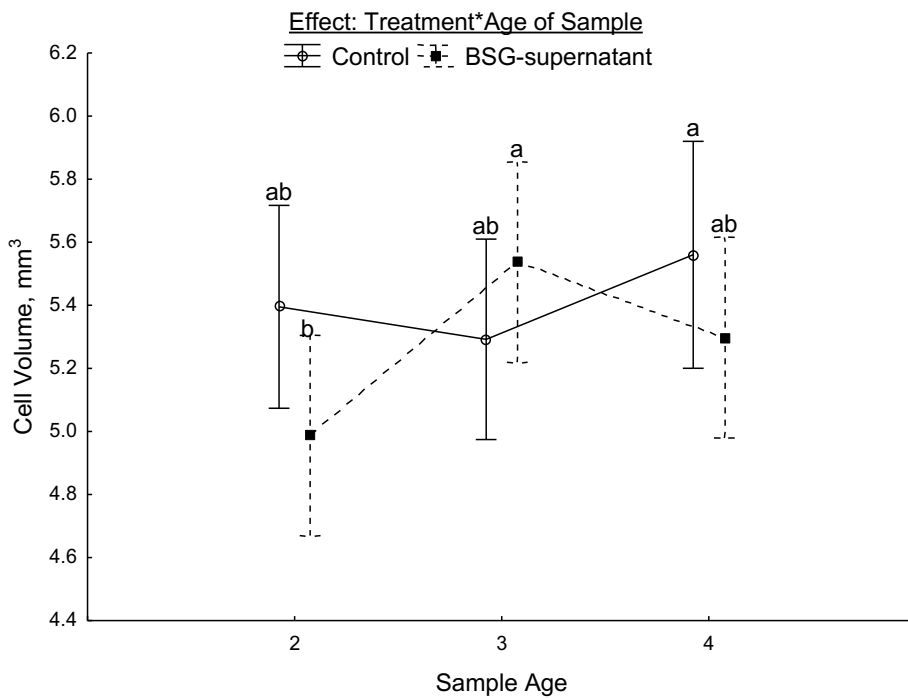


Figure 18 Volume of the cells within the bread slice, as measured by C-Cell VA and affected by the interaction between the treatment and the age of the bread sample. Vertical lines denote 95% confidence intervals. Indicated scripts that differ indicate a significant difference ($P \leq 0.05$).

The percentage (%) increase or decrease in bread quality, between control and BSG-supernatant formulation, was calculated for the parameters measured during C-Cell Visual Analysis (**Table 20**). The cell morphology measured during the two-dimensional C-Cell VA, included the cell diameter, -area, -volume, -wall thickness and -alignment relative to each other (**Table 20**). Upon comparison, these parameters did not differ significantly between the control and BSG-supernatant formulations on any of the considered shelf-life days. However, both formulations showed variation when considering their individual shelf-life quality. The cell-diameter, -area, -volume, and -wall thickness of the BSG-supernatant samples, all increased significantly from days two to three, whilst the control formulation's bread samples' cell wall thickness increased significantly from days three to four (**Table 20**).

The BSG-supernatant formulation significantly decreased the total concavity (%) of the bread samples (**Table 20**). The slice brightness and L*-colour value is unaffected by the treatment factor, although a significant decrease in the control samples is observed from days 2 to 3 (**Table 20**). The control bread samples showed a significant decrease in a*-colour value from days two to three, and a significant increase from days three to four (**Table 20**). On the second and fourth day of the bread sample's shelf-life (age) the measured a*-colour value was significantly greater for the BSG-supernatant samples than for the control samples.

The b*-colour value for the control samples, decreased significantly from days two to three, whilst significantly increasing from days three to four (**Table 20**). The BSG-supernatant samples remained consistent from days two to four, with the b*-colour value showing a significant difference between control- and BSG-supernatant formulation for only day three of sample age (**Table 20**).

Table 20 Bread quality parameters as measured by C-Cell visual analysis (Treatment*Age interaction). (n = 120 slices per Day)

	Day 2 (n = 12)	Day 3 (n = 12)	Day 4 (n = 12)		Day 2 (n = 12)	Day 3 (n = 12)	Day 4 (n = 12)
Total Concavity, %				Area of Cells, mm²			
Control	5.39±1.75 ^a	13837.25±607.68 ^a	13689.40±1011.73 ^a	Control	53.08±1.03 ^{ab}	52.88±1.25 ^{ab}	53.05±0.67 ^{ab}
BSG-supernatant	5.06±2.38 ^a	13641.02±565.00 ^{ab}	13226.74±758.45 ^b	BSG-supernatant	52.40±0.55 ^b	53.16±1.05 ^a	52.73±0.56 ^{ab}
% Increase/Decrease	-6.12	-1.42	-3.38	% Increase/Decrease	-1.28	0.53	-0.60
Slice Area, mm²				Volume of Cells, mm³			
Control	13655.42±819.00 ^a	141.47±3.27 ^b	144.65±7.16 ^a	Control	5.33±0.57 ^{ab}	5.29±0.88 ^{ab}	5.56±0.43 ^a
BSG-supernatant	13273.20±656.55 ^b	141.94±3.22 ^b	145.86±3.20 ^a	BSG-supernatant	4.97±0.49 ^b	5.55±0.71 ^a	5.29±0.45 ^{ab}
% Increase/Decrease	-2.80	0.33	0.84	% Increase/Decrease	-6.75	4.91	-4.86
Slice Brightness				Cell Wall Thickness, mm			
Control	145.62±3.84 ^a	56.75±3.15 ^b	60.09±2.33 ^a	Control	0.40±0.01 ^{abc}	0.40±0.02 ^{bc}	0.41±0.01 ^a
BSG-supernatant	145.25±2.33 ^a	57.36±2.81 ^b	59.60±1.57 ^a	BSG-supernatant	0.39±0.01 ^c	0.40±0.01 ^{ab}	0.40±0.01 ^{abc}
% Increase/Decrease	-0.25	1.07	-0.82	% Increase/Decrease	-2.5	0.00	-2.44
Colour L*				Cell Alignment			
Control	59.69±2.05 ^a	3.06±1.48 ^{bc}	2.39±0.92 ^c	Control	0.20±0.08 ^a	0.18±0.06 ^a	0.20±0.06 ^a
BSG-supernatant	59.63±1.15 ^a	3.32±1.25 ^{ab}	3.78±0.66 ^a	BSG-supernatant	0.22±0.04 ^a	0.22±0.07 ^a	0.23±0.05 ^a
% Increase/Decrease	-0.10	8.50	58.16	% Increase/Decrease	10.00	22.22	15.00
Colour a*				Number of Holes			
Control	2.53±0.95 ^c	18.52±2.89 ^b	20.46±1.36 ^a	Control	4.80±2.20 ^a	5.55±2.78 ^a	4.61±2.12 ^a
BSG-supernatant	3.66±1.12 ^{ab}	20.01±2.26 ^a	20.04±1.12 ^a	BSG-supernatant	5.23±2.91 ^a	4.16±2.12 ^a	5.06±2.75 ^a
% Increase/Decrease	44.66	8.05	-2.05	% Increase/Decrease	8.96	-25.05	9.76
Colour b*				Area of Holes, mm²			
Control	20.16±1.54 ^a	9757.70±1222.73 ^a	9239.24±914.80 ^a	Control	2.40±1.87 ^a	2.01±1.19 ^a	1.98±1.19 ^a
BSG-supernatant	20.65±1.51 ^a	9289.03±845.80 ^a	9219.73±732.42 ^a	BSG-supernatant	1.98±1.43 ^a	2.35±1.83 ^a	2.19±1.48 ^a
% Increase/Decrease	2.43	-4.80	-0.21	% Increase/Decrease	-17.5	16.92	10.61
Number of Cells				Volume of Holes, mm³			
Control	9398.06±869.83 ^a	1.69±0.22 ^{ab}	1.75±0.11 ^a	Control	80.89±31.63 ^a	75.81±24.48 ^a	74.02±25.21 ^a
BSG-supernatant	9638.34±914.41 ^a	1.75±0.19 ^a	1.69±0.12 ^{ab}	BSG-supernatant	74.23±26.81 ^a	77.03±30.88 ^a	76.88±26.41 ^a
% Increase/Decrease	2.5	3.55	-3.43	% Increase/Decrease	-8.23	1.61	3.86
Cell Diameter, mm							
Control	1.71±0.15 ^{ab}	1.69±0.22 ^{ab}	1.75±0.11 ^a				
BSG-supernatant	1.61±0.12 ^b	1.75±0.19 ^a	1.69±0.12 ^{ab}				
% Increase/Decrease	-5.58	3.55	-3.43				

Superscripts per measured parameter, within the same column or row, that differ, differ significantly from each other as P≤0.05.

X-ray micro-Computed Tomography Analyses

Bread size and porosity

The significance of the effects and their interaction(s) on the whole-bread sample morphology, including its surface area, total volume, volume of material- and air, and porosity are illustrated in the general linear models table (**Table 21**). These parameters were quantified during the first stage of this investigation's X-ray micro-Computed tomography analyses.

The treatment had a significant effect on the surface area of the bread samples (**Figure 19**). The age of the bread sample had a significant effect on the determined volume of material, included in the bread VOI, whilst it had an insignificant effect on the total volume of the sample (**Table 21 & 22**).

Table 21 General linear models for the Bread VOI morphology.

VOI = Bread	p-values		
Effect	Treatment	Age	Treatment*Age
Surface area, mm ²	0.03834	0.06547	0.17632
Total Volume, mm ³	0.18149	0.42754	0.27595
Volume of Material, mm ³	0.39277	0.02017	1.00000
Volume of Air, mm ³	0.16366	0.81970	0.23666
Porosity, %	0.89768	0.10815	0.47602

The effect or interaction of effects are significant when $P \leq 0.05$.

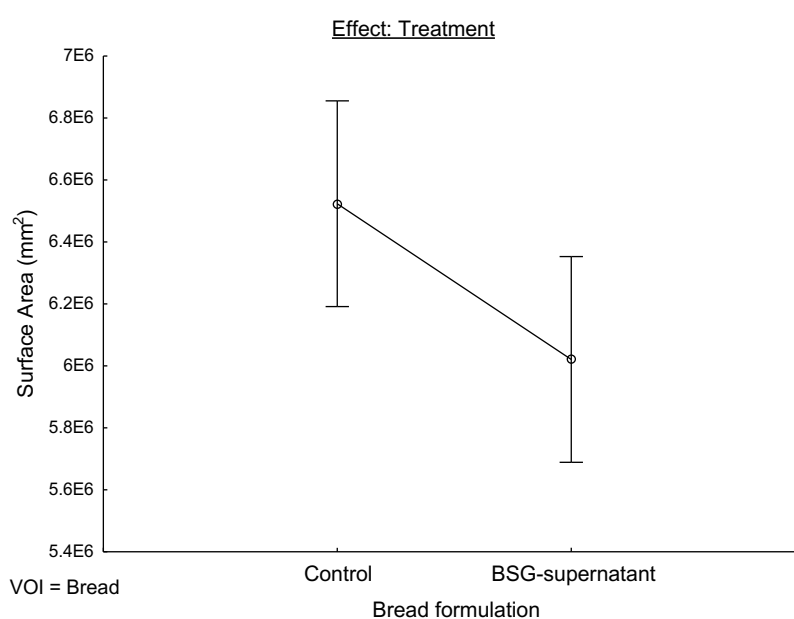


Figure 19 The area of the bread loaf, as measured by X-ray μ CT and affected by the treatment. Vertical lines denote 95% confidence intervals. Indicated scripts that differ indicate a significant difference ($P \leq 0.05$).

Table 22 Bread morphology as measured by X-ray μ CT, on three consecutive shelf-life days.

Treatment*Age			
VOI = Bread	Day 2 (n = 4)	Day 3 (n = 4)	Day 4 (n = 4)
Surface Area, mm²			
Control	6637055.00±244767.18 ^a	6550301.67±260964.69 ^a	6406771.67±162540.48 ^{ab}
BSG-supernatant	6546290.00±252076.09 ^a	5696700.00±838552.58 ^c	5841463.33±618371.46 ^{bc}
% increase/decrease	-1.36	-13.03	-8.82
Total Volume, mm³			
Control	3365639.51±101288.60 ^a	3357057.68±94266.43 ^a	3361763.58±116128.53 ^a
BSG-supernatant	3311383.77±49522.07 ^a	3318761.97±65120.78 ^a	3275918.90±65155.72 ^a
% increase/decrease	-1.61	-1.14	-2.55
Volume of Material, mm³			
Control	1651032.88±71527.82 ^{ab}	1644507.40±105855.13 ^{ab}	1531734.04±102942.23 ^{ab}
BSG-supernatant	1558221.91±13996.68 ^{ab}	1695022.07±218113.17 ^a	1445918.06±284963.12 ^b
% increase/decrease	-5.62	3.07	-5.60
Volume of Air, mm³			
Control	1714606.63±81131.16 ^a	1712550.28±98096.07 ^a	1830029.54±171351.80 ^a
BSG-supernatant	1753161.86±45186.86 ^a	1623739.91±259270.99 ^a	1775815.85±296950.35 ^a
% increase/decrease	2.25	-5.19	-2.96
Porosity, %			
Control	51.00±2.00 ^a	51.00±3.00 ^a	54.00±4.00 ^a
BSG-supernatant	53.00±1.00 ^a	49.00±7.00 ^a	54.00±9.00 ^a
% increase/decrease	2.00	-2.00	0.00

Superscripts per measured parameter, within the same column or row, that differ, differ significantly from each other as $P \leq 0.05$.

*represents an interaction.

The same object parameters were measured for each VOI within the Bread sample VOI reconstruction. The volume of interest (VOI) effect was significant for all measured object parameters (**Table 23**). The interaction between the treatment and the VOI, as well as the age of the bread sample with the VOI, are significant for the total volume and the volume of air within the bread sample, indicating that the volumes of interest within the Bread sample VOI reconstruction had different porosities (**Eq. 2**). The interaction between the VOI- and the age of the bread sample effect were significant on the volume of the VOI and the volume of air within, even though the volume of material was unaffected by these parameters.

The total volume of the top-crust VOI differed significantly between treatments, with the BSG-supernatant bread samples having a significantly greater top-crust volume than that of the control samples (**Table 24**). The interaction between the treatment and the VOI is significant on the volume of air, referred to as the porosity (%) of the bread micro-structure and is most evident for the top-crust VOI (**Table 23 & 24**). The bottom crust VOI had a significantly smaller porosity (%) than did

the other VOIs within the Bread sample VOI reconstruction (**Table 24**).

Table 23 General Linear Models for bread size parameters and porosity, regarding the Bread sample VOI reconstruction.

Effect	p-values						
	Treatment	Age	VOI	Treatment* Age	Treatment* VOI	Age*VOI	Treatment* Age*VOI
Surface Area, mm ²	0.74668	0.98545	0.00000	0.22632	0.21006	0.08839	0.90732
Total Volume, mm ³	0.41183	0,32541	0.00000	0.58647	0.04782	0.01219	0.81354
Volume of Material, mm ³	0.81480	0.29026	0.00000	0.53440	0.48826	0.45490	0.78737
Volume of Air, mm ³	0.28463	0.14970	0.00000	0.30022	0.03215	0.00296	0.97438
Porosity, %	0.41485	0.19027	0.00000	0.39196	0.10006	0.07305	0.90004

The effect or interaction of effects are significant when $P \leq 0.05$.

Although the interaction between the treatment and the age of the sample was insignificant, there was a significant increase in the volume of air within the control bread samples, from day two to four of the evaluated shelf-life period (**Table 25**).

The significant effect of the VOI-factor on the bread size and morphology parameters are illustrated graphically for the sample volume (**Figure 21**), the volume of air (**Figure 22**), and the volume of material (**Figure 23**).

The volume of air was also affected by the interaction between the age of the sample (shelf-life progression) and the VOI effects (**Figure 24**). From the aforementioned significant interactions, it is clear that the volume of air is dependent on the treatment, VOI and sample age effects.

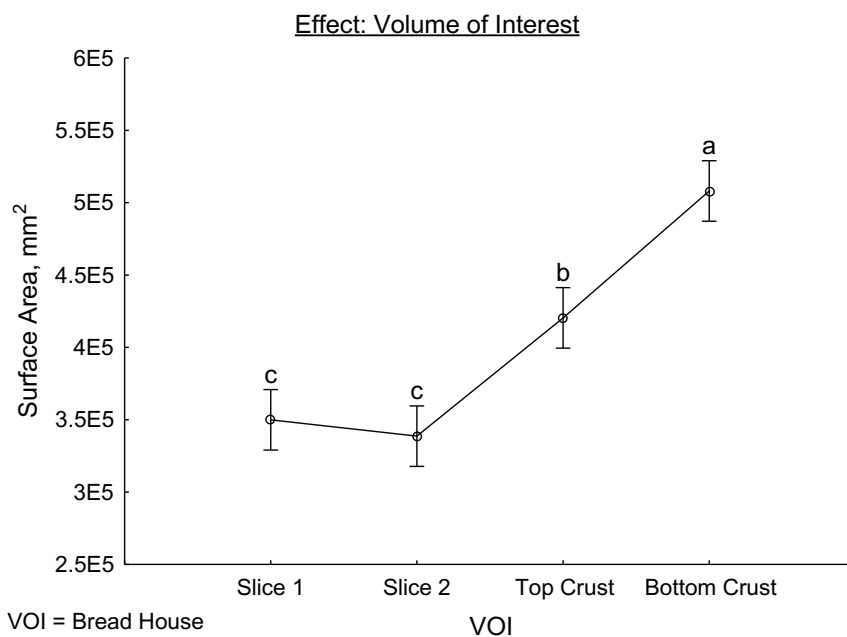


Figure 20 The area of the bread slice/crust, as affected by the VOI effect measured by X-ray μ CT. Vertical lines denote 95% confidence intervals. Indicated scripts that differ indicate a significant difference ($P \leq 0.05$).

Table 24 Determining the percentage increase/decrease, between Bread sample VOI reconstruction volumes of interest (VOI) due to the difference in bread formulation (treatment).

Treatment*VOI				
VOI = Bread House	Slice: 1 (n = 6)	Slice: 2 (n = 6)	Crust: Top (n = 6)	Crust: Bottom (n = 6)
Surface Area (mm²)				
Control	352922.68±17710.88 ^c	337131.46±15365.43 ^c	399176.56±40390.82 ^b	516253.63±38040.49 ^a
BSG-supernatant	342755.16±24982.34 ^c	340096.03±18114.62 ^c	437126.85±66502.20 ^b	502179.70±60054.35 ^a
% Increase/decrease	-2.88	0.88	9.51	-2.73
Total Volume (mm³) (p = 0.04782)				
Control	178983.24±7859.30 ^d	173938.43±6249.84 ^d	208724.16±19960.47 ^c	252206.19±14170.36 ^a
BSG-supernatant	175428.26±4038.36 ^d	174279.33±6323.13 ^d	231779.07±29374.89 ^b	244847.87±14947.75 ^{ab}
% Increase/decrease	-1.99	0.20	11.05	-2.92
Volume of Material (mm³)				
Control	82452.45±5922.16 ^c	80604.83±5106.37 ^c	99938.61±10663.82 ^b	129453.18±9440.88 ^a
BSG-supernatant	78806.10±7607.67 ^c	79833.83±5658.55 ^c	104497.13±10028.58 ^b	128448.98±10192.75 ^a
% Increase/decrease	-4.42	-0.96	4.56	-0.78
Volume of Air (mm³) (p = 0.03215)				
Control	96530.79±7288.41 ^{cd}	93333.59±7128.13 ^d	108785.54±13797.51 ^{bc}	122753.01±9961.12 ^a
BSG-supernatant	96622.16±5605.32 ^{cd}	94445.49±6456.84 ^{cd}	127281.94±24903.36 ^a	116398.89±11619.36 ^{ab}
% Increase/decrease	0.01	1.19	17.00	-5.18
Porosity (%)				
Control	54.00±3.00 ^{ab}	54.00±3.00 ^{ab}	52.00±3.00 ^b	49.00±3.00 ^c
BSG-supernatant	55.00±4.00 ^a	54.00±3.00 ^{ab}	55.00±5.00 ^{ab}	48.00±3.00 ^c
% Increase/decrease	1.85	0.00	5.77	1.69

Superscripts per measured parameter, within the same column or row, that differ, differ significantly from each other as P≤0.05.

*represents an interaction.

Table 25 Determining the percentage increase/decrease, between bread the control- and treatment bread formulations, across three shelf-life days (2, 3 and 4).

Treatment*Age			
VOI = Bread House	Day 2 (n = 4)	Day 3 (n = 4)	Day 4 (n = 4)
Surface Area (mm²)			
Control	401502.44±72454.60 ^a	408108.37±77320.04 ^a	394546.22±80971.59 ^a
BSG-supernatant	399767.85±73239.01 ^a	399271.13±76009.24 ^a	415655.46±96557.54 ^a
% Increase/decrease	-0.43	-2.17	5.35
Total Volume (mm³)			
Control	200582.96±32631.06 ^a	203741.64±34206.31 ^a	205104.39±35759.25 ^a
BSG-supernatant	204395.19±35824.54 ^a	207841.35±37288.29 ^a	206784.87±37068.69 ^a
% Increase/decrease	1.90	2.01	0.81
Volume of Material (mm³)			
Control	98655.01±17998.79 ^a	100559.06±21809.65 ^a	95303.65±23237.82 ^a
BSG-supernatant	98244.36±21802.61 ^a	98246.78±22208.18 ^a	97314.35±23416.86 ^a
% Increase/decrease	-0.42	-2.30	2.11
Volume of Air (mm³)			
Control	101927.95±15441.18 ^b	103182.58±13114.89 ^{ab}	109800.74±16397.71 ^a
BSG-supernatant	106150.83±16192.07 ^{ab}	109594.58±19847.55 ^{ab}	109470.53±22216.35 ^{ab}
% Increase/decrease	4.14	6.21	-0.30
Porosity (%)			
Control	51.00±2.00 ^a	51.00±3.00 ^a	54.00±5.00 ^a
BSG-supernatant	52.00±3.00 ^a	53.00±4.00 ^a	53.00±6.00 ^a
% Increase/decrease	1.00	2.00	-1.00

Superscripts per measured parameter, within the same column or row, that differ, differ significantly from each other as $P \leq 0.05$.

*represents an interaction between effects.

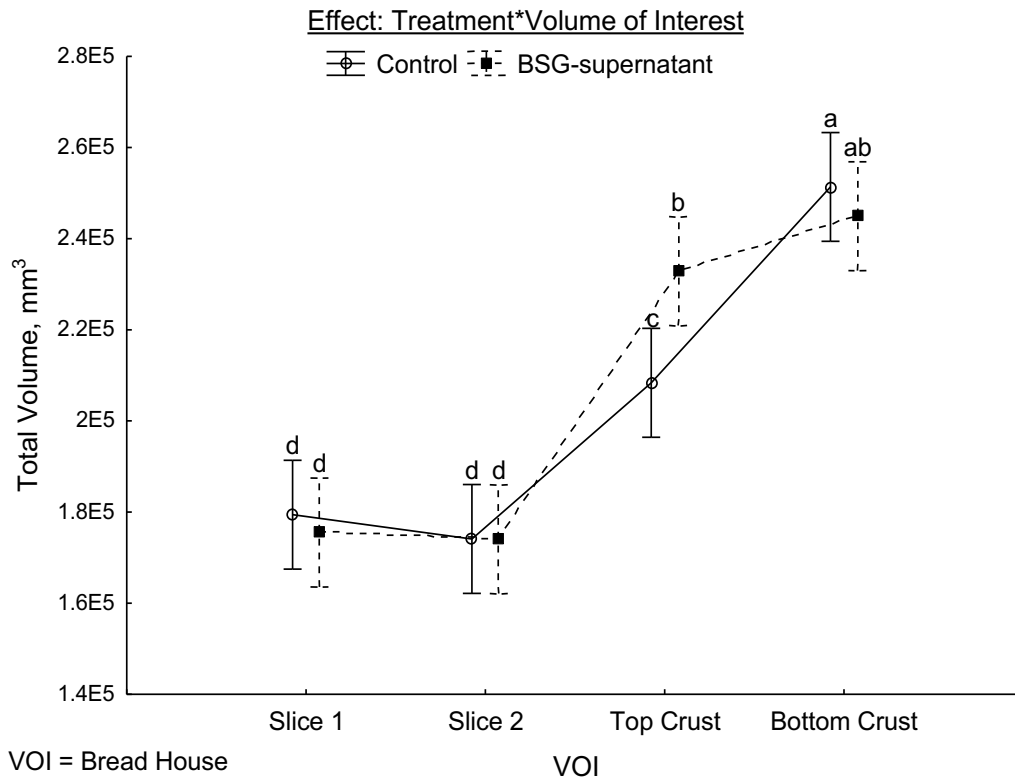


Figure 21 Total VOI volume as affected by the VOI effect, measured by X-ray μ CT. Vertical lines denote 95% confidence intervals. Indicated scripts that differ indicate a significant difference ($P \leq 0.05$).

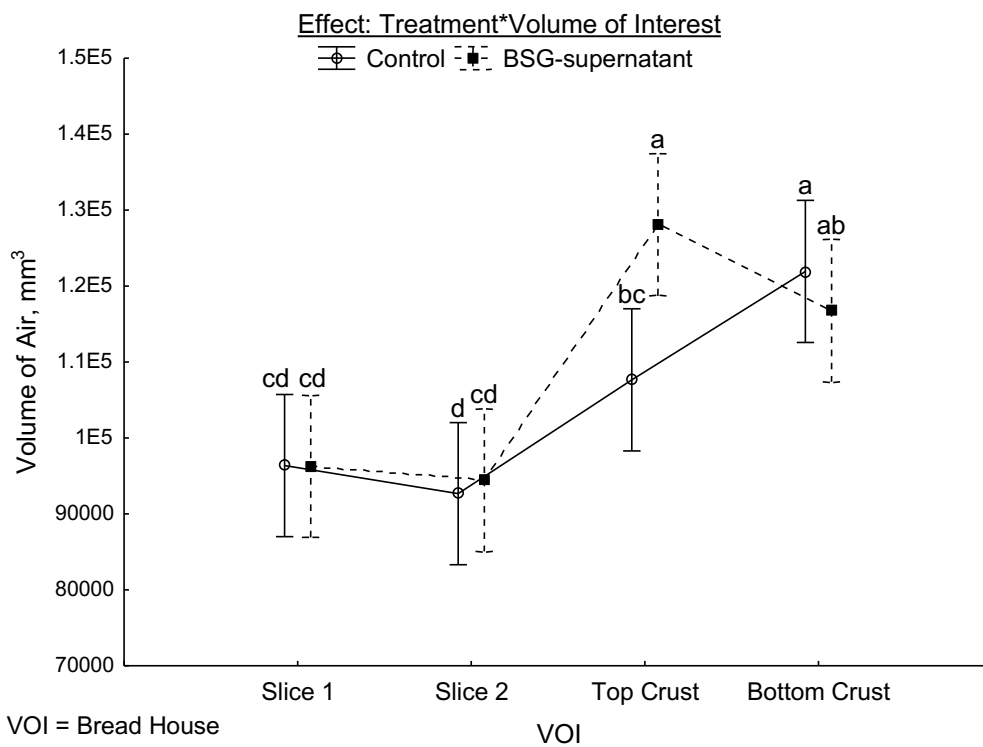


Figure 22 VOI porosity, as a function of its internal volume of air, as measured by X-ray μ CT, and affected by the interaction between the VOI, and the Treatment effects. Vertical lines denote 95% confidence intervals. Indicated scripts that differ indicate a significant difference ($P \leq 0.05$).

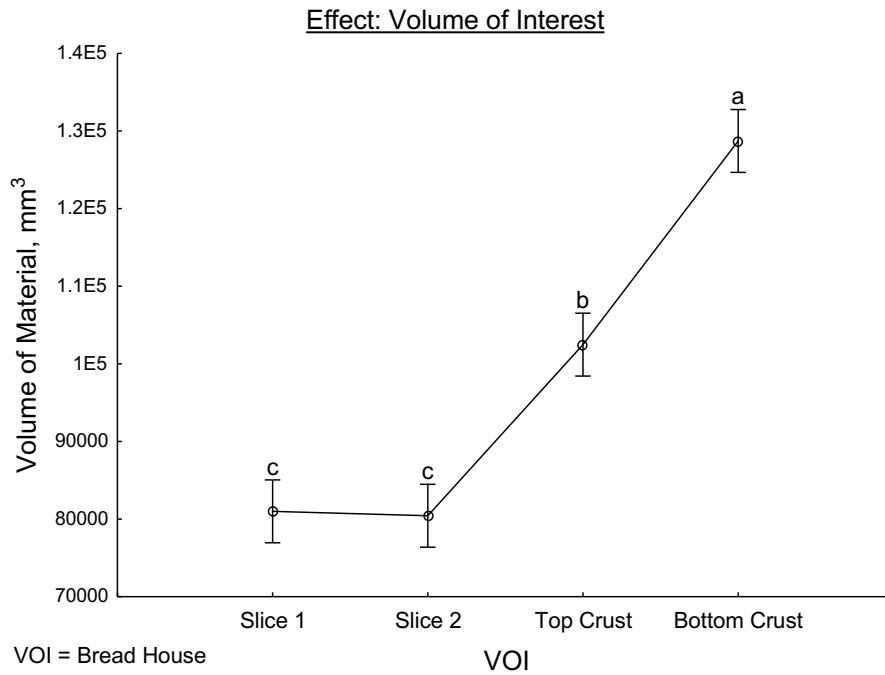


Figure 23 VOI porosity, as a function of its internal volume of material (crumb), as measured by X-ray μ CT and affected by the VOI-effect. Vertical lines denote 95% confidence intervals. Indicated scripts that differ indicate a significant difference ($P \leq 0.05$).

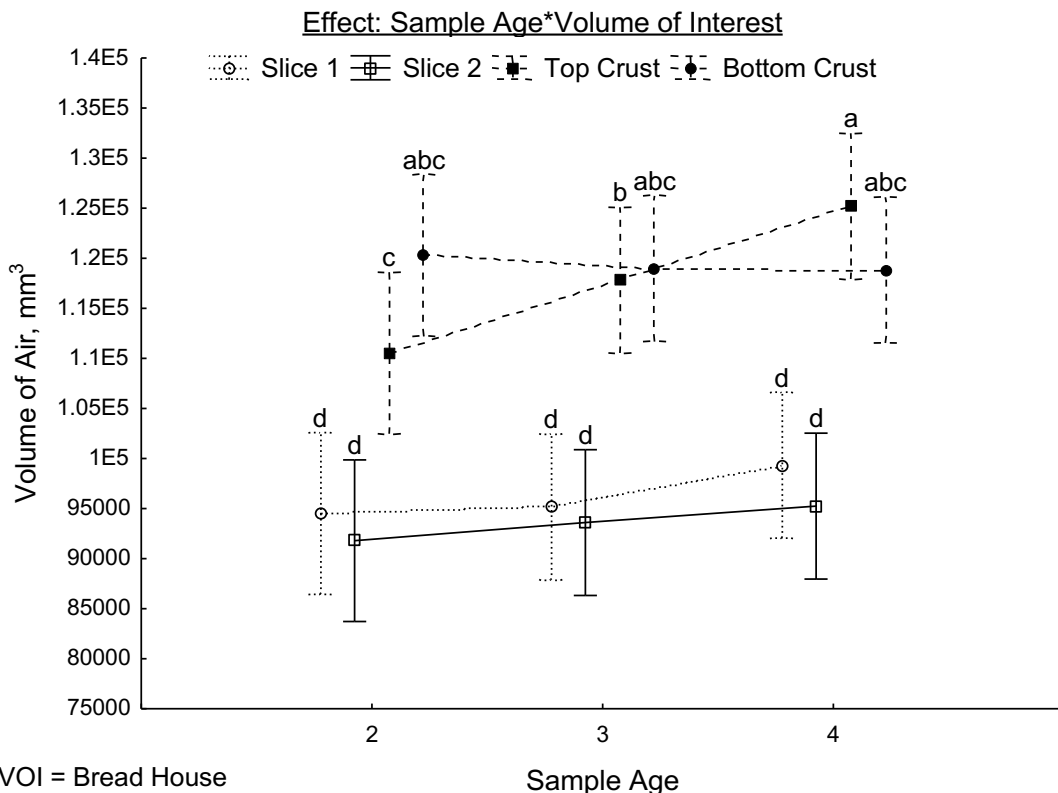


Figure 24 VOI porosity, as a function of its internal volume of air, as measured by X-ray μ CT, and affected by the interaction between the progress in loaf shelf-life (Sample Age) and its interaction with the VOI-effect. measured in days. Vertical lines denote 95% confidence intervals. Indicated scripts that differ indicate a significant difference ($P \leq 0.05$).

Bread Crumb Density

Both the attenuation of x-rays, referred to as the grey value distribution of the sample volume, and the relative density, calculated from these values (**Eq.1**) were significantly affected by both the age of the sample, and the VOI considered. Due to the Bread sample VOI reconstruction consisting of three geometrically different components, top- and bottom crust as well as two slices, the VOI was expected to have a significant effect on the grey value distribution (**Figure 25 & 26**) of the sample (**Table 26**).

Table 26 General Linear Models for the crumb density of bread samples as affected by the VOIs within the Bread sample VOI reconstruction VOIs, as affected by Treatment, Sample Age and Volume of Interest (VOI).

Effect	p-values						
	Treatment	Age	VOI	Treatment *Age	Treatment *VOI	Age*VOI	Treatment* Age*VOI
Grey value distribution, (\bar{x})	0.89621	0.04192	0.00946	0.50828	0.18574	0.66721	0.93439
Relative density (g/cm ³), (\bar{x})	0.74140	0.02831	0.00000	0.29517	0.54808	0.06216	1.00000

Probability values, $p \leq 0.05$, indicate significant interaction between parameter and variable, or between variables.

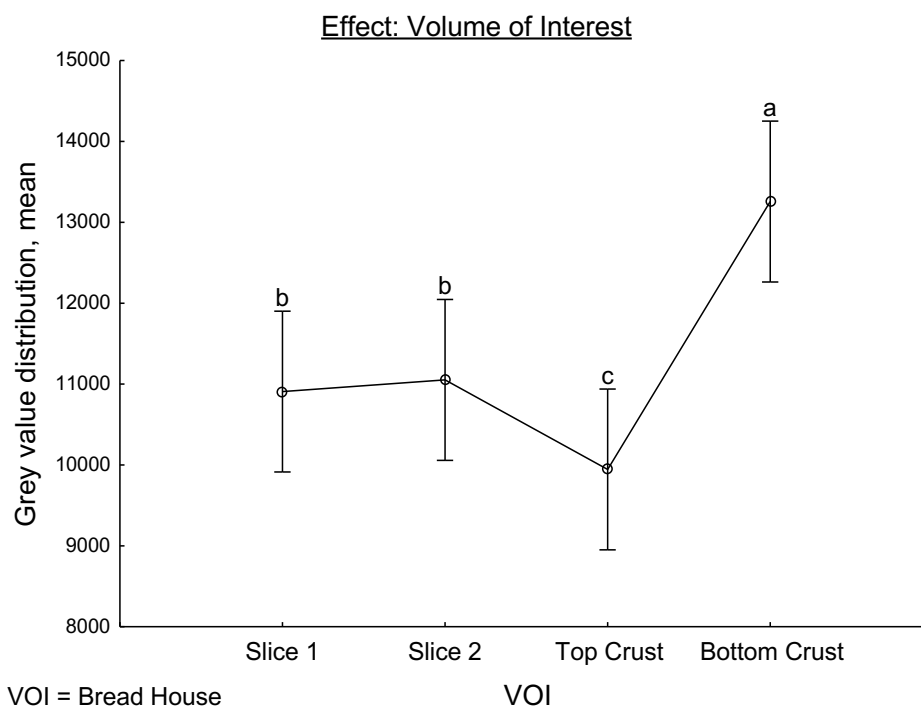
The bottom-crust VOI had a significantly greater grey-value distribution and mean relative density than the top-crust VOI, regardless of the treatment (**Table 27**). Simultaneously the top-crust VOI had a significantly greater grey-value distribution and mean relative density than both of the slice volumes, Slice 1 and 2 (**Table 27**). Although the increase was insignificant, the substitution of the baking water within the bread formulation, increased the grey-value distribution and mean relative density of all VOIs within the Bread sample VOI reconstruction (**Table 27**).

Table 27 Determining the difference, between the control- and treatment formulations as affected by the interaction between treatment*VOI factors.

Treatment*VOI				
VOI = Bread House	Slice: 1 (n = 6)	Slice: 2 (n = 6)	Crust: Top (n = 6)	Crust: Bottom (n = 6)
Grey value distribution, (\bar{x})				
Control	10947.77±1954.76 ^{ce}	11187.86±2025.13 ^{ce}	10085.21±2063.92 ^{df}	13116.77±1941.65 ^{ab}
BSG-supernatant	11392.12±2642.73 ^{bcd}	11420.17±2557.98 ^{bcd}	10373.89±2726.39 ^{ef}	13805.30±2968.67 ^a
% Increase/decrease	4.07	2.08	2.86	5.25
Relative density (g/cm³) (\bar{x})				
Control	0.40±0.07 ^{ce}	0.41±0.07 ^{ce}	0.37±0.08 ^{df}	0.48±0.07 ^{ab}
BSG-supernatant	0.42±0.10 ^{bcd}	0.42±0.09 ^{bcd}	0.38±0.10 ^{ef}	0.51±0.10 ^a
% Increase/decrease	5.00	2.44	2.70	6.25

Superscripts per measured parameter, within the same column or row, that differ, differ significantly from each other as $P \leq 0.05$.

*represents an interaction

**Figure 25** Grey-value distribution of the bread as affected by the VOI-effect. Vertical lines denote 95% confidence intervals. Indicated scripts that differ indicate a significant difference ($P \leq 0.05$).

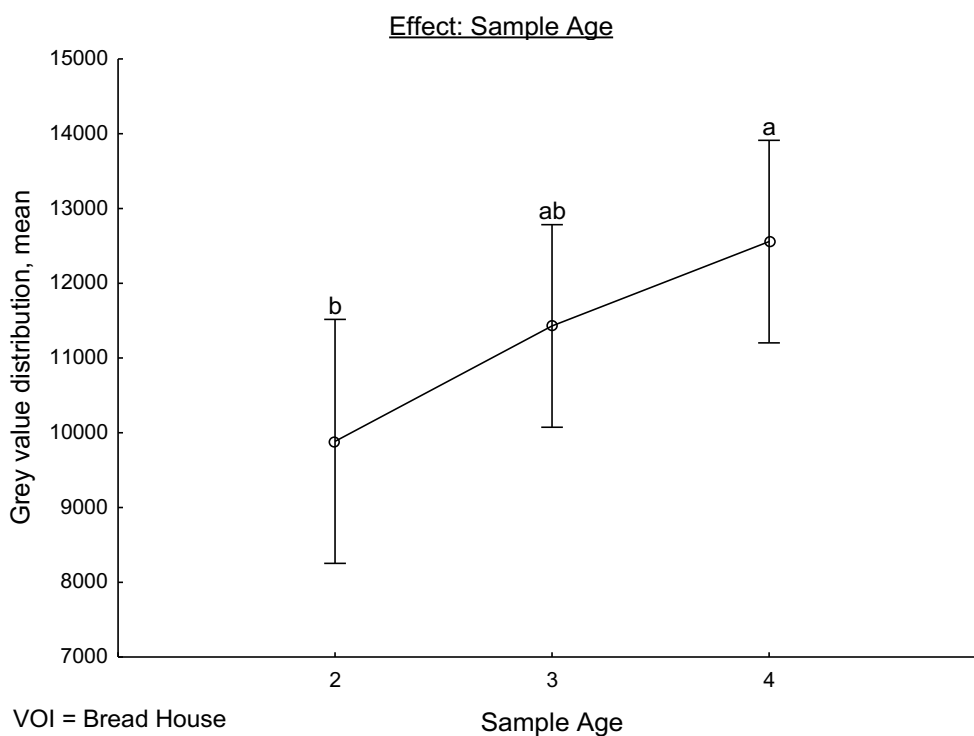


Figure 26 Grey-value distribution of the bread as affected by the age of the sample. Vertical lines denote 95% confidence intervals. Indicated scripts that differ indicate a significant difference ($P \leq 0.05$).

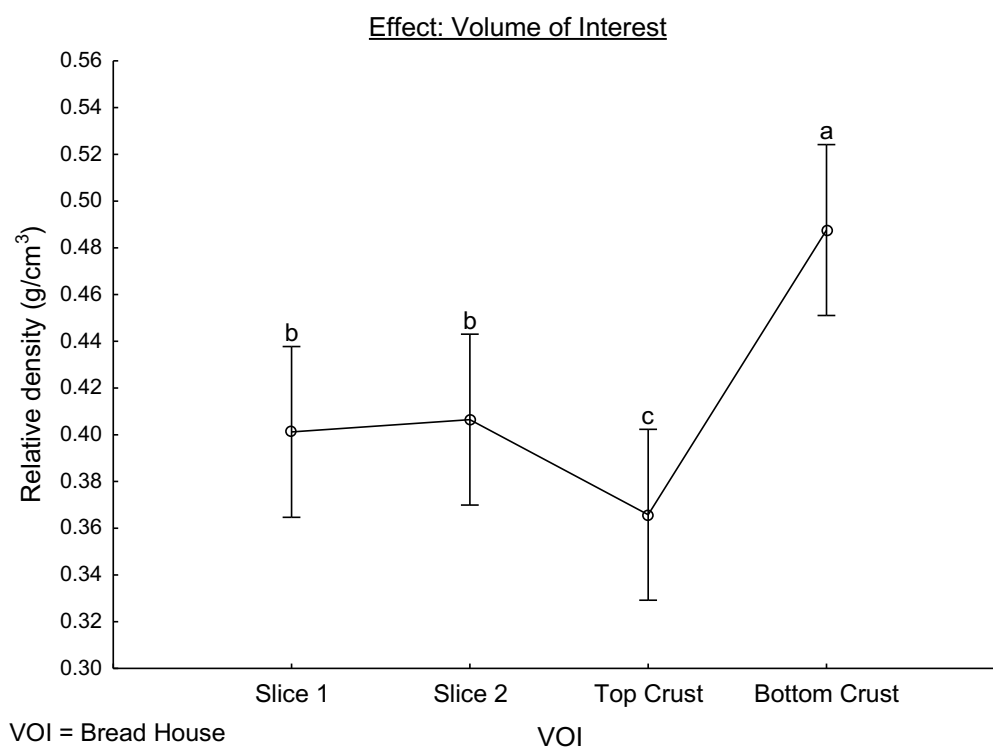


Figure 27 Relative density of the bread sample as affected by the VOI-effect. Vertical lines denote 95% confidence intervals. Indicated scripts that differ indicate a significant difference ($P \leq 0.05$).

The general linear models for the cell size- and distribution properties, as analysed using foam structure analysis during X-ray μ CT analyses, are illustrated in **Table 28**. The mean- and maximum cell size/volume within the bread's foam structure are the only parameters that are significantly affected by the VOI effect.

Table 28 General Linear Models for crumb properties as analysed using the Foam Structure analysis function of the VGStudio Max software package ($P \leq 0.05$)

Effect	p-values						
	Treatment	Age	VOI	Treatment *Age	Treatment *VOI	Age*VOI	Treatment *Age*VOI
Cell size, minimum	0.27158	0.49638	0.29681	0.1253	0.53323	0.38644	0.33448
Cell size, (\bar{x})	0.37929	0.38366	0.00000	0.12485	0.59582	0.93722	0.06611
Cell size, maximum	0.20050	0.89927	0.00155	0.42999	0.84952	0.44652	0.44652
Strut thickness, (\bar{x})	0.99525	0.92238	0.68340	0.08417	0.94673	0.79515	0.79515
Strut thickness, maximum	0.43712	0.77416	0.38787	0.49901	0.76023	0.50713	0.50713

Foam structure analysis: cell size and distribution within the bread sample foam structure

The purpose of measuring the distribution of cell- size and frequency was in order to compliment the two-dimensional C-Cell data extracted from the same sample sets, as a means of holistically describing the bread-foam structure, representing its micro-structure, and its potential change during a monitored three-day shelf-life period. The mean cell size of the slice VOIs (slice 1 and 2) were significantly smaller than that of the Top- and Bottom-crust VOIs (**Figure 28 & 29**), although the minimum cell size did not differ significantly per VOI or treatment, when evaluated at a 5% significance level (**Table 29**).

The control formulation showed a significant increase in minimum cell size from day 2 to 4 of the bread sample age (**Table 30**), whilst the mean cell size decreased significantly from days 2 to 3. There is no significant difference between treatments, although the BSG-supernatant samples showed a consistent minimum and mean cell size during the shelf-life period.

Table 29 Treatment vs. Volume of interest. Determining the difference, if any, between Bread sample VOI reconstruction volumes of interest (VOI) and treatment applied.

Treatment*VOI				
VOI = Bread House	Slice: 1 (n = 6)	Slice: 2 (n = 6)	Crust: Top (n = 6)	Crust: Bottom (n = 6)
Cell size (mm³) minimum				
Control	1.86±1.55 ^{ab}	1.69±1.80 ^{ab}	1.32±1.76 ^{ab}	0.91±1.25 ^b
BSG-supernatant	1.59±1.60 ^{ab}	2.48±1.42 ^a	1.55±1.99 ^{ab}	1.43±1.47 ^{ab}
% Increase/decrease	-14.52	46.75	17.42	57.14
Cell size (mm³) (\bar{x})				
Control	94.17±7.22 ^{bcd}	91.13±7.21 ^{cd}	100.57±13.58 ^{ab}	104.56±10.00 ^a
BSG-supernatant	88.99±8.63 ^d	87.67±7.63 ^d	101.15±13.12 ^{ab}	101.99±10.09 ^{abc}
% Increase/decrease	-5.50	-3.80	0.58	-2.46
Cell size (mm³) maximum				
Control	901.76±262.50 ^{cd}	1048.48±288.17 ^{bcd}	1818.61±657.47 ^a	1367.38±682.97 ^{abc}
BSG-supernatant	917.04±218.62 ^{cd}	828.55±166.79 ^d	1544.54±641.18 ^{ab}	1113.20±416.40 ^{bcd}
% Increase/decrease	1.69	-20.98	-15.07	-18.59
Strut thickness (mm) (\bar{x})				
Control	0.47±0.31 ^a	0.49±0.33 ^a	0.49±0.28 ^a	0.54±0.34 ^a
BSG-supernatant	0.52±0.32 ^a	0.57±0.31 ^a	0.51±0.30 ^a	0.56±0.32 ^a
% Increase/decrease	10.64	16.32	4.08	3.70
Strut thickness (mm) maximum				
Control	2.35±0.74 ^a	2.43±0.77 ^a	2.60±1.75 ^a	2.23±0.97 ^a
BSG-supernatant	2.06±0.59 ^a	2.14±0.59 ^a	2.38±0.84 ^a	2.20±0.61 ^a
% Increase/decrease	-12.34	-11.93	-8.46	-1.35

Superscripts per measured parameter, within the same column or row, that differ, differ significantly from each other as P≤0.05.

*represents an interaction

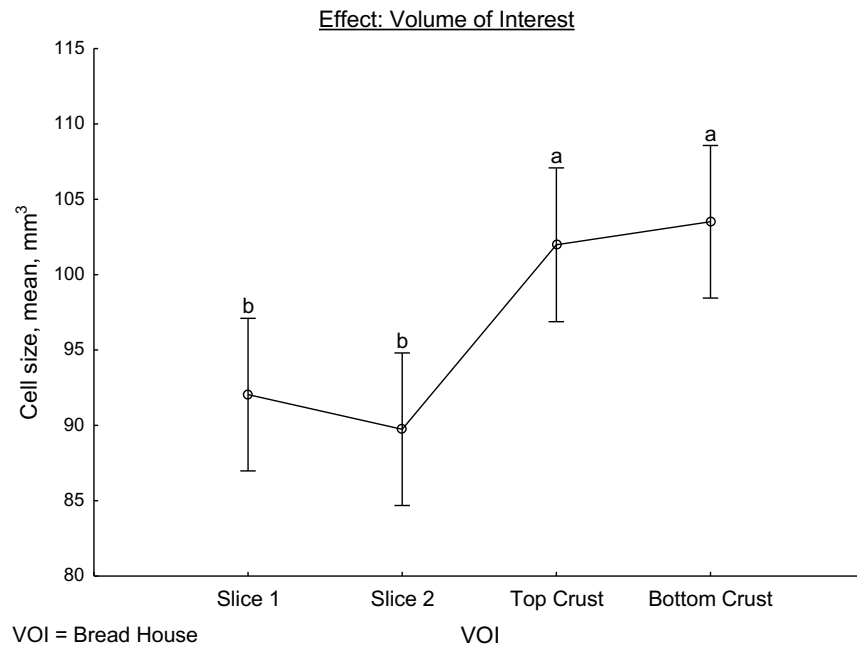


Figure 28 Foam structure analysis of the mean cell size within the bread micro-structure as affected by the VOI-effect. Vertical lines denote 95% confidence intervals. Indicated scripts that differ indicate a significant difference ($P \leq 0.05$).

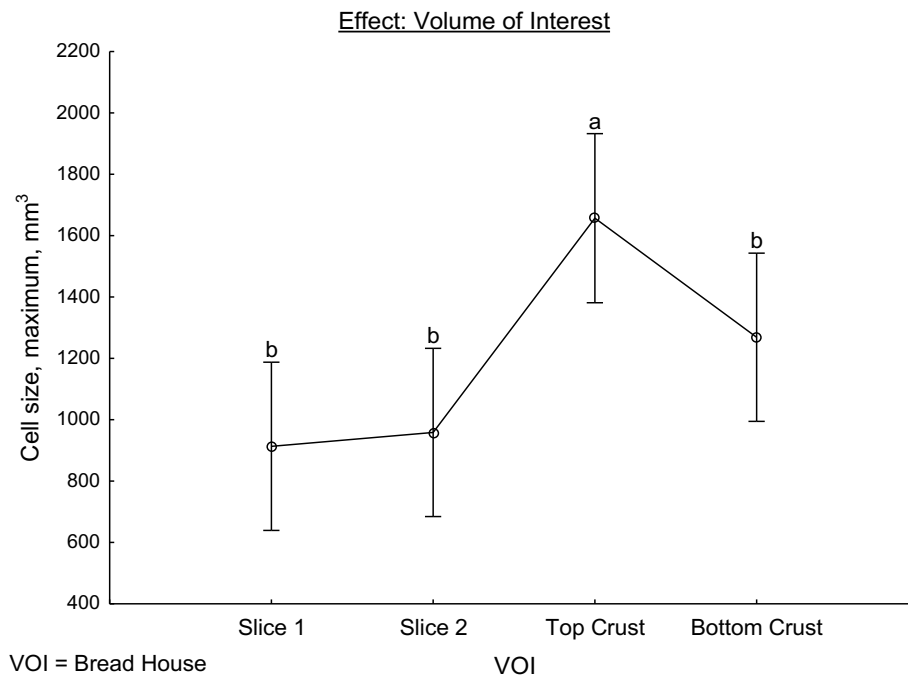


Figure 29 Foam structure analysis of the maximum cell size within the bread micro-structure as affected by the VOI-effect. Vertical lines denote 95% confidence intervals. Indicated scripts that differ indicate a significant difference ($P \leq 0.05$).

Table 30 Treatment vs. Sample Age. Determining the difference in foam structure (micro-structural) properties, between the two bread formulations, as affected by the interaction between the VOI and Treatment applied.

Treatment*Age			
VOI = Bread House	Day 2 (n = 12)	Day 3 (n = 12)	Day 4 (n = 12)
Cell size (mm³) minimum			
Control	0.78±1.40 ^b	1.42±1.63 ^{ab}	1.92±1.61 ^a
BSG-supernatant	1.85±1.99 ^{ab}	1.88±1.58 ^{ab}	1.59±1.53 ^{ab}
% Increase/decrease	137.18	32.39	-17.19
Cell size (mm³) (\bar{x})			
Control	100.52±15.21 ^a	96.82±10.77 ^b	96.46±7.45 ^b
BSG-supernatant	93.53±10.79 ^{ab}	95.91±12.24 ^{ab}	94.67±12.55 ^{ab}
% Increase/decrease	-6.95	-0.94	-1.86
Cell size (mm³) maximum			
Control	1345.69±620.26 ^a	1275.46±662.69 ^a	1251.57±578.98 ^a
BSG-supernatant	1078.79±515.51 ^a	1115.17±467.06 ^a	1081.91±483.75 ^a
% Increase/decrease	-19.83	-12.57	-13.56
Strut thickness (mm) (\bar{x})			
Control	0.48±0.33 ^a	0.41±0.31 ^a	0.60±0.28 ^a
BSG-supernatant	0.55±0.31 ^a	0.60±0.29 ^a	0.47±0.31 ^a
% Increase/decrease	14.58	46.34	-21.67
Strut thickness (mm) maximum			
Control	2.45±0.59 ^a	2.13±0.76 ^a	2.64±1.57 ^a
BSG-supernatant	2.10±0.65 ^a	2.28±0.61 ^a	2.18±0.73 ^a
% Increase/decrease	-14.29	7.04	-17.42

Superscripts per measured parameter, within the same column or row, that differ, differ significantly from each other as $P \leq 0.05$.

*represents an interaction

Chapter 5

Discussion

BSG-supernatant composition

The supernatant consists of 97.99% water, measured as moisture content and 2.01% accounted for by the TDS(%) and TSS(%) (**Table 7**). The pH of the supernatant (**Table 7**) was determined to be below that of water (*ca.* pH=7), possibly attributed to the acetic acid concentration, *ca.* 0.56% (g/L), detected within the supernatant (**Table 8**). The BSG-supernatant, with a pH (4.2) is below that of the isoelectric point of wheat gluten-proteins, glutenin and gliadin (Avramenko *et al.*, 2018). The decrease in pH of the dough system has the potential to be beneficial to the bread sample quality. In the baking industry the pH of the dough is reduced as a result of subjecting the bread flour to a chlorination pre-treatment (DAFF, 2017).

The sum of the total dissolved solids (TDS) and total suspended solids (TSS) (**Table 7**) consisted of the fine spent barley particulate matter within the supernatant, extracted as a consequence of the applied shear-force from the screw-press used to extract the BSG-liquid fraction (**Figure 1**). The mineral content of the supernatant is reflected in the measured ash percentage (**Table 7**). These minerals are estimated to be calcium, phosphorous and selenium, based on the analyses of BSG in reviewed literature (Duarte *et al.*, 2008; Meneses *et al.*, 2013).

In order to analyse the supernatant using HPLC, the samples were subjected to acid hydrolyses (Gil-Martinez, 2016). The acid hydrolysis of triacylglycerols results in the formation of glycerol and carboxylic acid by-products. The carboxylic acid concentration within the supernatant was measured as the acetic acid content (**Table 8**). The combination of the glycerol and acetic acid detected during analysis reflects, to a certain degree of the triacylglycerol concentration within the BSG-supernatant. As the triacylglycerols are from the spent barley grains and of plant origin it is estimated to have a low degree of saturation. This is substantiated by the empirical ratio of glycerol to acetic acid which is greater than 1:3. BSG typically contains *ca.* 7 to 10% lipid concentration, as measured on a dry basis (del Río *et al.*, 2013). The lipid content of the BSG-supernatant was also attributed to the applied shear-force from the screw-press used to extract the BSG-liquid fraction. The ethanol (EtOH) concentration detected within the BSG-supernatant is attributed to EtOH produced as a by-product of the degradation of triacylglycerols, which occurs during the acid-hydrolysis sample preparation required to analyse the supernatant sample, according to the HPLC analyses (**Table 8**).

Due to the inherent inefficiency of the mashing step during beer production, *ca.* 5 to 10% of the total fermentable sugars are still present in the “Spent Grain” after the wort has been drained into the boiling tank (Mussatto *et al.*, 2006). The range in concentration of the residual fermentable sugars is dependant on the difference between the extraction efficiency of different brewing systems/brew houses.

Through the use of a refractometer, the oligosaccharide concentration within the BSG-

supernatant was determined in degrees Brix (°Bx) (AACC International, 1999e). Refractometer results indicated that the supernatant contains ca. 5.0 g of sucrose per litre of BSG-supernatant (**Table 7**). The glucose concentration is close to this estimation, at ca. 6.6 g per litre of supernatant (**Table 8**). Using the BSG-supernatant as a baking water thus increases the concentration of mono- and oligosaccharide concentration within the lean bread formulation from 1.0% sucrose to ca. 1.3% (g/g of flour) along with an increase in glucose of ca. 0.4% (g/g of flour). The increase of mono- and oligosaccharide concentration within a bread formulation has been determined to decrease the rate of retrogradation of both amylopectin and amylose starch components (Wang *et al.*, 2015)

Both sucrose and glucose are metabolised by yeast to produce CO₂ and EtOH, limited by the concentration of fermentable sugars, when under favourable conditions (<40°C) (FAO, 1947). Increasing the fermentable sugar content within a bread formulation has the potential to increase the dough proof height, due to the increased CO₂(g) produced. This was observed for the BSG-supernatant dough samples during bread production.

The detected NSPs, within the BSG-supernatant, unequivocally originated from the spent barley grains used to extract the BSG-supernatant. The NSP concentration within the BSG-supernatant includes AXs (**Table 8**), which are known to be beneficial to the micro-structural homogeneity of the bread product, as well as the rate of bread-staling (Gray and Bemiller, 2003; Izydorczyk, 2009; Kwaśniewska *et al.*, 2014). HMF and furfural are known to be prevalent in BSG, whilst it could also have been produced during the acid hydrolysis of glucose within the supernatant, as part of its sample preparation for HPLC analysis. Since the detected concentration of these two compounds were low, their origin is assumed to be from the BSG, and extracted during screw-press processing (**Figure 1**).

Bread flour quality

A lean dough formulation comprises wheat flour, water, yeast, salt, sugar, and shortening (FAO, 1947; Cauvain and Young, 2000). The two main ingredients that determine the resulting bread's quality are the quality of the wheat flour and the amount of water used (Mondal and Datta, 2008; Shehzad *et al.*, 2013). The ingredients that are mixed, and how they are mixed to form a dough, determines the sensory aesthetic of the bread loaf produced (Mondal and Datta, 2008).

For the purpose of this investigation, proximate- and rheological analyses were employed to verify the quality of the bread flour, as well as evaluate and measure how replacing the water with BSG-supernatant affects the resulting bread dough and -loaf quality. In order to reduce additional variation, the bread flour was not treated with chlorine, as per convention and did not contain any shelf-life or nutrient improving additives (DAFF, 2017). According to the wheat quality guidelines and regulations from the South African Department of Agriculture, Forestry, and Fisheries (DAFF), the wheat (**Table 9**) and flour (**Tables 10, 11, 13, and 14**) used to produce bread flour and bake bread samples with for this investigation, was of 1st Grade quality (DAFF, 2016, 2017; SAGL, 2018).

Bread flour quality was confirmed during rheological analyses (**Tables 10, 11, 13 and 14**). The

stability (P), distensibility (L), curve configuration ratio (P/L) and dough strength (W) measured for the bread flour used in this investigation (**Table 11**), were all indicative of a bread flour that will produce a bread product of excellent quality, according to the standards stipulated in regulations (DAFF, 2017; SAGL, 2018). These parameters correlate with the dough-matrix's gas retention capacity, the loaf volume, bread crumb- and pore- structure homogeneity, and overall consumer acceptability (Vodovotz, 2007; Cauvain, 2009b).

The colour of the wheat flour determines the colour of the white-bread product (SAGL, 2018). With regards to this investigation, the colour of the flour was a controlled variable (**Table 20**). The observed whiteness index (WI) of a slice of white bread is an important sensory parameter to consumers (Vodovotz, 2007; Kwaśniewska *et al.*, 2014).

Effect of BSG-supernatant on Rheology

Due to the modernisation of instruments used to perform rheological analysis, only some of the rheological analysis could be performed with the BSG-supernatant as the source of water. The analyses were repeated for the water-flour mixtures. The Mixo- and Farinograph methods were used to quantify how the dough, made from flour and its bread formulation's source of water, deformed and flowed (Delcour and Hosenev, 2010c).

Farinographic measurements illustrated that replacing the water with BSG-supernatant is beneficial to the BA of the bread formulation, whilst showing a slight decrease in dough development time (DDT) and stability. The Falling Number was determined for the bread flour, which was greater than the stipulated minimum of 250 s, when using either dH₂O or BSG-supernatant during analysis (**Table 13**) (AACC International, 1999h; DAFF, 2016).

The effect of replacing water with BSG-supernatant, on the rate of hydration and the gelatinisation of starch was quantified during the analysis of the pasting properties of the bread flour (**Table 14**). The general linear models (**Table 15**) indicate that the treatment, age of the supernatant, as well as their interaction significantly affected the pasting properties of the bread flour ($P \leq 0.05$). Irrespective of the "age" of the supernatant, it had a significant effect on all measured parameters encompassing the pasting properties of the bread flour, including the peak viscosity, the trough depth, the final viscosity and the time required to reach the peak viscosity (**Table 14**). The sample age of the supernatant also had a significant effect on the bread flour's pasting properties (**Table 14**). The *treatment* effect on the pasting properties of the flour was attributed to the sum of the TSS(%) and TDS(%) within the supernatant, as well as the possible residual amylolytic activity, measured as part of the falling number analysis. The effect of the BSG-supernatant's "age" could also be attributed to the residual enzyme activity within the supernatant, increasing slightly per day it was refrigerated post-defrosting (**Figure 2**).

As BSG is produced from malted barley, it is possible that this could be due to the presence of residual alpha- and beta-glucanase (Mussatto *et al.*, 2006) activity which was extracted, into the supernatant through the shear-force of the screw-press. It was possible to deduce that the BSG-

supernatant showed an enzyme activity of its own, as it also significantly decreased the Falling Number of the bread flour (**Table 13**).

The decrease in dough resistance-to-mixing, measured during Mixo- and Farinographic analysis (**Table 13**) agrees with the possibility of the BSG-supernatant having its own amylolytic activity. The increase in the overall amylolytic activity within the bread formulation, could benefit the dough proof volume and the homogeneity of the bread product's crumb, as well as the rate of starch retrogradation as the bread product ages (Della Valle *et al.*, 2014; Wang *et al.*, 2015).

Bread Analyses

Texture Analysis

The texture of a bread product directly influences the consumer's perception of product freshness (Cauvain, 2009b). The micro-structural deterioration of bread quality is a consequence of bread staling, which is the perceived loss of bread product freshness, independent of microbial deterioration (Choi *et al.*, 2010). The most obvious effect of bread staling is the increase in bread crumb- firmness accompanied by a decrease in its resilience (Vodovotz, 2007).

Bread's micro-structure has been described as having a viscoelastic nature, due to its non-linear response to strain (Lagrain *et al.*, 2012). The firmness of the bread's crumb is measured, by a Texture Analyser with a pre-programmed stress profile, mimicking a consumer's bite.

As the texture of bread's foam-like structure is the result of its mixing, proofing, sheeting and shaping and baking conditions (Della Valle *et al.*, 2014) these breadmaking parameters were controlled and monitored (**Table 3**) for all of the bread samples produced during this investigation. This was done in order to measure only the effect of replacing the baking water with BSG-supernatant in a lean dough formulation (**Table 2**). The texture of a slice of bread is dependent on many factors, including the crumb-size and density, the crust thickness, the porosity of the bread's structure and the amount of moisture within the bread at the time of consumption and texture analysis. The bread samples made from BSG-supernatant did not differ significantly from the control formulation samples on either of the considered shelf-life days (Days 2, 3 and 4 post-baking).

C-Cell Visual Analysis

BSG-supernatant has an opaque appearance. The effect of replacing water with BSG-supernatant in a lean bread formulation, on the colour of the crumb of white bread, was determined to be insignificant.

The slice shape and colour properties were significantly influenced by the replicate effect. It is postulated that the replicate effect only became significant due to inconsistent loaf sizes. The replicate size variation is also noticeable in the measured slice area of the bread samples, regardless of their age. The interaction between the treatment and replicate effects were significant and so further substantiates the possibility that bread loaf size varied between replicates, regardless of the treatment. As the production of bread samples were outsourced to an external baking laboratory,

because of the calibre of their baking equipment, it is reasonable to assume that the variation in loaf size was attributed to the fact that the bread samples were baked in a pan without a lid, which would have constricted the expansion of the dough during baking and proofing stages. The replicate effect is also evident in the a^* and b^* colour properties (**Figures 15 & 16**), with only a^* being affected by both the treatment, BSG-supernatant and the variation between replicates.

The general linear models from the C-Cell VA (**Table 19**) indicate that the age of the bread sample (Days 2, 3, and 4) significantly affected the concavity (%) (**Figure 12**) and slice area of the bread loaves (**Figure 13**). The age of the bread sample also significantly affected the slice brightness (**Figure 14**) as well as the measured CIElab (Kenten Jones) colours (**Figure 15, 16 & 17**). Although the cavity/hole morphology was quantified, there were no significant differences in the size (number, area, and volume) between the control- and BSG-supernatant breads as they progressed along the monitored shelf-life period (**Table 19 & 20**).

X-ray micro-Computed Tomography

The results of the bread sample analyses were used to determine if there was a significantly different rate of the bread sample's staling during its shelf-life, attributed to the replacement of the baking water in a lean bread formulation with BSG-supernatant (**Table 2**). Baked food samples (Laverse *et al.*, 2002; Lim and Barigou, 2004; Koksel *et al.*, 2016), including bread (Cafarelli *et al.*, 2014; Van Dyck *et al.*, 2014; Guessasma and Nouri, 2015) have been analysed using X-ray μ CT.

As the bread proceeded across its shelf-life, the surface area, total volume, volume of material and porosity did not change significantly for bread samples made from either the control- or BSG-supernatant bread formulation (**Table 21**). The volume of the bread material, excluding air, was significantly affected by the interaction of the treatment and age of the bread sample, although the two bread formulations did not differ significantly from each other, on any of the considered shelf-life days. The age of the sample still had a significant interaction with both the grey value distribution and the relative density (**Table 26**). It would seem that the only explanation for this is due to the change in relative density during the ageing of the bread samples as a consequence of bread staling.

This correlates with the observed shrinkage/expansion observed for the bread sample crumb-structure when evaluating the foam structure of the Bread reconstruction VOIs (**Table 29 & 30**).

Microstructural changes: A consequence of bread staling

From the general linear models for the cell size, which was determined during the three-dimensional foam structure analyses enabled by X-ray micro-Computed Tomography it could be deduced that the cell size, mean and maximum were significantly dependent on the VOI evaluated (**Table 28**). And so, it was possible to confirm that the foam structure of the slices, representing the crumb size and distribution of the bread, were significantly different from the crumb-structure within the Top- and Bottom crust VOI. The interface between the crust and the surrounding atmosphere has been determined to be where the greatest rate of moisture loss occurs (Monteau *et al.*, 2017), which indicates that an open pore structure is more susceptible to moisture loss than a more densely-

packed pore structure.

Purhagen *et al.*, (2008), determined through the use of Textural Analysis (TA) and Differential Scanning Calorimetry (DSC), that the loss and migration of moisture (water) plays a greater role in the staling of bread than does the occurrence of amylopectin-retrogradation (Purhagen *et al.*, 2008). During the shelf-life period, the moisture in the bread becomes redistributed (Czuchajowska and Pomeranz, 1989; Buera *et al.*, 1998).

The water entrapped within the structural confines of the bread product is able to soften the food foam as it ages, due to water's ability to plasticize glassy polymers found within the micro-structure of bread (Ablett *et al.*, 1986). Fessas *et al.* determined that the water in the bread product has a high thermodynamic activity (>95%), enabling the water to migrate freely through the pore- and crumb-structure of a bread-foam as long as the favourable chemical potential gradient exists within the bread's structural confines (Fessas and Schiraldi, 2001). As the different polymer phases within the bread product become increasingly incompatible as the bread product ages (hours, days) the polymers can utilise their water's thermodynamic activity to aid in conformational and phase changes during the product's shelf-life (Vodovotz, 2007) such as which occurs during the retrogradation of starch components amylopectin, and amylose. The rate of retrogradation is determined by the rate of moisture migration primarily due to hysteresis (Hoseney, 1986; Gray and Bemiller, 2003; Vodovotz, 2007). It is hypothesised that the hysteresis taking place during bread ageing, can be attributed to capillary condensation within the bread's pore- and crumb-structure (Andrade *et al.*, 2011).

The recorded grey values were the result of X-ray attenuation by the sample, recorded as integers in Hounsfield Units (HU) (Wall and Rajagopalan, 2013). By convention, water is assigned an HU value of zero whilst air has a -1000 HU (Wall and Rajagopalan, 2013). The smaller the mean grey value, related to the attenuation of X-rays by the sample, the less dense the sample volume is (Wall and Rajagopalan, 2013; Schoeman *et al.*, 2016).

The measurements completed during C-Cell Visual Analysis, were all two dimensional, whilst those made during X-ray micro-computed tomographic analyses were three dimensional. And so, it is important to consider the similarities and differences when the same parameters are measured, with- or without considering the third dimension. X-ray micro-Computed tomographic results are considered more representative of the sample parameters measured as it is measured with greater accuracy and precision than that of the established two-dimensional analyses. As it is still a relatively new technique, processing techniques/methods have not yet been established for all areas of research.

Whilst comparing the results from both C-Cell and X-ray μ CT analyses the following could be deduced. The number of cells, cell diameter and area of cells measured by the C-Cell VA reflecting the crumb-fineness did not differ significantly between formulations on either of the monitored shelf-life days (**Table 20**). The crumb fineness was measured during X-ray μ CT post-acquisition processing, as the frequency of cells per identified cell size (mm^3) and recorded as the mean cell

size (mm^3) within each bread sample VOI. The control formulation showed a significant increase in minimum cell size from day 2 to 4 of sample age, whilst the mean cell size decreased significantly from days 2 to 3 (**Table 30**). There was no significant difference between treatments, although the BSG-supernatant samples showed a consistent minimum and mean cell size during the monitored shelf-life period (**Table 30**).

The X-ray μCT analyses measured the increase in slice-firmness as the increase in relative density (g/cm^3) of the bread sample's various VOIs. This was made possible through quantifying the X-ray attenuation of the individual voxels within the sample VOI, along with an internal reference standard during each bread sample's image acquisition. The results gained correlated with that of the TA of the bread sample slices, with regards to the increase in firmness of the bread samples. The benefit of the μCT analyses is that the relative density, can be related to the WHC of the bread samples. Based on the TA of samples from both bread formulations, there is no significant difference in the measured resistance to compression (firmness), between the control- and treatment samples. The increased relative density of the bread slice VOIs, of the BSG-supernatant samples, are indicative of a greater moisture content within the treatment samples. It can thus be said that the WHC of the treatment samples crumb-structure, and foam-structure as a whole, was greater than that of the control samples.

Chapter 6

Conclusion

The fine spent barley particulate matter present within the supernatant was extracted as a consequence of the applied shear-force from the screw-press used to extract the BSG-liquid fraction. The ash content of the supernatant originated from the suspended BSG particulate, and so the use of the supernatant as an alternative baking water could benefit the mineral concentration incorporated into a bread formulation. The composition of BSG-supernatant is very close to that of water's, consisting of ca. 98% moisture (water), and a small fraction of TDS and TSS. In the context of bread formulations, the supernatant was determined to have a notable concentration of glucose and AX, with AX measured as the combined arabinose and xylose concentration.

Within the context of established baking-industry bread quality standards, the effect of using BSG-supernatant as an alternative baking water on the rheological properties of the bread flour was insignificantly different from that of the interaction of water and the bread flour. The factors within the research assignment's experimental design and their interaction(s) were evaluated and illustrated in order to substantiate the insignificant difference between treatments.

BSG-supernatant was determined to be an effective alternative baking water, when incorporated into a lean bread formulation. The evaluation of bread quality parameters currently used by the baking industry, were completed for both the control- and treatment formulation, across a shelf-life period (Days 2, 3 and 4), according to this research assignment's experimental design.

X-ray micro-Computed Tomography proved a useful method of evaluating the change in density of the bread's microstructure, across the monitored shelf-life period, accompanied by established TA and C-Cell VA methods used by the baking industry. From the statistical evaluation of bread quality parameters, from both control- and BSG-supernatant formulations, it was possible to deduce that there were no significant detrimental effects on both dough- and bread product quality when the baking water was completely replaced by BSG-supernatant. However, based on the difference in relative density and X-ray attenuation values between formulations, it could be deduced that the WHC of the bread-crumbs within treatment bread samples was greater than that of the control samples on all monitored shelf-life days (Days 2, 3, and 4), which is known to be beneficial to decreasing the rate at which bread staling occurs.

The use of BSG-supernatant as an alternative baking water could potentially decrease the amount of safe, clean drinking water that is currently used to produce white bread loaves, as well as several other popular types of bread. The use of the BSG-supernatant is also a viable method of increasing the shelf-life of the BSG-solid, fibrous material in order to be utilised within other industrial sectors such as livestock feed, the extraction of value-added components for the nutraceutical and pharmaceutical industry, as well as other proposed innovative routes reviewed in the literature. Increasing the shelf-life of the BSG-solid, would increase its potential for utilisation prior to being

designated to landfills and becoming an environmental hazard.

It is suggested that the screw-press operation, proposed in this investigation, be connected directly to the point of BSG removal connected to the brewery's mash-tun. The removal of the majority of the moisture from the BSG increases its ease of transport from its production point, to other processing facilities. The extraction of the supernatant requires no chemical pre-treatments and reduces the weight of the fresh BSG which needs to be relocated to its final destination, whether it be another food processing plant, a nearby farm, biorefinery or landfill.

Recommendations

In order to holistically evaluate the intricacies of the BSG-supernatant and its potential for use as an alternative baking water, the following are suggested objectives for a future research project in order to further characterise the supernatant and its potential.

The proximate and compositional analyses of BSG-supernatant extracted from different beer styles and breweries, would enable standardisation of the composition of the supernatant. Microbial analyses would shed light on the sustainable use of BSG-supernatant in food products, with regards to consumer health and safety. Sensory evaluation of bread samples made with BSG-supernatant as its baking water would impact the feasibility of the bread industry adopting the BSG-supernatant as an alternative baking water.

The quantification and evaluation of the residual enzyme activity within the supernatant would aid in evaluating its potential for application into baked food product formulations.

In order to proceed with a pilot-scale study, the logistics concerning the implementation of a screw-press within a brewery, including its operation and maintenance need to be evaluated. This includes the transport of the extracted BSG-supernatant to bakeries.

Chapter 7:

References

- AACC. (1999). Measurement of Bread Firmness by Universal Testing Machine, Method: 74-09. In: *AACC International Approved Methods*. Pp. 7–10. St. Paul, MN, U.S.A.: AACC International.
- AACC International. (1999a). Experimental Milling-Batch Method for Hard Wheat Method: 26-22.01. In: *AACC International Approved Methods*. Pp. 1–5. St. Paul, MN, U.S.A.: AACC International.
- AACC International. (1999b). *Moisture-Air-Oven Method: 44-15.02. AACC International Approved Methods*.
- AACC International. (1999c). Crude Protein-Combustion Method: 46-30.01. In: *AACC International Approved Methods*. Pp. 1–2. AACC International.
- AACC International. (1999d). Ash-Rapid (Magnesium Acetate) Method: 08-02.01. In: *AACC International Approved Methods*. Pp. 1–2. St. Paul, MN, U.S.A.: AACC International.
- AACC International. (1999e). Solids in Syrups — Refractometer Method: 80-51.01. In: *AACC International Approved Methods*. Pp. 1–4.
- AACC International. (1999f). Moisture: Modified Vacuum-Oven Method (44-40.01). In: *AACC International Approved Methods*. Pp. 16–17. St. Paul, MN, U.S.A.: AACC International.
- AACC International. (1999g). Mixograph Method: 54-40.02. In: *AACC International Approved Methods*. Pp. 1–6. AACC International.
- AACC International. (1999h). Determination of Falling Number Method: 56-81.03. In: *AACC International Approved Methods*. Pp. 1–4. AACC International.
- AACC International. (1999i). Alveograph Method for Soft and Hard Wheat Flour Method: 54-30.02. In: *AACC International Approved Methods*. Pp. 1–8. AACC International.
- AACC International. (2007). Damaged Starch-Amperometric Method: 76-33.01. In: *AACC International Approved Methods*. Pp. 1–2. AACC International.
- AACC International. (2009). General Pasting Method for Wheat or Rye Flour of Starch Using the Rapid Visco Analyser Method: 76-21.02. In: *AACC International Approved Methods*. Pp. 1–4. AACC International.
- AACC International. (2011). Rheological Behavior of Flour by Farinograph: Constant Flour Weight Procedure Method: 54-21.02. In: *AACC International Approved Methods*. Pp. 1–8.
- AACC International. (2017). Grains & Pulses. *Cereal Foods World*, **62**, 192–193.
- Ablett, S., Attenburrow, G.E. & Lillford, P.J. (Unilever R.L.U. (1986). The Significance of Water in the Baking Process. In: *Chemistry and physics of baking : materials, processes and products : the proceedings of an international symposium organised by the Food Chemistry Group of the Royal Society of Chemistry and the School of Agriculture of the University of Nottingham* (edited by J.M.V. Blanshard, P.J. Frazier & T. Galliard). Pp. 30–41. Royal Society of Chemistry.
- Aggelopoulos, T. & Bekatorou, A. (2013). Discarded Oranges and Brewer ' s Spent Grains as

Promoting Ingredients for Microbial Growth by Submerged and Solid State Fermentation of Agro-industrial Waste Mixtures, 1885–1895.

Ahmed, J. & Thomas, L. (2015). Effect of β -Glucan Concentrate on the Water Uptake, Rheological and Textural Properties of Wheat Flour Dough. *International Journal of Food Properties*, **18**, 1801–1816.

Aliyu, S. & Bala, M. (2011). Brewer's spent grain : A review of its potentials and applications, **10**, 324–331.

Aliyu, S. & Bala, M. (2013). Brewer's spent grain: A review of its potentials and applications. *African Journal of Biotechnology*, **10**, 324–331.

Andrade, R.D., Lemus, R. & Perez, C.E. (2011). Models of Sorption Isotherms for Food: Uses and Limitations. *Vitae-Revista De La Facultad De Quimica Farmaceutica*, **18**, 324–333.

Angold, R. (The L.R.R.C.U. (1975). Wheat Starch (structural aspects). In: *Bread: Social, Nutritional and Agricultural Aspects of Wheaten Breads* (edited by A. Spicer). Pp. 141–160. London: Applied Science Publishers Ltd.

Anonymous. (2017). Saving water in your home.

Avramenko, N.A., Tyler, R.T., Scanlon, M.G., Hucl, P. & Nickerson, M.T. (2018). The chemistry of bread making: The role of salt to ensure optimal functionality of its constituents. *Food Reviews International*, **34**, 204–225.

Barak, S., Mudgil, D. & Khatkar, B.S. (2014). Influence of Gliadin and Glutenin Fractions on Rheological, Pasting, and Textural Properties of Dough. *International Journal of Food Properties*, **17**, 1428–1438.

Barrera, G.N., Pérez, G.T., Ribotta, P.D. & León, A.E. (2007). Influence of damaged starch on cookie and bread-making quality. *European Food Research and Technology*, **225**, 1–7.

Bartolomé, B., Faulds, C.B. & Williamson, G. (1997). Enzymic Release of Ferulic Acid from Barley Spent Grain. *Journal of Cereal Science*, **25**, 285–288.

Beck, M., Jekle, M. & Becker, T. (2012). Impact of sodium chloride on wheat flour dough for yeast-leavened products. I. Rheological attributes. *Journal of the Science of Food and Agriculture*, **92**, 585–592.

Bloksma, A.H. (TNO C.F. and B.I.T. (1986). Rheological Aspects of Structural Changes during Baking. In: *Chemistry and physics of baking: materials, processes and products: the proceedings of an international symposium organised by the Food Chemistry Group of the Royal Society of Chemistry and the School of Agriculture of the University of Nottingham* (edited by J.M.V. Blanshard, P.J. Frazier & T. Galliard). Pp. 170–178. Royal Society of Chemistry.

Buera, M.P., Jouppila, K., Roos, Y.H. & Chirife, J. (1998). Differential Scanning Calorimetry Glass Transition Temperatures of White Bread and Mold Growth in the Putative Glassy State. *Cereal Chemistry Journal*, **75**, 64–69.

Cafarelli, B., Spada, A., Laverse, J., Lampignano, V. & Nobile, M.A. Del. (2014). X-ray microtomography and statistical analysis: Tools to quantitatively classify bread microstructure.

Journal of Food Engineering, **124**, 64–71.

Calibre Control International. (2014). C-Cell Colour Operational Manual (CC.400).

Carvalho, F., Esteves, M.P., Parajo, J.C., Pereira, H. & Gírio, F.M. (2004). Production of oligosaccharides by autohydrolysis of brewery's spent grain. *Bioresource Technology*, **91**, 93–100.

Cauvain, S.P. (2001). Breadmaking. In: *Cereals Processing Technology* (edited by G. Owens). Pp. 204–230. Cambridge: Woodhead Publishing.

Cauvain, S.P. (2009a). Other bakery ingredients. In: *More Baking Problems Solved*. Pp. 52–82.

Cauvain, S.P. (2009b). Bread and fermented products. In: *More Baking Problems Solved*. Pp. 83–127.

Cauvain, S.P. & Young, L.S. (2000). *Bakery Food Manufacture and Quality: Water Control and Effects*. Wiley.

Choi, Y.J., Kim, B.Y. & Baik, M.Y. (2010). Analytical methodology for bread staling. *Journal of Applied Biological Chemistry*, **53**, 389–400.

CSIR. (2008). Sustainability: Reducing the Human Footprint. *Science Scope*, 23–24.

Curren, M.S.S. & King, J.W. (2002). Sampling and Sample Food Analysis Preparation. In: *Comprehensive Analytical Chemistry* (edited by J. Pawliszyn). Pp. 873–874. Elsevier Science B.V.

Czuchajowska, Z. & Pomeranz, Y. (1989). Differential scanning calorimetry, water activity, and moisture contents in bread center and near-crust zones of bread during storage. *Cereal Chemistry*.

DAFF. (2016). Agricultural Product Standards Act (Act no. 119 of 1990). *Staatskoerant*, 17–29.

DAFF. (2017). Regulations relating to the grading, packing and marking of wheat products intended for sale in the Republic of South Africa. *Staatskoerant*, 11–27.

Davidou, S., Meste, M. Le, Debever, E. & Bekaert, D. (1996). A contribution to the study of staling of white bread: Effect of water and hydrocolloid. *Food Hydrocolloids*, **10**, 375–383.

Delcour, J.A. & Hosney, R.C. (2010a). Chapter 1: Structure of Cereals. In: *Principles of Cereal Science and Technology* (edited by J.A. Delcour & R.C. Hosney). Pp. 1–22. Minnesota: St. Paul, Minn.: AACC International.

Delcour, J.A. & Hosney, R.C. (2010b). Chapter 6: Glass Transition and Its Role in Cereals. In: *Principles of Cereal Science and Technology* (edited by J.A. Delcour & R.C. Hosney). Pp. 97–105. Minnesota: St. Paul, Minn.: AACC International.

Delcour, J.A. & Hosney, R.C. (2010c). Chapter 5: Rheology of Doughs and Batters. In: *Principles of Cereal Science and Technology* (edited by J.A. Delcour & R.C. Hosney). Pp. 87–96. Minnesota: St. Paul, Minn.: AACC International.

Delcour, J.A. & Hosney, R.C. (2010d). Chapter 2: Starch. In: *Principles of Cereal Science and Technology* (edited by J.A. Delcour & R.C. Hosney). Pp. 23–51. Minnesota: St. Paul, Minn.: AACC International.

- Delcour, J.A. & Hosney, R.C. (2010e). *Principles of Cereal Science and Technology. Journal of Cereal Science*. St. Paul, Minn: AACC International.
- Duarte, L.C., Carvalheiro, F. & Lopes, S. (2008). Yeast Biomass Production in Brewery 's Spent Grains Hemicellulosic Hydrolyzate, 119–129.
- Dyck, T. Van, Verboven, P., Herremans, E., Defraeye, T., Campenhout, L. Van, Wevers, M., Claes, J. & Nicolai, B. (2014). Characterisation of structural patterns in bread as evaluated by X-ray computer tomography. *Journal of Food Engineering*, **123**, 67–77.
- El-Shafey, E.I., Gameiro, M.L.F., Correia, P.F.M. & Carvalho, J.M.R. de. (2004). Dewatering of brewer's spent grain using a membrane filter press: A pilot plant study. *Separation Science and Technology*, **39**, 3237–3261.
- Fadda, C., Sanguinetti, A.M., Caro, A. Del, Collar, C. & Piga, A. (2014). Bread Staling: Updating the View. *Comprehensive Reviews in Food Science and Food Safety*, **13**, 473–492.
- Falcone, P.M., Baiano, A., Zanini, F., Mancini, L., Tromba, G., Montanari, F. & Nobile, M.A. Del. (2004). A Novel Approach to the Study of Bread Porous Structure: Phase-contrast X-Ray Microtomography. *Journal of Food Science*, **69**.
- FAO. (1947). Food and Agriculture Organization of the United Nations: Cereals Processing Toolkit. *International Organization*, **1**, 350.
- Fessas, D. & Schiraldi, A. (2001). Water properties in wheat flour dough I: classical thermogravimetry approach. *Food Chemistry*, **72**, 237–244.
- Gao, J., Wong, J.X., Lim, J.C.-S., Henry, J. & Zhou, W. (2015). Influence of bread structure on human oral processing. *Journal of Food Engineering*, **167**, 147–155.
- García-Aparicio, M., Parawira, W., Rensburg, E. Van, Diedericks, D., Galbe, M., Rosslander, C., Zacchi, G. & Görgens, J. (2011). Evaluation of steam-treated giant bamboo for production of fermentable sugars. *Biotechnology Progress*, **27**, 641–649.
- Gil-Martinez, J. (ABInBev). (2016). *Life Refreshment: Refreshment-Pilot for environmentally friendly, efficient, sustainable and healthy products development. LIFE15 ENV/BE/000267*.
- Giroto, F., Alibardi, L. & Cossu, R. (2015). Food waste generation and industrial uses: A review. *Waste Management*, **45**, 32–41.
- Goesaert, H., Brijs, K., Veraverbeke, W.S., Courtin, C.M., Gebruers, K. & Delcour, J.A. (2005). Wheat flour constituents: How they impact bread quality, and how to impact their functionality. *Trends in Food Science and Technology*, **16**, 12–30.
- Gray, J.A. & Bemiller, J.N. (2003). Bread Staling: Molecular Basis and Control. *Comprehensive Reviews in Food Science and Food Safety*, **2**, 1–21.
- Guessasma, S. & Nouri, H. (2015). Compression behaviour of bread crumb up to densification investigated using X-ray tomography and finite element computation. *Food Research International*, **72**, 140–148.
- Haraszi, R., Gras, P.W., Tömösközi, S., Salgó, A. & Békés, F. (2004). Application of a Micro Z-Arm Mixer to Characterize Mixing Properties and Water Absorption of Wheat Flour. *Cereal*

Chemistry Journal, **81**, 555–560.

- Hassan, A. & El-Shazly, H. (2013). Influence of Substituting Water with Fermented Skim Milk, Acid Cheese Whey or Buttermilk on Dough Properties and Baking Quality of Pan Bread. *World Journal of Dairy & Food Sciences*, **8**, 100–117.
- Hemdane, S., Jacobs, P.J., Bosmans, G.M., Verspreet, J., Delcour, J.A. & Courtin, C.M. (2017). Study of biopolymer mobility and water dynamics in wheat bran using time-domain ¹H NMR relaxometry. *Food Chemistry*, **236**, 68–75.
- Hemdane, S., Langenaeken, N.A., Jacobs, P.J., Verspreet, J., Delcour, J.A. & Courtin, C.M. (2018). Study of the role of bran water binding and the steric hindrance by bran in straight dough bread making. *Food Chemistry*, **253**, 262–268.
- Hoseney, R.C. (1986). Component Interaction during Heating and Storage of Baked Products. In: *Chemistry and physics of baking: materials, processes and products: the proceedings of an international symposium organised by the Food Chemistry Group of the Royal Society of Chemistry and the School of Agriculture of the University of Nottingham: the p* (edited by J.M.V. Blanshard, P.J. Frazier & T. Galliard). Pp. 216–226.
- Hug-Iten, S., Escher, F. & Conde-Petit, B. (2003). Staling of Bread: Role of Amylose and Amylopectin and Influence of Starch-Degrading Enzymes. *Cereal Chemistry Journal*, **80**, 654–661.
- Hug-Iten, S., Handschin, S., Conde-Petit, B. & Escher, F. (1999). Changes in Starch Microstructure on Baking and Staling of Wheat Bread. *LWT - Food Science and Technology*, **32**, 255–260.
- Ikram, S., Huang, L.Y., Zhang, H., Wang, J. & Yin, M. (2017). Composition and Nutrient Value Proposition of Brewers Spent Grain. *Journal of Food Science*, **82**, 2232–2242.
- Irvine, N.G. (1975). Milling and Baking Quality. In: *Bread: Social, Nutritional and Agricultural Aspects of Wheaten Bread social, nutritional and agricultural aspects of wheaten bread* (edited by A. Spicer). Pp. 115–126. London: Applied Science Publishers Ltd.
- Izydorczyk, M.S. (2009). Arabinoxylans. In: *Handbook of Hydrocolloids*. Pp. 653–692. Elsevier.
- Izydorczyk, M.S. & Dexter, J.E. (2008). Barley β -glucans and arabinoxylans: Molecular structure, physicochemical properties, and uses in food products—a Review. *Food Research International*, **41**, 850–868.
- Jahromi, S.H.R., Yazdi, F.T., Karimi, M. & Mortazavi, S.A. (2014). Bread-Making Process Optimization: Staling Kinetics, Relationship of Batter Rheology, Shelf Life, Quality and Sensory Characteristics of Barbari Bread. *Journal of Food Processing and Preservation*, **38**, 1447–1460.
- Kemppainen, K., Rommi, K., Holopainen, U. & Kruus, K. (2016). Steam explosion of Brewer's spent grain improves enzymatic digestibility of carbohydrates and affects solubility and stability of proteins. *Applied Biochemistry and Biotechnology*, **180**.
- Kent, N.L. & Evers, A.D. (1994a). Flour Quality. In: *Kent's Technology of Cereals*. Pp. 170–190. Woodhead Publishing Limited.
- Kent, N.L. & Evers, A.D. (1994b). Bread-baking Technology. In: *Kent's Technology of Cereals*. Pp. 191–217. Woodhead Publishing Limited.

- Kleyn, M.E. (2018). *Influence of waxy wheat flour blends on dough and bread baking quality as well as shelf life by.*
- Koksel, F., Aritan, S., Strybulevych, A., Page, J.H. & Scanlon, M.G. (2016). The bubble size distribution and its evolution in non-yeasted wheat flour doughs investigated by synchrotron X-ray microtomography. *Food Research International*, **80**, 12–18.
- Kotlar, C.E., Belagardi, M., Agüero, M.V. & Roura, S.I. (2011). Brewer's spent grain standardization and upstream processes for enzymatic hydrolysate production. P. 5. Buenos Aires, Argentina.
- Ktenioudaki, A., Alvarez-Jubete, L., Smyth, T.J., Kilcawley, K., Rai, D.K. & Gallagher, E. (2015). Application of bioprocessing techniques (sourdough fermentation and technological aids) for brewer's spent grain breads. *Food Research International*, **73**, 107–116.
- Ktenioudaki, A., Crofton, E., Scannell, A.G.M., Hannon, J.A., Kilcawley, K.N. & Gallagher, E. (2013a). Sensory properties and aromatic composition of baked snacks containing brewer's spent grain. *Journal of Cereal Science*.
- Ktenioudaki, A., O'Shea, N. & Gallagher, E. (2013b). Rheological properties of wheat dough supplemented with functional by-products of food processing: Brewer's spent grain and apple pomace. *Journal of Food Engineering*.
- Kwaśniewska, I., Rosicka-Kaczmarek, J. and & Krala, L. (2014). Factors influencing quality and shelf life of baking products. *Journal on Processing and Energy in Agriculture*, **18**, 1–7.
- Lagrain, B., Wilderjans, E., Glorieux, C. & Delcour, J.A. (2012). Importance of Gluten and Starch for Structural and Textural Properties of Crumb from Fresh and Stored Bread. *Food Biophysics*, **7**, 173–181.
- Larsson, K. (1986). Functionality of Wheat Lipids in Relation to Gluten Gel Formation. In: *Chemistry and physics of baking : materials, processes and products : the proceedings of an international symposium organised by the Food Chemistry Group of the Royal Society of Chemistry and the School of Agriculture of the University of Nottingham* (edited by J.M.V. Blanshard, P.J. Frazier & T. Galliard). Pp. 62–74. Royal Society of Chemistry.
- Laverse, J., Frisullo, P., Conte, A., Alessandro, M. & Nobile, D. (2002). X-Ray Microtomography for Food Quality Analysis. In: *Food Industrial Processes – Methods and Equipment*. Pp. 339–362.
- Leung, H.K., Magnuson, J.A. & Bruinsma, B.L. (1983). Water Binding of Wheat Flour Doughs and Breads as Studied by Deuteron Relaxation. *Journal of Food Science*, **48**, 95–99.
- Li, J., Kang, J., Wang, L., Li, Z., Wang, R., Chen, Z.X. & Hou, G.G. (2012). Effect of water migration between arabinoxylans and gluten on baking quality of whole wheat bread detected by magnetic resonance imaging (MRI). *Journal of agricultural and food chemistry*, **60**, 6507–14.
- Lim, K.S. & Barigou, M. (2004). X-ray micro-computed tomography of cellular food products. *Food Research International*, **37**, 1001–1012.
- Lind, I. & Rask, C. (1991). Sorption isotherms of mixed minced meat, dough, and bread crust. *Journal of Food Engineering*, **14**, 303–315.
- Linlaud, N.E., Puppo, M.. C. & Ferrero, C. (2009). Effect of hydrocolloids on water absorption of

- wheat flour and farinograph and textural characteristics of dough. *Cereal Chemistry*, **86**, 376–382.
- Lu, X., Brennan, M.A., Serventi, L. & Brennan, C.S. (2018). Incorporation of mushroom powder into bread dough—effects on dough rheology and bread properties. *Cereal Chemistry*, **95**, 418–427.
- Luo, D., Kou, X., Zhang, T., Nie, Y., Xu, B., Li, P., Li, X., Han, S. & Liu, J. (2018). Original article Effect of inulin on rheological properties of soft and strong wheat dough. *International Journal of Food Science & Technology*, **53**, 1648–1656.
- Lynch, K.M., Steffen, E.J. & Arendt, E.K. (2016). Brewers' spent grain: a review with an emphasis on food and health. *Journal of the Institute of Brewing*, **122**, 553–568.
- Macmurray, T.A. & Morrison, W.R. (1970). Composition of wheat-flour lipids, **21**.
- MacRitchie, F. (1986). Physicochemical Processes in Mixing. In: *Chemistry and physics of baking : materials, processes and products : the proceedings of an international symposium organised by the Food Chemistry Group of the Royal Society of Chemistry and the School of Agriculture of the University of Nottingham* (edited by J.M.V. Blanshard, P.J. Frazier & T. Galliard). Pp. 132–146. Royal Society of Chemistry.
- Madubuike, P.C. & Okolo, T.C. (2016). Quality estimation of Brewer's Spent Grains and its Potential: A Product of Beer Industries. *The International Journal Of Engineering and Science (IJES)*, **5**, 21–25.
- Mani, K., Trägårdh, C., Eliasson, A.C. & Lindahl, L. (1992). Water Content, Water Soluble Fraction, and Mixing Affect Fundamental Rheological Properties of Wheat Flour Doughs. *Journal of Food Science*, **57**, 1198–1209.
- Mbagwu, J.S.C. & Ekwealor, G.C. (1990). Agronomic potential of brewers' spent grains. *Biological Wastes*, **34**, 335–347.
- McCarthy, A.F. (2013). *Novel ingredients from brewers' spent grain - bioactivity in cell culture model systems and bioactivity retention in fortified food products*.
- McCarthy, A.L., O'Callaghan, Y.C., Piggott, C.O., FitzGerald, R.J. & O'Brien, N.M. (2013). Brewers' spent grain; bioactivity of phenolic component, its role in animal nutrition and potential for incorporation in functional foods: a review. *Proceedings of the Nutrition Society*, **72**, 117–125.
- Meneses, N.G.T., Martins, S., Teixeira, J.A. & Mussatto, S.I. (2013). Influence of extraction solvents on the recovery of antioxidant phenolic compounds from brewer's spent grains. *Separation and Purification Technology*, **108**, 152–158.
- Meuser, F. & Suckow, P. (1986). Non-starch Polysaccharides. In: *Chemistry and physics of baking : materials, processes and products : the proceedings of an international symposium organised by the Food Chemistry Group of the Royal Society of Chemistry and the School of Agriculture of the University of Nottingham* (edited by J.M.V. Blanshard, P.J. Frazier & T. Galliard). Pp. 42–61. Royal Society of Chemistry.
- Michniewicz, J., Biliaderis, G.G. & Bushuk, W. (1992). Effect of added pentosans on some properties

of wheat bread. *Food Chemistry*, **43**, 251–257.

- Mills, E.N.C., Salt, L.J., Jenkins, J.A., Skeggs, P.K. & Wilde, P.J. (2005). Bubbles in bread - The potential role of the aqueous phase of doughs in determining crumb structure. In: *Using Cereal Science and Technology for the Benefit of Consumers - Proceedings of the 12th International ICC Cereal and Bread Congress 23-26th May 2004, Harrogate, UK*. (edited by S.P. Cauvain, S.S. Salmon & L.S. Young). Pp. 138–141. Harrogate: Woodhead Publishing Series in Food Science, Technology and Nutrition.
- Mondal, A. & Datta, A.K. (2008). Bread baking - A review. *Journal of Food Engineering*, **86**, 465–474.
- Monteau, J.Y., Purlis, E., Besbes, E., Jury, V. & Le-Bail, A. (2017). Water transfer in bread during staling: Physical phenomena and modelling. *Journal of Food Engineering*, **211**, 95–103.
- Moreira, M.M., Morais, S., Carvalho, D.O., Barros, A.A., Delerue-Matos, C. & Guido, L.F. (2013). Brewer's spent grain from different types of malt: Evaluation of the antioxidant activity and identification of the major phenolic compounds. *Food Research International*, **54**, 382–388.
- Moreira, M.M., Morais, S. & Guido, L.F. (2012). A novel application of microwave-assisted extraction of polyphenols from brewer's spent grain with HPLC-DAD-MS analysis, 1019–1029.
- Morren, S., Ho, Q.T., Stoops, J., Dyck, T. Van, Claes, J., Verboven, P., Nicolaï, B. & Campenhout, L. Van. (2017). Effect of Product Microstructure and Process Parameters on Modified Atmosphere Packaged Bread. *Food and Bioprocess Technology*, **10**, 328–339.
- Mussatto, S.I. (2014). Brewer's spent grain: A valuable feedstock for industrial applications. *Journal of the Science of Food and Agriculture*, **94**, 1264–1275.
- Mussatto, S.I., Dragone, G. & Roberto, I.C. (2006). Brewers' spent grain: Generation, characteristics and potential applications. *Journal of Cereal Science*, **43**, 1–14.
- Mussatto, S.I. & Roberto, I.C. (2006). Chemical characterization and liberation of pentose sugars from brewer's spent grain. *Journal of Chemical Technology and Biotechnology*, **81**, 268–274.
- Niemi, P., Tamminen, T., Smeds, A., Viljanen, K., Ohra-Aho, T., Holopainen-Mantila, U., Faulds, C.B., Poutanen, K. & Buchert, J. (2012). Characterization of lipids and lignans in brewer's spent grain and its enzymatically extracted fraction. *Journal of Agricultural and Food Chemistry*, **60**, 9910–9917.
- Osella, C.A., Sánchez, H.D. & La Torre, M.A. De. (2007). Effect of dough water content and mixing conditions on energy imparted to dough and bread quality. *Cereal Foods World*, **52**, 70–73.
- Öztürk, S., Özboy, Ö., Ox, D., Köksel, H. & Brew, J.I. (2002). Effects of brewer's spent grain on the quality and dietary fibre content of cookies. *Journal of the Institute of Brewing of Brewing*, **108**, 23–27.
- Pareyt, B., Finnie, S.M., Putseys, J.A. & Delcour, J.A. (2011). Lipids in bread making: Sources, interactions, and impact on bread quality. *Journal of Cereal Science*, **54**, 266–279.
- Plessis, A. du, Broeckhoven, C., Guelpa, A. & Roux, S.G. le. (2017). Laboratory x-ray micro-computed tomography: A user guideline for biological samples. *GigaScience*, **6**, 1–11.

- Poladyan, A., Trchounian, K., Vassilian, A. & Trchounian, A. (2018). Hydrogen production by *Escherichia coli* using brewery waste : Optimal pretreatment of waste and role of different hydrogenases. *Renewable Energy*, **115**, 931–936.
- Puhr, D.P. & D'Appolonia, B.L. (1992). Effect of baking absorption on bread yield, crumb moisture, and crumb water activity. *Cereal Chemistry*, **69**, 582–586.
- Purhagen, J.K., Sjöo, M.E. & Eliasson, A.-C. (2011). Starch affecting anti-staling agents and their function in freestanding and pan-baked bread. *Food Hydrocolloids*, **25**, 1656–1666.
- Purhagen, J.K., Sjöo, M.E. & Eliasson, A.C. (2008). Staling effects when adding low amounts of normal and heat-treated barley flour to a wheat bread. *Cereal Chemistry*, **85**, 109–114.
- Rahman, M.S. (2009). Applications of macro–micro region concept in the state diagram and critical temperature concepts in determining the food stability. *International Journal of Food Properties*, **12**, 726–740.
- Reis, S.F., Coelho, E., Coimbra, M.A. & Abu-ghannam, N. (2015). Influence of grain particle sizes on the structure of arabinoxylans from brewer ' s spent grain. *Carbohydrate Polymers*, **130**, 222–226.
- Reis, S.F., Gullón, B., Gullón, P., Ferreira, S., Maia, C.J., Alonso, J.L., Domingues, F.C. & Abu-Ghannam, N. (2014). Evaluation of the prebiotic potential of arabinoxylans from brewer's spent grain. *Applied Microbiology and Biotechnology*, **98**, 9365–9373.
- Río, J.C. del, Prinsen, P. & Gutiérrez, A. (2013). Chemical composition of lipids in brewer's spent grain: A promising source of valuable phytochemicals. *Journal of Cereal Science*, **58**, 248–254.
- Roels, S.P., Cleemput, G., Vandewalle, X., Nys, M. & Delcour, J.A. (1993). Bread volume potential of variable-quality flours with constant protein level as determined by factors governing mixing time and absorption levels. *Cereal Chemistry*, **70**, 318–323.
- Roman-Gutierrez, A.D., Guilbert, S. & Cuq, B. (2002). Distribution of water between wheat flour components: A dynamic water vapour adsorption study. *Journal of Cereal Science*, **36**, 347–355.
- Rosell, C.M. (2011). The Science of Doughs and Bread Quality. In: *Flour and Breads and their Fortification in Health and Disease Prevention*. Pp. 3–14. Elsevier.
- SAGL. (2018). *South African Wheat Crop Quality Report 2017/2018 Season*. Pretoria, South Africa.
- Santos, M., Jiménez, J.J., Bartolomé, B., Gómez-Cordovés, C. & Nozal, M.J. Del. (2003). Variability of brewer's spent grain within a brewery. *Food Chemistry*, **80**, 17–21.
- Schoeman, L., Williams, P. & Manley, M. (2016). Trends in Food Science & Technology characterisation of food microstructure. *Trends in Food Science & Technology*, **47**, 10–24.
- Schofield, J.D. (1986). Flour Proteins: Structure and Functionality in Baked Products. In: *Chemistry and physics of baking : materials, processes and products : the proceedings of an international symposium organised by the Food Chemistry Group of the Royal Society of Chemistry and the School of Agriculture of the University of Nottingham* (edited by J.M.V. Blanshard, P.J. Frazier & T. Galliard). Pp. 14–29. Royal Society of Chemistry.

- Sęczyk, Ł., Świeca, M., Dzik, D., Anders, A. & Gawlik-Dziki, U. (2017). Antioxidant, nutritional and functional characteristics of wheat bread enriched with ground flaxseed hulls. *Food Chemistry*, **214**, 32–38.
- Severini, C., Azzollini, D., Jouppila, K., Jussi, L., Derossi, A. & Pilli, T. De. (2015). Effect of enzymatic and technological treatments on solubilisation of arabinoxylans from brewer's spent grain. *Journal of Cereal Science*.
- Shehzad, A., Khan, M.R., Shabbir, M.A. & Shoaib, M. (2013). A comprehensive review on wheat flour dough rheology. *Pakistan Journal of Food Sciences*, **23**, 105–123.
- Sobukola, O.P., Babajide, J.M. & Ogunsade, O. (2013). Effect of brewers spent grain addition and extrusion parameters on some properties of extruded yam starch-based pasta. *Journal of Food Processing and Preservation*, **37**, 734–743.
- Stojceska, V. (2011). Dietary Fiber from Brewer's Spent Grain as a Functional Ingredient in Bread Making Technology. In: *Flour and Breads and their Fortification in Health and Disease Prevention*. Pp. 171–181. Manchester, UK.
- Stojceska, V., Ainsworth, P., Plunkett, A. & Ibanoglu, S. (2008). The recycling of brewer's processing by-product into ready-to-eat snacks using extrusion technology. *Journal of Cereal Science*, **47**, 469–479.
- Švec, I. & Hrušková, M. (2018). Effect of golden and brown linseed fibre on wheat flour pasting, dough properties and bread quality. *Cereal Research Communications*, **46**, 114–123.
- Thiago, R.D.S.M., Pedro, P.M.D.M. & Eliana, F.C.S. (2014). Solid wastes in brewing process: A review. *Journal of Brewing and Distilling*, **5**, 1–9.
- Thorvaldsson, K. & Skjöldebrand, C. (1998). Water Diffusion in Bread During Baking. *LWT - Food Science and Technology*, **31**, 658–663.
- Valle, G. Della, Chiron, H., Cicerelli, L., Kansou, K., Katina, K., Ndiaye, A., Whitworth, M. & Poutanen, K. (2014). Basic knowledge models for the design of bread texture. *Trends in Food Science & Technology*, **36**, 5–14.
- Vodovotz, Y. (2007). Soy-enriched bread. In: *Technology of functional cereal products* (edited by B.R. Hamaker). Pp. 388–408. The University of Ohio, USA: Woodhead Publishing.
- Volume Graphics. (2017). VGSTUDIO MAX 3.1.
- Wall, M.C. & Rajagopalan, S. (2013). Computed Tomographic Angiography. In: *Vascular Medicine: A Companion to Braunwald's Heart Disease*. Pp. 184–198. Elsevier Inc.
- Wang, L., Fayin, Y., Sheng, L., Wei, F., Chen, J. & Zhao, G. (2017). Wheat flour enriched with oat β -glucan: A study of hydration, rheological and fermentation properties of dough. *Journal of Cereal Science*, **75**, 143–150.
- Wang, S., Li, C., Copeland, L., Niu, Q. & Wang, S. (2015). Starch Retrogradation: A Comprehensive Review. *Comprehensive Reviews in Food Science and Food Safety*, **14**, 568–585.
- Waters, D.M., Jacob, F., Titze, J., Arendt, E.K. & Zannini, E. (2012). Fibre, protein and mineral fortification of wheat bread through milled and fermented brewer's spent grain enrichment.

European Food Research and Technology, **235**, 767–778.

Weger, A., Jung, R., Stenzel, F. & Hornung, A. (2017). Optimized Energetic Usage of Brewers' Spent Grains. *Chemical Engineering & Technology*, **40**, 306–312.

Whitworth, M.B., Cauvain, S.P. & Cliffe, D. (2005). Measurement of Bread Cell Structure by Image Analysis. In: *Using Cereal Science and Technology for the Benefit of Consumers - Proceedings of the 12th International ICC Cereal and Bread Congress 23-26th May 2004, Harrogate, UK*. (edited by S.P. Cauvain, S.S. Salmon & L.S. Young). Pp. 193–198. Harrogate: Woodhead Publishing Series in Food Science, Technology and Nutrition.

Zeleznak, K.J. & Hosney, R.C. (1996). The Role of Water in the Retrogradation of Wheat Starch Gels and Bread Crumb. *Cereal Chemistry*, **63**, 407–411.

Zghal, M.C., Scanlon, M.G. & Sapirstein, H.D. (2001). Effects of flour strength, baking absorption, and processing conditions on the structure and mechanical properties of bread crumb. *Cereal Chemistry*, **78**, 1–7.

Zhou, X., Wang, R., Yoo, S.H. & Lim, S.T. (2011). Water effect on the interaction between amylose and amylopectin during retrogradation. *Carbohydrate Polymers*, **86**, 1671–1674.

Addendum: A

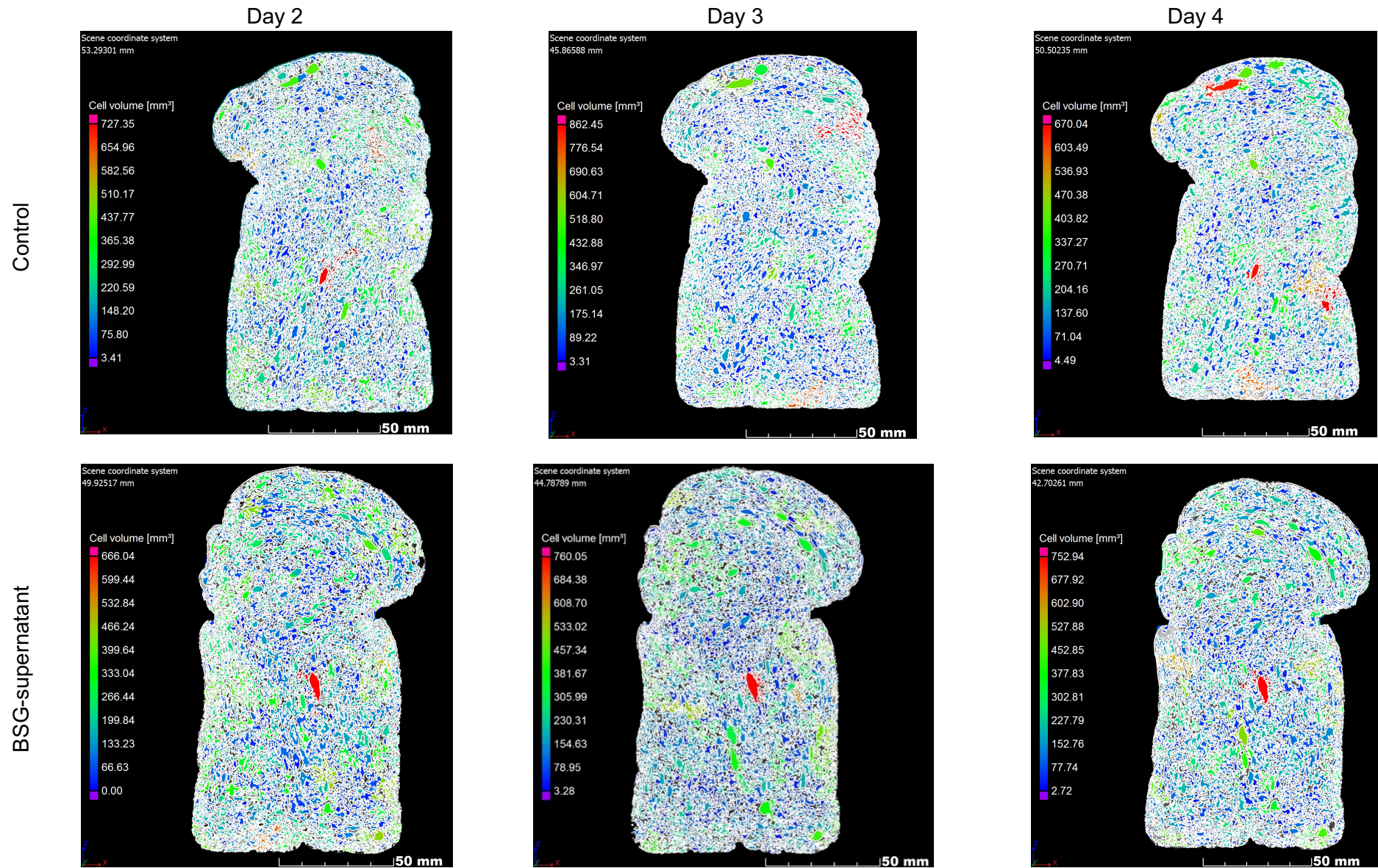


Figure A.1 Images form Foam Structure Analysis of VOI: Slice 1, across shelf-life days 2, 3 and 4

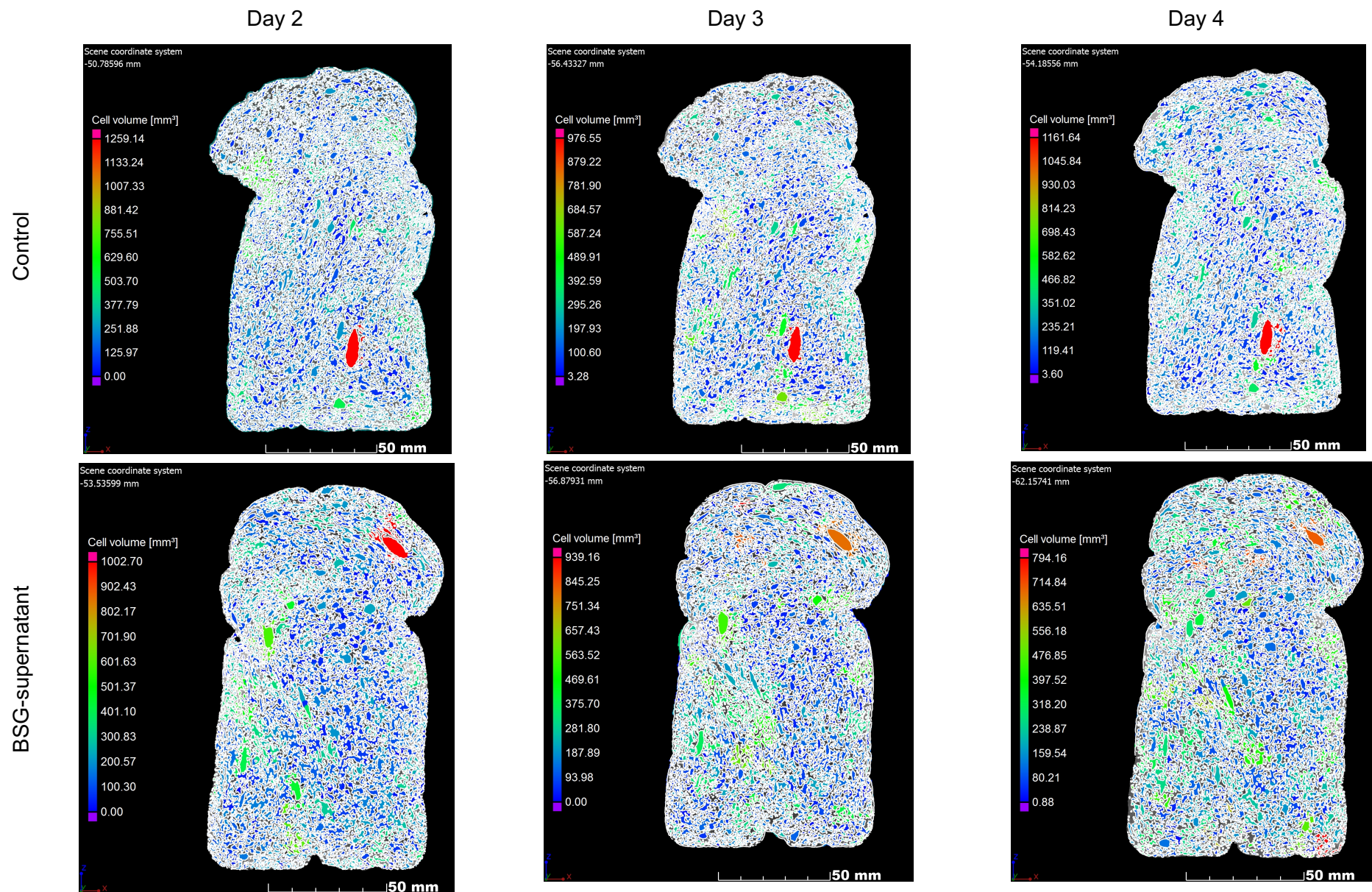


Figure A.2 Images from Foam Structure Analysis of VOI: Slice 2, across shelf-life days 2, 3 and 4

